UNIVERSAL BOUND STATES OF TWO- AND THREE-BODY QUANTUM SYSTEMS

A Dissertation
Presented to
The Academic Faculty

By

Kevin J. Driscoll

In Partial Fulfillment
of the Requirements for the Degree
Doctor of Philosophy in Physics

Georgia Institute of Technology

August 2020

UNIVERSAL BOUND STATES OF TWO- AND THREE-BODY QUANTUM SYSTEMS

Approved by:

Dr. Shina Tan, Advisor
School of Physics
Peking University

Dr. Brian Kennedy, Advisor
School of Physics
Georgia Institute of Technology

Dr. Predrag Cvitanović
School of Physics
Georgia Institute of Technology

Dr. Evans Harrell
School of Mathematics
Georgia Institute of Technology

Dr. Colin Parker
School of Physics
Georgia Institute of Technology

Date Approved: July 22, 2020

ACKNOWLEDGEMENTS

Every PhD thesis wraps one author's name around the gifts of thousands. Although I have calculated, written, and edited each and every element of this work, the final product remains a dividend on the investment of those, named and unnamed, who have touched my life.

The principal belongs to my parents, Brenda and Kenneth. I am forever indebted for their example and their sacrifice. Their unwavering support sustains my universe of possibilities and no acknowledgement can capture the size of that contribution.

I am also grateful for the spark and the insight of Dr. Shina Tan, which underlies all of this work. His unparalleled excitement and curiosity inspired me to travel this path and to approach each problem from a unique angle. I continue to appreciate and benefit from the meticulous research skills that he taught me.

A thesis will put up a fight, and Dr. Brian Kennedy has been a dedicated and persistent co-combatant. His analysis and advice greatly honed the quality and clarity of my work, allowing me to present my best efforts to the community. Most importantly, his personal support and encouragement restored my hope when there was little left.

My thesis committee members, Dr. Predrag Cvitanović, Dr. Evans Harrell, and Dr. Colin Parker also deserve praise for their flexibility, attention, and thoughtful feedback, both before and during the thesis process. I am especially grateful for their kind words and consideration.

I would have been lost years ago without the help of Heather Pynne (and Pandora). Her unwarranted patience and understanding lifted me to push past the terror and move forward. Dr. Edwin Greco has also been an ever-present friend and confidant who never gave up on me. It has been a pleasure to learn from his example of positive impact.

Many colleagues have contributed to my growth. I am happy to thank Dr. Shangguo Zhu and Dr. Ran Qi for sharing many ideas and correcting errors before they multiplied. I appreciated learning many useful new ideas from Dr. Paul Goldbart and Dr. Predrag Cvitanović. Dr. Kurt Wiesenfeld and Dr. JC Gumbart several times gave especially helpful and encouraging research and personal advice. As a teacher, I have also benefited from excellent mentors: Dr. Michael Schatz, Dr. Edwin Greco, Dr. Emily Alicea-Muñoz, and Dr. Brian Thoms.

Graduate school is about more than work, and I would like to especially thank Dr. Chien-Yuan Chang, Di Chen, Hauzia Conyers, Dr. Michael Dimitriyev, Dr. Matthew Dinehart, Dr. Perry Ellis, Dr. Alexandros Fragkopoulos, Dr. John Hyatt, Dr. Yue Jiang, Dr. Mark Kingsbury, Dr. Daegene Koh, Dr. Ravi Kumar Pallantla, Dr. Gregory Richards, Alex Riviere, Brendan Szulik, Dr. Owen Vail, and Dr. Hsin-Ju Wu for many important hours away from the office. I wish all the best to Anshul, Chelly, Evren, Galen, Kimmai, Kotaro, Nick, Saad, Sarah, Sophia, Terri, and Weiping. Thank you for bringing me into your circle. And, I owe so much to Andy for helping me turn down the noise; this would not have happened without you.

Finally, I acknowledge support from the National Science Foundation under Grant No. PHY-1068511 and No. PHY-1352208. I would also like to thank the leadership of the School of Physics, especially Dr. David Ballantyne, for generous advising and support, as well as the many staff without whom nothing would run.

TABLE OF CONTENTS

LIST OF TABLES

LIST OF FIGURES

SUMMARY

This thesis investigates the consequences of a simple physical intuition: waves scattered from objects of the same approximate size but different shapes will be virtually the same if their wavelength is much larger than the size of the objects, even if there is a low-energy resonance. We apply this idea to the interaction of quantum particles at energy scales much smaller than the characteristic scale of any internal degrees of freedom, for example collisions of trapped cold atoms or elastic nuclear scattering. Using zero-range models, which avoid making arbitrary choices about the interaction by replacing them with appropriately chosen boundary conditions, we investigate the interaction between two particles and a flat surface as well as that between three particles. We show how zero-range interactions can bind multiple particles together when the underlying potential is close to supporting a bound state at zero energy. Taking a different approach from many previous studies, we reduce these problems to solving a one-dimensional singular integral equation and demonstrate several analytical and numerical solutions with greater precision that prior techniques. Further, we show how asymptotic analysis based on the Mellin transform can extract the important parameters that describe the short-range correlations in the system, called the contacts. These results may be useful in many-particle systems if the states we describe play an important role and the methods developed can be applied to many other zero-range models.

CHAPTER 1
INTRODUCTION AND BACKGROUND

In principle, every physical system can be described according to a very small set of fundamental physical laws. However, none of these laws have known general solutions that would allow us to mechanically generate predictions from either a physical or mathematical description of the system. So, although the laws are known (at least to some level of approximation), we must still create more specific models to make testable predictions. Every physical model then faces the competing concerns of accuracy and broad applicability. Models that account for all the details of a particular system can be incredibly accurate, but then usually have a narrow range of applicability. Tractable models that apply to a broad range of very different systems can reach general conclusions, but may fail in practice because important physics is neglected. Within quantum mechanics, for example, the Schrodinger Equation can be solved essentially exactly when applied to a system of two interacting particles, say, a proton and either an electron or a neutron. However, for several particles we must often either drastically limit the strength of the interactions to apply analytical tools or use numerical techniques that require specific details about the system and its interactions to operate.

Our work attempts to chart an intermediate course for some strongly interacting systems. We strive for some degree of analytical tractability and thus we must use a greatly simplified model of interactions between just a few (2 to 3) particles. In our model, particles interact only when they overlap; the force has a range of zero. However, we can identify regimes where we expect this simple model to apply to broad classes of atomic and nuclear systems. The advantage of this approach is that we can make qualitative and quantitative predictions regardless of how strongly the constituents are interacting. And, we are sometimes able to identify features that should persist regardless of the number of

interacting particles. The disadvantage is that we must ignore many details of the interaction – such ignorance can cause both mathematical and empirical difficulties – and we do not have direct access to the many-body regime. The precise degree to which we can understand systems of many particles from studying their interacting sub-systems remains an interesting open question.

The most obvious path between two-body systems and many-body systems is, of course, to add a third interacting particle, the quantum mechanical three-body problem. In the context of our zero-range model, this problem was studied by Thomas in 1935 who found that its spectrum is unbounded from below [1]. The model was therefore essentially discarded, until Efimov showed in 1970 that at energy scales much lower than that of the deepest bound states, zero-range forces tuned to have a zero energy two-body bound state give rise to a sequence of many low-energy three-body bound states, dubbed the Efimov effect. Efimov discussed specifically the cases of the carbon-12 nucleus as well as the triton (a tritium nucleus); however his work has found its broadest application within atomic physics. Unlike nuclear physics where the interaction strengths are fixed by nature, atomic interactions can be tuned using a magnetic Feshbach resonance. It is thus possible to create atomic systems that are much more accurately described by Efimov's original theory than almost any nuclear system.

In this thesis, we both build on the existing literature for the Efimov effect and investigate a new direction for supplementing two-body interactions, resonant interactions between two particles and some external geometry. In Chapter 1 we discuss the foundations of our model, including two particle interactions via zero-range forces, and briefly summarize necessary prior work. In Chapter 2 we introduce a model for two particles interacting resonantly with a plane and derive an integral equation for this system which we then solve analytically in several special cases and numerically for arbitrary interaction strengths. Chapter 3 continues this work using asymptotic techniques to relate the behavior of this system during two- and three-particle collisions to its momentum distribution,

energy, and response to changes in the interaction strength. Finally, in Chapter II we return to the Efimov effect, derive a similar integral equation to that of Chapter 2, solve it analytically for zero binding energy and use this solution to compute the two- and three-body contacts.

1.1 What Are the Relevant Length Scales in Cold Atom Experiments?

The natural world spans many orders of magnitude in length, from the size of the observable universe ($\sim 10^{27}$m) to subnuclear structures ($< 10^{15}$m), and we must identify which length scales are relevant for the physics that we wish to describe and which length scales are irrelevant. Typically, length scales either much larger or much smaller than the overall size of our system can be safely ignored.

For example, in a system of cold atoms, we can immediately identify a hierarchy of length scales. Neutral atoms interact primarily through a Van der Waals potential,

$$V_{VdW}(r) = -\frac{C_6}{r^6},$$

which is much shorter ranged than Coulomb or magnetic dipole interactions because it is inversely proportional to the sixth power of the distance between atoms. The characteristic length scale associated with this potential is called the Van der Waals length,

$$r_{VdW} = \frac{1}{2}\left(\frac{mC_6}{\hbar^2}\right)^{\frac{1}{4}},$$

which is a few nanometers (10^{-9}m) for the atoms most commonly used in cold atom experiments.

By contrast, the overall size of the system combined with the number of atoms present gives a scale for the average separation between atoms,

$$L = \left(\frac{N}{V}\right)^{\frac{1}{3}}. \tag{1.1}$$

For the typical size of atom traps and the number of atoms present, the average separation is a few microns (10^{-6}m). When treated as point-like objects, the atoms would almost never be within the characteristic range of the potential. However, when cooled the atoms can maintain internal coherence over longer and longer length scales, making them behave more as wave-like objects. Their characteristic wavelength, which acts as a kind of average size for a cold atom, is known as the de Broglie wavelength,

$$\Lambda = \sqrt{\frac{2\pi\hbar^2}{mk_BT}}, \tag{1.2}$$

and can range from 100 nanometers for microkelvin systems to more than a micron as the system is cooled to the nanokelvin range.

Therefore, throughout the range of experimental parameters the Van der Waals length is much smaller than the length scales that characterize the system overall,

$$r_{VdW} \ll \Lambda \sim L. \tag{1.3}$$

We might therefore expect that at the experimental scale, the interactions between atoms should be largely negligible and we should be able to think about the system primarily as a collection of non-interacting wave-like objects. And, in fact, many experiments with cold atomic gases take exactly this view and show very good agreement with non-interacting or weakly interacting models. However, as we shall see in the next section, quantum scattering can produce pathological cases where interactions over a very short length scale modify the system's behavior at much larger scales.

1.2 Two Particle Scattering at Low Energy

Consider the case of scattering between two particles interacting via an isotropic potential. We can derive two important results, known as the Effective Range Expansion and the

Bethe-Peierls boundary condition, which illuminate how the length scale of scattering may be much larger than that of the underlying potential.

The Schrodinger equation for two particles of mass m with center of mass $R \in \mathbb{R}^3$ and relative position $s \in \mathbb{R}^3$ interacting via a potential that depends only on their relative position vector $V(s)$ is given by

$$\left(-\frac{\hbar^2}{2m}\nabla^2 + V(s)\right)\Psi(R,s) = E\,\Psi(R,s). \tag{1.4}$$

Because the potential depends only on the relative coordinates, we can separate out the center of mass variables using a product ansatz,

$$\Psi(R,s) = \phi(R)\psi(s),$$

which leads to the differential equations

$$\left(-\nabla_s^2 + U(s)\right)\psi(s) = k^2\psi(s) \tag{1.5}$$

$$-\nabla_R^2\phi(R) = K^2\phi(R) \tag{1.6}$$

with the wavenumbers k, K satisfying $\frac{\hbar^2K^2}{4m} + \frac{\hbar^2k^2}{m} = E$ and $V(s) \equiv \frac{\hbar^2}{m}U(s)$. For a spherically symmetric potential $U(s) = U(r)$, $r = |s|$, and if we expand the relative wavefunction as

$$\psi(s) = \chi(r)Y_{lm}(\theta,\phi), \tag{1.7}$$

with the Y_{lm} constructed such that with

$$\nabla_s^2 = \frac{1}{r^2}\frac{\partial}{\partial r}\left(r^2\frac{\partial}{\partial r}\right) - \frac{\hat{L}^2}{r^2},$$
$$\hat{L}^2 \equiv -\frac{1}{\sin^2\theta}\left(\sin\theta\frac{\partial}{\partial\theta}\left(\sin\theta\frac{\partial}{\partial\theta}\right) + \frac{\partial^2}{\partial\phi^2}\right),$$

they satisfy [2]

$$\hat{L}^2 Y_{lm} = l(l+1)Y_{lm},$$

then for the radial component we are left with

$$-\frac{d^2}{dr^2}\left(r\chi(r)\right) + \frac{l(l+1)}{r^2} r\chi(r) + U(r)r\chi(r) = k_l^2 r\chi(r) \tag{1.8}$$

provided that $\sum_{l=0}^{\infty} k_l^2 = k^2$. And finally letting $r\chi(r) \equiv u(r)$ in the s-wave ($l = 0$) channel we have a radial Schrodinger equation which is equivalent to a one dimensional Schrodinger equation

$$-\frac{d^2}{dr^2}u(r) + U(r)u(r) = k_0^2 u(r). \tag{1.9}$$

If the potential U has compact support, that is $U(r) = 0,\ r > r^*$, then outside this range of interaction, $u(r)$ satisfies a free Schrodinger equation and we can write a general solution as

$$u(r) = \frac{\sin\left(k_0 r + \delta(k_0)\right)}{\sin\left(\delta(k_0)\right)}, \tag{1.10}$$

where the s-wave scattering phase shift $\delta(k_0)$ must be determined by matching the logarithmic derivative of the radial wavefunction at $r = r^*$ and the normalization is chosen purely for convenience. That leaves for the logarithmic derivative

$$\frac{u'(r)}{u(r)} = k_0 \cot\left(k_0 r + \delta(k_0)\right). \tag{1.11}$$

Returning to our discussion of length scales, because the thermal deBroglie wavelength is so large compared to the Van der Waals length and k_0 characterizes the wavelength of the particles outside the range of interaction, we will investigate the range where $k_0 r^* \ll 1$.

We can neglect $k_0 r^*$ on the right-hand side leaving only the r-independent $k_0 \cot\left(\delta(k_0)\right)$ and relate this logarithmic derivative to the difference between the radial Schrodinger solution with and without the interaction potential by considering two solutions with different

eigenvalues [3, 4, 5, 6]

$$-\frac{d^2}{dr^2}v(r) + U(r)v(r) = v_0^2 v(r),$$
$$-\frac{d^2}{dr^2}w(r) + U(r)w(r) = w_0^2 w(r).$$

Further, divide the solutions into inner and outer sections

$$v(r) = \begin{cases} v_<(r) & r < r^*, \\ v_>(r) & r > r^*, \end{cases}$$

$$w(r) = \begin{cases} w_<(r) & r < r^*, \\ w_>(r) & r > r^*. \end{cases}$$

If we cross-multiply and subtract the Schrodinger equations associated to these two solutions, the terms dependent on the potential cancel and we are left with

$$v(r)\frac{d^2}{dr^2}w(r) - w(r)\frac{d^2}{dr^2}v(r) = (v_0^2 - w_0^2)v(r)w(r).$$

The left-hand side is, in fact, a total derivative with respect to r, which can be integrated from 0 to some arbitrary point R giving

$$\left[v(r)\frac{d}{dr}w(r) - w(r)\frac{d}{dr}v(r)\right]_0^R = (v_0^2 - w_0^2)\int_0^R v(r)w(r)\,dr$$

for the full solution, and repeating this process considering only the solution outside the range of interaction

$$\left[v_>(r)\frac{d}{dr}w_>(r) - w_>(r)\frac{d}{dr}v_>(r)\right]_0^R = (v_0^2 - w_0^2)\int_0^R v_>(r)w_>(r)\,dr.$$

If we let $R > r^*$, then $v(r) = v_>(r),\ w(r) = w_>(r)$ and so when subtracting these

equations, the upper limit on the left-hand side cancels. In addition, the full solutions will have $v(0) = w(0) = 0$ and so in that relation, the lower limit will also be zero. Therefore subtracting gives

$$(v_0^2 - w_0^2)\int_0^R v_>(r)w_>(r) - v(r)w(r)\,dr = v_>(0)\frac{d}{dr}w_>(0) - w_>(0)\frac{d}{dr}v_>(0)$$
$$= w_0\cot(\delta(w_0)) - v_0\cot(\delta(v_0)).$$

Let w_0, v_0 be small compared to the energy scale of the potential, then these solutions will be small correction to the solutions at zero energy, $v(0,r), w(0,r)$. Further, let $v_0 \to 0$, then

$$w_0\cot(\delta(w_0)) = \lim_{v_0\to 0} v_0\cot(\delta(v_0)) + w_0^2\int_0^{r^*} w(0,r)^2 - w_>(0,r)^2\,dr + \mathcal{O}(w_0)^3.$$

We define $\lim_{v_0\to 0} v_0\cot(\delta(v_0)) = -\frac{1}{a}$ to be the inverse of the s-wave scattering length and we refer to the coefficient of the second term as the s-wave effective range

$$\frac{1}{2}r_s = \int_0^{r^*} w(0,r)^2 - w_>(0,r)^2\,dr.$$

These are the first two terms in the Effective Range Expansion

$$k\cot(\delta(k)) = -\frac{1}{a} + \frac{1}{2}r_s k^2 + \mathcal{O}(k^4), \tag{1.12}$$

and we will apply this parameterization to the logarithmic derivative which we derived earlier,

$$\frac{u'(r)}{u(r)} = -\frac{1}{a} + \frac{1}{2}r_s k_0^2 + \mathcal{O}(k_0^4). \tag{1.13}$$

This implies that

$$\frac{\psi'(r)}{\psi(r)} = -\frac{1}{r} + \frac{u'(r)}{u(r)},$$

and then integrating and considering the small-r behavior, we find that

$$\psi(r) = \frac{1}{r} - \frac{1}{a} + \mathcal{O}(r). \tag{1.14}$$

This expression, which we arrived at by considering the exact behavior of the wavefunction anywhere outside the range of interaction and applying the results of the effective range expansion, leads to what is called the Bethe-Peierls boundary condition [3]. At first glance, this appear to be an extremely local condition on the wavefunction; it only considers the behavior at the range of interaction. However, its consequence can propagate to scales much large than that.

The Bethe-Peierls boundary condition implies that the wavefunction has a node outside the range of interaction at

$$\psi(a) \approx 0.$$

If the scattering length is of order the range of interaction,

$$a \sim r^*,$$

then $\psi(a) \approx \psi(r^*) \approx 0$ and the wavefunction will be close to zero just outside the range of interaction. The difference then between the scattering solution and the free solution (the solution of the Schrodinger equation with no potential at all) is just that the node of the free solution at $r = 0$ has been displaced to $r \sim r^*$. Because r^* is negligible compared to the wavelength $1/k_0 \sim \Lambda$ this amounts to only a small change of phase of the solution. In this

case, the scattering solution is almost the same as the free solution everywhere outside the range of interaction. By contrast, if the scattering length is much larger than the range of interaction,

$$a \gg r^*,$$

then the wavefunction just outside the range of interaction has a very large value, in fact it is near a maximum/minimum, and therefore the phase shift is near $\pi/2$. The solution outside the range of interaction is then altered in the most radical way possible compared to the free solution everywhere outside the range of interaction.

We see then that when the scattering length is large, we cannot necessarily neglect interactions that have a small range because they alter the behavior of the wavefunction over lengths of order the scattering length, much larger than the size of the underlying potential. Our hierarchy of length scales will be disrupted, then, when we have

$$r_{VdW} \ll a \sim \Lambda \sim L. \tag{1.15}$$

In these situations, our starting point cannot be a non-interacting model because the length scale of our interactions is comparable to the average size of the atoms and the average distance between them.

1.3 Zero Range Models

The effective range expansion demonstrates that regardless of the functional form of the interaction potential, systems that have the same scattering length, effective range, and/or higher-order shape parameters behave similarly at low energies. We may therefore choose interaction potentials that are especially convenient for our analysis, confident that the results do not depend on the particular choice up the appropriate order. For a potential of finite range, this would involve specifying the range of the potential and requiring that both the wavefunction and its derivative be continuous at $r = r^*$. However, we can further

eliminate this arbitrary choice by considering a potential of zero range.

The main idea of this approach is that we extend the behavior given by the Bethe-Peierls boundary condition all the way in to the origin, collapsing the potential into an infinitesimal region. Doing this in a naive way with no fine-tuning would eliminate the scattering altogether since as the size of the scatterer shrinks, so generally does the probability of a scattering event and thus the cross section. However, in the zero-range procedure, as the range of interaction goes to zero, we keep the potential tuned so that the scattering length is fixed. This fixes the low energy cross section and preserves the scattering even in the limit of an infinitesimal scatterer [7]. Note that it is not possible to carry out this procedure with all of the (infinite) coefficients in the expansion of the scattering phase shift fixed; only a finite number may be fixed. Inverse scattering theory shows that the scattering amplitude due to a finite ranged potential is an analytic function of the incoming wavenumber and therefore the scattering phase shift is given everywhere by its expansion about zero [8]. As such, the full effective range expansion uniquely specifies a short-range potential and it is therefore not possible to reduce the range of the potential and keep the entire expansion fixed. Nevertheless, we can fix any finite number of the coefficients and carry out our procedure.

This procedure can lead to mathematical difficulties; for example, the resulting wavefunctions may no longer be within the domain of the kinetic energy operator, or the implied Hamiltonian may fail to be essentially self-adjoint [9]. As they arise, we will need to navigate such issues while keeping in mind that this model should always be thought of as a particular limiting procedure involving finite-ranged potentials. With that understanding, we realize why particular mathematical issues arise and how their solution is settled by the short-range physics which our models neglect.

Throughout this thesis, we follow a particular method to implement zero-range models and the Bethe-Peierls boundary condition which we will now summarize. So long as two or more particles are not overlapping, the zero-range wavefunction will satisfy the

free Schrodinger equation. Extending that behavior to the entire configuration space naturally leads to a system of free particles. However, we will show that we can enforce the Bethe-Peierls boundary condition by considering a non-homogeneous Schrodinger equation perturbed by a delta function. The solution can then be written in terms of the free Green's function and will automatically have the appropriate singular behavior present in the Bethe-Peierls boundary condition. We will however still need to match our solution to the regular part of the Bethe-Peierls boundary condition which will lead to an integral equation involving the weight of the non-homogeneous term in the Schrodinger equation. It is this integral equation that will be the primary object of study in each of our investigations.

1.4 The Shallow Dimer

To illustrate the methods that we discussed in the previous section, let us begin with the simplest zero-range model; that of two identical spinless bosons of mass m interacting with an s-wave scattering length a in free space. This system is well-known in the literature and therefore our methods should reproduce the known wavefunctions and eigenenergies.

Let $(x, y) \in \mathbb{R}^3 \times \mathbb{R}^3$ be the positions of these bosons. The bosons are unconfined, but experience an interparticle interaction, which we take to be of zero-range. Then, whenever the two particles are not in contact (almost everywhere) the system obeys the free Schrodinger equation:

$$\left(-\frac{\hbar^2}{2m}\nabla_x^2 - \frac{\hbar^2}{2m}\nabla_y^2\right)\psi(x,y) = E\psi(x,y), \quad x \neq y. \tag{1.16}$$

And in the center of mass and relative coordinates

$$R = \tfrac{x+y}{2}, \quad r = x - y,$$

$$\left(-\frac{\hbar^2}{4m}\nabla_R^2 - \frac{\hbar^2}{m}\nabla_r^2\right)\,\psi\left(R+\frac{r}{2}, R-\frac{r}{2}\right) = E\,\psi\left(R+\frac{r}{2}, R-\frac{r}{2}\right), \quad r \neq 0. \tag{1.17}$$

To satisfy the Bethe-Peierls boundary condition, our prescription includes adding a source

term to the Schrodinger equation

$$\left(-\frac{\hbar^2}{4m}\nabla_R^2 - \frac{\hbar^2}{m}\nabla_r^2\right)\ \psi\left(R+\frac{r}{2}, R-\frac{r}{2}\right) - E\ \psi\left(R+\frac{r}{2}, R-\frac{r}{2}\right) = \frac{\hbar^2}{m} f(R)\delta(r), \tag{1.18}$$

where the unknown function $f(R)$ appears in the boundary condition,

$$\psi\left(R+\frac{r}{2}, R-\frac{r}{2}\right) \sim f(R)\left(\frac{1}{r}-\frac{1}{a}\right), \quad r \to 0.$$

Taking the Fourier Transform over all 6 coordinates,

$$\widetilde{\psi}(K,q) \equiv \int_{\mathbb{R}^6} \psi\left(R+\frac{r}{2}, R-\frac{r}{2}\right) e^{iK\cdot R} e^{iq\cdot r}\ d^3R\, d^3r,$$

$$\widetilde{f}(K) \equiv \int_{\mathbb{R}^3} f(R) e^{iK\cdot R}\ d^3R,$$

$$\left(\frac{\hbar^2}{4m}K^2 + \frac{\hbar^2}{m}q^2\right)\ \widetilde{\psi}(K,q) - E\ \widetilde{\psi}(K,q) = \frac{\hbar^2}{m}\widetilde{f}(K), \tag{1.19}$$

and therefore a particular solution to Eq. 1.18 is

$$\psi\left(R+\frac{r}{2}, R-\frac{r}{2}\right) = \frac{1}{(2\pi)^6}\int_{\mathbb{R}^6} \frac{\frac{\hbar^2}{m}\widetilde{f}(K)}{\frac{\hbar^2}{4m}K^2 + \frac{\hbar^2}{m}q^2 - E} e^{-iK\cdot R} e^{-iq\cdot r}\ d^3K\ d^3q. \tag{1.20}$$

The dependence on q is entirely explicit and so we can carry out the integral. There will, however, be a pole when $\frac{\hbar^2}{4m}K^2 + \frac{\hbar^2}{m}q^2 - E = 0$ that must be bypassed. In this case, both ways of avoiding the pole lead to the same expression,

$$\psi\left(R+\frac{r}{2}, R-\frac{r}{2}\right) = \frac{1}{32\pi^4}\int_{\mathbb{R}^3}\left[\frac{e^{-iK\cdot R - r\sqrt{\frac{K^2}{4}-\frac{mE}{\hbar}}}}{r}\widetilde{f}(K)\,\Theta\left(\frac{\hbar^2K^2}{4m}-E\right)\right.$$
$$\left. + \frac{e^{-iK\cdot R + ir\sqrt{\frac{mE}{\hbar}-\frac{K^2}{4}}}}{r}\widetilde{f}(K)\,\Theta\left(E-\frac{\hbar^2K^2}{4m}\right)\right] d^3K,$$

where $\Theta(x)$ is the Heaviside theta function. This expression can be combined in the form

$$\psi\left(R+\frac{r}{2},R-\frac{r}{2}\right)=\frac{1}{32\pi^4}\int_{\mathbb{R}^3}\frac{e^{-iK\cdot R+ir\sqrt{\frac{mE}{\hbar}-\frac{K^2}{4}}}}{r}\widetilde{f}(K)\,d^3K,$$

provided that we understand that for negative arguments, we take the principal branch of the square root function. Rewriting this expression using the Fourier convolution theorem gives

$$\psi\left(R+\frac{r}{2},R-\frac{r}{2}\right)=-\frac{mE}{(2\pi)^3\hbar^2}\int_{\mathbb{R}^3}f(R')\frac{K_2\left(-\frac{i}{\hbar}\sqrt{4mE}\sqrt{(R-R')^2+\left(\frac{r}{2}\right)^2}\right)}{(R-R')^2+\left(\frac{r}{2}\right)^2}\,d^3R'.$$

For the first time, we introduce $K_n(x)$, the modified Bessel function of the second kind of order n, sometimes also called the MacDonald function. The properties of this family of special functions that will be relevant to several points of analysis through the thesis are summarized in Appendix G At this point, we need to investigate the behavior of the wavefunction when two atoms closely approach each other to enforce the Bethe-Peierls boundary condition by taking the limit $r\to 0$. However, the integrand in our particular solution has a non-integrable singularity in this limit at $R=R'$. We therefore divide the region of integration and treat each region separately.

Let

$$r << \epsilon << \left|\sqrt{\frac{\hbar^2}{4mE}}\right|.$$

Then, when $|R-R'|\leq\epsilon$ we have that

$$\frac{\sqrt{4mE}}{\hbar}\sqrt{(R-R')^2+\left(\frac{r}{2}\right)^2}<<1$$

and we can replace the Bessel function with its expansion for small arguments in this re-

gion. In the outer region, $|R-R'|>\epsilon$ and we may thus neglect r directly,

$$= \frac{f(R)}{4\pi^2}\int_0^{\epsilon}\frac{|R''|^2}{\left(|R''|^2+\left(\frac{r}{2}\right)^2\right)^2}\,d|R''|+$$
$$-\frac{mE}{(2\pi)^3\hbar^2}\int_{|R-R'|>\epsilon} f(R')\frac{K_2\left(-\frac{i}{\hbar}\sqrt{4mE}|R-R'|\right)}{|R-R'|^2}\,d^3R'+\mathcal{O}(r)$$

$$= \frac{f(R)}{8\pi r}-\frac{f(R)}{4\pi^2\epsilon}-\frac{mE}{(2\pi)^3\hbar^2}\int_{|R-R'|>\epsilon} f(R')\frac{K_2\left(-\frac{i}{\hbar}\sqrt{4mE}|R-R'|\right)}{|R-R'|^2}\,d^3R'+\mathcal{O}(r)+\mathcal{O}(\frac{r}{\epsilon}).$$

We will take a sequence of limits to match this expression to the Bethe-Peierls boundary condition. First, we let $r\to 0$ and then let $\epsilon\to 0$ with the result that

$$\frac{f(R)}{a}=\lim_{\epsilon\to 0}\left(\frac{mE}{\pi^2\hbar^2}\int_{|R-R'|>\epsilon} f(R')\frac{K_2\left(-\frac{i}{\hbar}\sqrt{4mE}|R-R'|\right)}{|R-R'|^2}\,d^3R'+\frac{2f(R)}{\pi\epsilon}\right).$$

It is this integral equation which determines the particular function $f(R)$ that characterizes our system.

Noting that the integral operator on the right-hand side resembles a convolution operator, we can try an ansatz,

$$f(R)=e^{iK_0\cdot R}, \tag{1.21}$$

with K_0 to be determined. Substituting this ansatz into the integral equation and also shifting the origin in the integral, we have

$$\frac{e^{iK_0\cdot R}}{a}=\lim_{\epsilon\to 0}\left(\frac{mE}{\pi^2\hbar^2}\int_{|R'|>\epsilon} e^{iK_0\cdot(R-R')}\frac{K_2\left(-\frac{i}{\hbar}\sqrt{4mE}|R'|\right)}{|R'|^2}\,d^3R'+\frac{2e^{iK_0\cdot R}}{\pi\epsilon}\right).$$

The dependence on R cancels and K_0 must be chosen so that

$$\frac{1}{a}=\lim_{\epsilon\to 0}\left(\frac{mE}{\pi^2\hbar^2}\int_{|R|\geq\epsilon} e^{iK_0\cdot R}\frac{K_2\left(-\frac{i}{\hbar}\sqrt{4mE}|R|\right)}{R^2}\,d^3R+\frac{2}{\pi\epsilon}\right). \tag{1.22}$$

Performing the integrals over the direction of R gives

$$\frac{1}{a} = \lim_{\epsilon \to 0} \left(\frac{4mE}{\pi \hbar^2} \int_{\epsilon}^{\infty} K_2 \left(-\frac{i}{\hbar} \sqrt{4mE} |R| \right) \frac{\sin K_0 |R|}{K_0 |R|} \, d|R| + \frac{2}{\pi \epsilon} \right). \tag{1.23}$$

Rather than compute this integral via a subtraction regularization, we instead compute

$$\frac{1}{a} = \lim_{\alpha \to 1} \frac{4mE}{\pi \hbar^2} \int_{0}^{\infty} K_{2\alpha}(-\frac{i}{\hbar} \sqrt{4mE} |R|) \frac{\sin K_0 |R|}{K_0 |R|^{\alpha}} \, d|R|, \tag{1.24}$$

which exists as an ordinary integral for $|\alpha| < \frac{1}{2}$ and can be expressed as a sum of several Gauss hypergeometric functions of $\frac{K_0^2}{\beta^2}$. The limit however gives the relatively simple relation

$$-\frac{1}{a} = \frac{i}{2\hbar} \sqrt{4mE - \hbar^2 K_0^2}. \tag{1.25}$$

For a real scattering length, this relation is only satisfiable when

$$\frac{\hbar^2 K_0^2}{4m} > E, \tag{1.26}$$

and because we have taken the principal branch of the square root, there are no solutions when the scattering length is negative. When both conditions are satisfied, we can find a solution with

$$K_0^2 = \frac{4mE}{\hbar^2} + \frac{4}{a^2}. \tag{1.27}$$

Given this result for $f(R)$,

$$\widetilde{f}(K) = (2\pi)^3 \delta^3 (K - K_0), \tag{1.28}$$

and therefore

$$\begin{aligned}\psi_{K_0}\left(R+\frac{r}{2},R-\frac{r}{2}\right) &= \frac{1}{32\pi^4}\int_{\mathbb{R}^3}\frac{e^{-iK\cdot R+ir\sqrt{\frac{mE}{\hbar}-\frac{K^2}{4}}}}{r}\widetilde{f}(K)\,d^3K,\\ &= \frac{e^{-iK_0\cdot R+ir\sqrt{\frac{mE}{\hbar}-\frac{K_0^2}{4}}}}{4\pi r}\\ &= \frac{e^{-\frac{r}{a}}}{4\pi r}e^{-iK_0\cdot R}.\end{aligned}$$

We can normalize this wavefunction such that

$$\int_{\mathbb{R}^6}\psi^*_{K_1}\left(R+\frac{r}{2},R-\frac{r}{2}\right)\psi_{K_2}\left(R+\frac{r}{2},R-\frac{r}{2}\right)\,d^3R\,d^3r=(2\pi)^3\delta^3(K_1-K_2)$$

and therefore the normalized wavefunction is given by

$$\psi_{K_0}\left(R+\frac{r}{2},R-\frac{r}{2}\right)=\frac{1}{\sqrt{2\pi a}}\frac{e^{-\frac{r}{a}}}{r}e^{-iK_0\cdot R}, \tag{1.29}$$

with $a>0$, $K_0\in\mathbb{R}^3$ arbitrary, and

$$E=\frac{\hbar^2K_0^2}{4m}-\frac{\hbar^2}{ma^2}$$

We have found then a single bound state within the zero-range model for two particles in free space, commonly referred to as the shallow dimer. Our expressions for both the wavefunction and the binding energy of this state agree with those found in the literature [10]. This validates that we can implement a zero-range model via our non-homogeneous Schrodinger equation, and we will continue by applying a similar procedure for the interaction of more than two particles and for two particles interacting with a surface.

1.5 The Efimov Effect

The Efimov Effect is the spontaneous generation of relatively long range effective three-body forces within a system of three (or more) particles with scattering lengths (see Section 1.2) that are much larger than the characteristic length scale of the underlying two-body potentials. It was first predicted in 1970 by Efimov [11], who was investigating the interaction between neutrons and protons at low energies, and he predicted that such three-body forces should create a sequence of three-body bounds states regardless of the size and shape of the particular microscopic potential. The system's properties are said to be "universal" in that all of the details of the interaction can be summarized by just two parameters, the scattering length a and what is known as the Efimov parameter, which we will refer to as β_0 [10, 12, 13]. Efimov himself later showed how the binding energy of the triton (a bound state of two neutrons and a proton) could be predicted within this paradigm; however, it would take several decades before his original prediction for identical bosons could be verified.

Cold atomic gases later replaced nucleons as the most natural setting in which to consider Efimov's predictions, both because many trappable atomic species behave as composite bosons and because the presence of magnetic Feschbach resonances allow systems to be tuned so that the scattering length becomes very large. We will postpone any technical details describing or setting up the three-boson problem until the appropriate chapter within this thesis. However, we will for now summarize several known facts about the Efimov Effect in the three-boson problem to set the stage for later work. We do not give here a comprehensive list of facts about Efimov trimers because several comprehensive review articles exist; rather, we list only the central elements that set a foundation for our work.

In the zero-range model, the main feature of the Efimov Effect is a series of three body bound states which exist for arbitrary scattering length. These states can be understood as a consequence of an effective inverse square potential which arises in the problem when viewed in the hyperspherical coordinate system [11, 14, 15]. As is well-known, inverse

square potentials exhibit a "fall to the center" effect which would lead to probability "escaping" into the origin; however, this is generally remedied by applying a boundary condition at the edge of the region of configuration space where three particles collide such that probability is conserved [9, 1, 16, 17, 18, 19]. One would expect from the classical action of such a potential that a continuous scale symmetry exists within the system; however, that symmetry is broken at the quantum level by this additional boundary condition to a discrete scaling symmetry [20]. Within a real system, the short-range physics will create a cut-off such that these mathematical issues do not arise. The phase of the three-body wavefunction will be determined by the details of the interparticle interaction, which will set the Efimov parameter, and there will be some deepest bound Efimov trimer of size comparable to the range of interaction such that the spectrum is bounded from below [21].

Whenever we find a trimer state with a binding energy β at a scattering length a, we can find an entire sequence of associated trimer states at binding energies $\beta_n = e^{\frac{n\pi}{s_0}}\beta$ at scattering lengths $a_n = e^{-\frac{n\pi}{s_0}}a$ for $n \in \mathbb{Z}$. These trimers are all identical up to this scale transformation [22]. The numbers $\pm is_0$ are the only imaginary roots of the transcendental equation

$$\frac{8}{\sqrt{3}}\sin\left(\frac{\pi\nu}{6}\right) - \nu\cos\left(\frac{\pi\nu}{2}\right) = 0. \tag{1.30}$$

and $\lambda = e^{\frac{\pi}{s_0}} \approx 22.7$. If we define the binding wavenumber of a particular trimer at unitarity ($a \to \pm\infty$) as β_0, then away from unitarity, we can follow the binding wavenumber of that particular state as the scattering length is tuned. On the positive side, the ratio of the binding energies of adjacent trimers at fixed scattering length is generally smaller than λ^2. Each binding energy approaches that of the universal two-body bound state (the shallow dimer) as the scattering length is decreased to a critical value, where that state disappears into the continuum. Specifically, the trimer with binding wavenumber β_0 at unitarity decays into one free atom and a universal dimer at $a^* = 0.070764509\beta_0^{-1}$ [10].

On the negative side, the opposite is true as the ratio of the binding energies of adjacent trimers at fixed scattering length generally becomes larger than the ratio at unitarity. Each

trimer eventually reaches a negative critical scattering length; if its binding wavenumber was $beta_0$ at unitarity, then at a scattering length $a'^* = -1.507639982\beta_0^{-1}$ the binding energy of the trimer approaches zero and it disassociates into three free atoms [23]. It is this limit that will be the focus of our work on the Efimov effect.

1.6 The Contacts

Effective calculations of the properties of a many-body quantum system typically rely on finding a representation of the system in which the degrees of freedom are relatively uncorrelated. For strongly interacting systems, such a representation rarely overlaps significantly with the stationary states of the non-interacting system, which are typically well-known. However, in the case of zero-range interactions, the short-range correlations can be characterized by a quantity called the contact which determines both how changes in the collective properties of the system are related to changes in the interaction parameters and also how the energy of the interacting system depends on the degrees of freedom relevant for a non-interacting system.

This surprising result was first derived by Tan for the two-component Fermi gas [24, 25, 26]. It has been extended in several directions, including being defined for a system of N identical particles with wavenumbers $k_1, ..., k_N \in \mathbb{R}^3$ and wavefunction $\widetilde{\psi}(k_1, ..., k_N)$ as the leading coefficient in the asymptotic expansion of the single particle momentum distribution,

$$C_2 \equiv \lim_{k\to\infty} k^4 n(k), \tag{1.31}$$

$$n(k) \equiv \sum_{i=1}^{N} \int |\widetilde{\psi}(k_1, ..., k_N)|^2 \prod_{j\neq i} d^3k_j. \tag{1.32}$$

Precisely the same contact also characterizes the small-distance limit of the pair distribution function, $G_2(r, r')$, which describes the probability distribution of finding one particle at r and a second at r'. When integrated, the total probability of finding a pair of size r

somewhere in the system is proportional to the contact,

$$\int G_2(R+r, R-r)\, d^3R \sim \frac{C_2}{r^2}, \quad r \to 0. \tag{1.33}$$

Further, due to the duality between smoothness and decay for the Fourier Transform, the contact for an unconstrained gas of particles can also be related to the behavior of the wave-function when two or more particles are close. According to the Bethe-Peierls boundary condition,

$$\Psi(r_1, ..., r_N) \sim \left(\frac{1}{|r_i - r_j|} - \frac{1}{a}\right) A\left(\frac{r_1 + r_j}{2}, \{r_k\}_{k\neq i,j}\right) \quad r_i \to r_j, \tag{1.34}$$

and the contact is then related via [25]

$$C_2 \sim \int \left| A\left(\frac{r_1 + r_j}{2}, \{r_k\}_{k\neq i,j}\right)\right|^2 \prod_{l\neq i,j} d^3 r_l. \tag{1.35}$$

Despite the fact that the contact is defined by the behavior of the wavefunction in a particular region of configuration space, it is also directly related to the overall properties of the system. For instance, after accounting for the contact, the internal energy of the interacting gas can be written in a form reminiscent of the non-interacting gas [24]:

$$E = \frac{\hbar^2 C_2}{4\pi m a} + \sum_k \frac{\hbar^2 k^2}{2m}\left(n(k) - \frac{C_2}{k^4}\right). \tag{1.36}$$

Essentially, after removing the high-momentum component of the distribution, the kinetic energy of the system can be calculated by ignoring any correlation between particles in different modes. Given that this formula holds even for very strongly interacting systems, it suggests that the contact completely characterizes the correlations between modes that results from zero-range scattering. The contact has also been shown to relate changes in

the scattering length to changes in the energy of the system

$$\frac{\partial E}{\partial\left(\frac{-1}{a}\right)} \sim C_2 \tag{1.37}$$

as well as to the pressure of a uniform Fermi gas [25],

$$P = \frac{2}{3}\frac{E}{V} + \frac{\hbar^2 C_2}{12\pi a m}. \tag{1.38}$$

Beyond these results first established by Tan, parameters analogous to the contact have been extended to bosonic systems [27, 28], systems in dimension other than 3 [29, 30], higher partial waves [31, 32, 33, 34, 35, 36], finite-range interactions [37, 38], spin systems including spin-orbit coupling [39, 40], and nuclear systems [41, 42, 43, 44, 45]. Due to the proliferation of "contacts," the original quantity defined by Tan has come to be known as the s-wave two-body contact (or Tan's contact), hence C_2. For our analysis here, the bosonic extensions are the most important since they relate directly the the Efimov effect, which we have already discussed. In particular, the three-body contact similarly describes the probability that three particles cluster within a small region and is also related to a sub-leading correction to the asymptotic expansion of the momentum distribution [27]:

$$n(k) - \frac{C_2}{k^4} \sim C_3 \frac{L(k)}{k^5}, \quad k \to \infty, \tag{1.39}$$

where $L(k)$ is a log-periodic function of k. The change in the energy as the Efimov parameter, mentioned in a previous section on the Efimov effect, is varied is also proportional to the three-body contact

$$\frac{\partial E}{\partial \log \kappa^*} \sim C_3. \tag{1.40}$$

The three-body contact has been shown to be related to the the behavior of the wavefunction in regions of configuration space where three or more particles are closely clustered, and Werner and Castin have further shown that the loss rate of particles due to recombination

to deeply bound dimer states is proportional to C_3 [28].

Clearly, the contact plays a central role in characterizing systems with zero-range interactions; therefore, a variety of tools must be developed to investigate this quantity. Within this thesis we will show several methods by which relations involving the contact can be derived, even for systems exhibiting less symmetry than a gas of particles in free space. We will also show how to derive governing equations for the unknown function that appears in the Bethe-Peierls boundary condition and which characterizes short-range correlations and therefore the contact. These equations allow us to determine the contact analytically and numerically for a variety of systems with zero-range interactions.

1.6.1 Measurement of the contact

Because the contact appears in many exact universal relations, several experimental probes of it have been developed and suggested, including measuring pair correlations directly via Bragg spectroscopy, the momentum distribution via time-of-flight photography, and the transition rate between internal states via rf-spectroscopy.

The first verification of the universal relations proposed by Tan and measurement of the two-body contact for a unitary Fermi gas were carried out by the Jin group at JILA. They used time-of-flight imaging, photo emission spectroscopy, and rf spectroscopy to independently measure the single-particle momentum distribution, the disassociation energy within a trap, and the number of atoms transferred to a different internal state by an rf pulse. The measurement of the contact from all three probes agreed to within the precision of the experiment, providing the first measurement of this quantity and verifying two of the universal relations propsed by Tan [46]. The Vale group at Swinburne University instead used Bragg spectroscopy to measure the static structure factor of a Fermi gas, which is the Fourier transform of the two-point correlation function and proportional to the contact. Their measurements near unitarity were consistent with those of the Jin group [47, 48]. One recent approach has suggested that momentum distributions may be measured *in situ*

in the trap via Raman spectroscopy, although challenges remain in applying this technique to strongly interacting systems [49].

Extending beyond the two-component Fermi gas, several groups have measured contact-like parameters in bosonic systems and in spin-polarized systems dominated by p-wave interactions. In weakly interacting BEC as well as the p-wave case, analogous universal relations were observed in both the single particle momentum distribution and the rf transition rate. For strongly interacting bosonic systems, however, the instability of the system complicates measurement, and even at wavenumbers approximately twice the natural scale (set by the density of the gas), the universal scaling of the momentum distribution was not observed. It is also important to note that these experiments also investigated the possibility of sub-leading corrections proportional to contact-like parameters beyond the typical two-body contact, but all measurements were consistent with a value of zero for these additional contacts, though with relatively large errors [50, 51, 35]. However, later work has since shown using Ramsey interferometry that the three-body contact can be measured in strongly interacting bosonic systems and is indeed necessary to accurately predict the properties of the gas [52, 53]. Nevertheless, more work needs to be completed refining experimental procedures and developing new relations where sub-leading corrections to the momentum distribution appear as dominant terms in order to access these parameters.

Part I

Two Bosons Resonantly Interacting with a Plane

CHAPTER 2

UNIVERSAL BOUND STATES BETWEEN TWO PARTICLES AND A SURFACE

A potential that supports a near zero-energy bound state will strongly scattering incoming particles with wavelengths much larger than the characteristic size of the potential. Moreover, potentials with very different shapes but the same energy for this near-threshold bound state have similar scattering properties. These ideas allow extremely complicated interactions to be summarized by simple models that have only a few parameters. Several surprising results, particularly that three identical bosons possess a geometric sequence of three-body bound states and that macroscopic properties like the energy and pressure of a gas are intimately related to particle correlations as small distances, have been discovered and later observed by applying these models to systems of a few or many interacting particles. Applying the same idea to potentials that are generated by a line or a surface rather than a point particle has drawn much less attention, despite the fact that such potentials can be engineered more easily than ever before. In this work, we investigate the consequences of modelling a short-range potential created by a surface as a "zero-range force" imposing the condition that the normal derivative of the wavefunction must vanish at the surface (homogeneous Neumann boundary conditions). We give the bound states of this model and find that even under conditions where two unconstrained atoms would have no low energy bound states, they can nevertheless form states that are bound to the surface. We further investigate the properties of these bound states as a function of the inter-particle scattering length, including the binding energies, the inter-particle Tan's Contact, and a further Contact involving both atoms and the surface which is analogous to the three-body Contact from Efimov physics.

2.1 Boundary Conditions for One Particle Resonantly Interacting with a Plane

To motivate and investigate the use of homogeneous Neumann boundary conditions, consider a single spinless particle of mass m, with position $x = (x_1, x_2, x_3)$, interacting with a planar surface, which we take to be the x_2x_3-plane. Let the surface subject the particle to a potential, $V(x_1)$, (Figure 2.1) which is translationally invariant in the x_2 and x_3 directions, but in the x_1 direction is given by

$$V(x_1) = \begin{cases} \infty & x_1 < 0 \\ V_0(x_1) & 0 < x_1 < x_0 \\ 0 & x_1 > x_0, \end{cases}$$

with $V_0(x_1)$ smooth and therefore bounded on the compact set $[0, x_0]$. One optical method

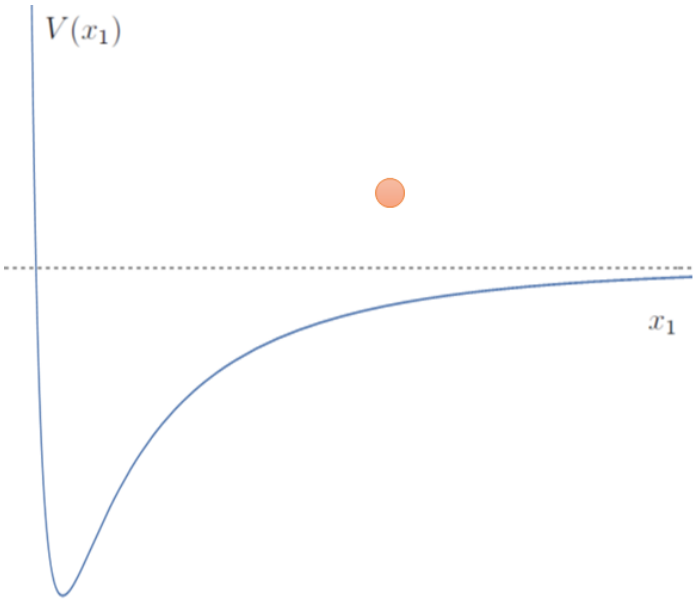

Figure 2.1: Surface potential, $V(x_1)$. The potential should have a "well" so that bound states are possible. It should also increase rapidly at small distance to form a barrier at the origin.

for creating such a potential that interacts with neutral atoms is by using the evanescent

light wave created when a laser beam undergoes total internal reflection from the inner surface of a prism. The exponentially decreasing electric field will polarize neutral atoms, which creates a dipole interaction between the atoms and the field. By using two such beams, both the intensity and the frequency of each beam can be tuned to alter both the depth and the range of the result. The typical size of the potential is roughly in the range that we require, with reported ranges varying from 100-300 nanometers [54, 55]. In this regime, they will be significantly longer-ranged than the nanometer length scale Van der Waals interaction, but not so large that they dwarf a tuned scattering length in size.

The Schrödinger equation is then

$$\hat{H}\Psi(x_1, x_2, x_3) = E\Psi(x_1, x_2, x_3),$$

with the Hamiltonian for this system given by

$$\hat{H} = \frac{\hat{p}_1^2}{2m} + \frac{\hat{p}_2^2}{2m} + \frac{\hat{p}_3^2}{2m} + V(\hat{x}_1),$$

with $\hat{p}_i$ the momentum operator conjugate to $\hat{x}_i$.

Since the potential depends only on the x_1-coordinate, separation of variables

$$\Psi(x_1, x_2, x_3) \equiv \psi(x_1)\phi(x_2, x_3)$$

leads to a free particle description in the directions parallel to the surface, and a one-dimensional equation in the perpendicular direction where the particle is restricted to the half-space $x > 0$:

$$\left(\frac{\hat{p}_{x_2}^2}{2m} + \frac{\hat{p}_{x_3}^2}{2m}\right)\phi(x_2, x_3) = E_{2,3}\,\phi(x_2, x_3),$$
$$\left(\frac{\hat{p}_{x_1}^2}{2m} + V(\hat{x}_1)\right)\psi(x_1) = E_1\,\psi(x_1),$$

with the eigenvalue relation $E = E_{2,3} + E_1$.

From here, our strategy will be to investigate the behavior of the wavefunction and its derivative outside the range of interaction, x_0, with the surface. Then, we will take the limit that the range of interaction goes to 0. However, we will not take this limit with all other aspects of the potential fixed because this would cause the scatting by the potential to become weaker and weaker. Instead, we will take this limit while holding the scattering length, a, between the particle and the surface constant so that the low-energy scattering behavior remains unchanged. The goal will be to arrive at an effective model where the surface potential is completely replaced by a boundary condition at $x_1 = 0$, valid for energy scales $E_1 << \frac{\hbar^2}{mx_0^2}$.

Focusing on the x_1-direction, when $x_1 > x_0$ we have that $V(x_1) = 0$ and so we can represent the solution in this region as a standing wave

$$\psi(x_1) = A \sin\left(k_1 x_1 + \delta(k_1)\right), \tag{2.1}$$

with the coefficient A determined by the choice of normalization for scattering states and $E_1 = \frac{\hbar^2 k_1^2}{2m}$. The scattering phase-shift $\delta(k_1)$ is determined by requiring continuity of the wavefunction and its derivative at $x_1 = x_0$. However, rather than solve the Schrödinger equation and for $x_1 < x_0$ and match at the boundary, instead we take the the scattering length, a, which appears in the effective range expansion (see Section 1.2),

$$k_1 \cot\left(\delta(k_1)\right) = -\frac{1}{a} + \frac{1}{2} r_s k_1^2 + \mathcal{O}(k_1^4), \tag{2.2}$$

as empirically given. Then for $k_1 x_0 \to 0$,

$$\frac{\psi'(x_0)}{\psi(x_0)} = k_1 \cot\left(\delta(k_1)\right) - \left(1 + \cot\left(\delta(k_1)\right)^2\right) k_1^2 x_0 + \mathcal{O}(k_1^3 x_0^2) \tag{2.3}$$

$$= -\frac{1}{a} + \left(\frac{r_s}{2} - x_0\right) k_1^2 + \mathcal{O}\left(\frac{x_0}{a^2}\right) + o(r_s k_1^2). \tag{2.4}$$

Typically, the effective range r_s scales as the range of interaction ($r_s \sim x_0$), which can be seen by noting that the interval of integration in the definition of r_s, Eq. 1.2, goes to zero. Therefore, if the interaction between the surface and the particle is tuned such that $a \to \infty$, then in the limit that $x_0 \to 0$ (and consequently $r_s \to 0$), we have that $\psi'(x_0) \to 0$. Thus for a finite range potential that has been tuned to resonance with the particle ($a \to \pm\infty$), the wavefunction will have a normal derivative of 0 at the boundary. That is, the wavefunction satisfies homogeneous Neumann boundary conditions at the surface.

2.2 Two Particles Resonantly Interacting with a Plane: A Formal Solution

Consider next a system of two particles interacting resonantly with the surface described in the previous section (see Figure 2.2). When a particle approaches the surface and the

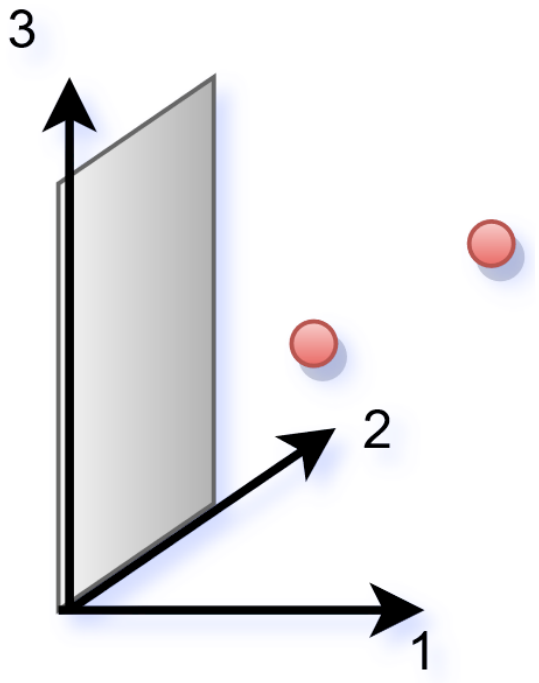

Figure 2.2: Two particles and a resonant surface. By convention, the 1-direction always points perpendicular to the surface while the $2, 3$-directions always point parallel to it.

other particles are far away (compared to the range of interaction), then asymptotically the wavefunction will approximately factorize and obey this Nuemann boundary condition.

Previously, models where the Bethe-Peierls boundary condition (which we introduced in Section 1.2) is enforced in many-particle systems, although it is only exactly valid for two particles, have been studied extensively [10]. We extend in a similar way the homogenous Neumann boundary condition at the surface derived from the one-particle model to the case of two particles. We enforce that this condition should be satisfied by each particle exactly, without respect to the location of the second particle (at least so long as the two particles are not both coincident with the surface; a case which we investigate in Appendix B). Simultaneously, we will model the inter-particle interaction as a zero-range force satisfying the Bethe-Peierls boundary condition. The result is then a model Hamiltonian with two particles that have positions $x = (x_1, x_2, x_3)$ and $y = (y_1, y_2, y_3)$ respectively, and at least when $|x - y| > 0,\ x_1 > 0,\ y_1 > 0$ we have the Schrödinger equation

$$-\frac{\hbar^2}{2m}\Big(\frac{\partial^2}{\partial x_1^2} + \frac{\partial^2}{\partial y_1^2} + \frac{\partial^2}{\partial x_2^2} + \frac{\partial^2}{\partial y_2^2} + \frac{\partial^2}{\partial x_3^2} + \frac{\partial^2}{\partial y_3^2}\Big)\psi(x, y) = E\ \psi(x, y), \tag{2.5}$$

simultaneously subject to the boundary conditions

$$\psi(x, y) = \mathcal{N}\mathcal{A}\Big(\frac{x + y}{2}\Big)\Big(\frac{1}{|x - y|} - \frac{1}{a}\Big) + O(|x - y|),\ \ |x - y| \to 0, \tag{2.6}$$

$$\frac{\partial\psi(x, y)}{\partial x_1}\Big|_{x_1=0} = 0, \quad \frac{\partial\psi(x, y)}{\partial y_1}\Big|_{y_1=0} = 0, \tag{2.7}$$

(with $\mathcal{N}$ a normalization constant) due to both the interparticle zero-range interaction and the zero-range interaction with the surface. As in our model with a single particle, we take the surface to act as an infinite potential whenever at least one particle would be inside the surface and therefore

$$\psi(x, y) \equiv 0, \quad x < 0,\ y < 0. \tag{2.8}$$

The function $\mathcal{A}$ we refer to as the "source distribution" (for reasons that will become more clear later), must be in $C^2(0, \infty)$ so that it can satisfy the Schrödinger Equation and must

also be square-integrable so that the wavefunction is normalizable, but is otherwise as yet undetermined. The source distribution must be chosen appropriately so that all terms within the Bethe-Peierls boundary conditon are indeed satisfied, and we will later accomplish this by finding a singular integral equation that the source distribution must satisfy.

Having developed a Schrödinger Equation valid for $|x - y| > 0$, we seek an extension of this equation that automatically incorporates the behavior dictated by the Bethe-Peierls boundary condition (2.6). Using the coordinates

$$R = (R_1, R_2, R_3),$$
$$r = (r_1, r_2, r_3),$$

$$R_1 = \frac{x_1 + x_2}{2}, \quad R_2 = \frac{y_1 + y_2}{2}, \quad R_3 = \frac{z_1 + z_2}{2},$$
$$r_1 = x_1 - x_2, \quad r_3 = y_1 - y_2, \quad r_3 = z_1 - z_2.$$

The Schrödinger equation is tranformed to

$$-\frac{\hbar^2}{m}\Big(\frac{1}{4}\nabla_R^2 + \nabla_r^2\Big)\psi\left(R + \frac{r}{2}, R - \frac{r}{2}\right) = E\,\psi\left(R + \frac{r}{2}, R - \frac{r}{2}\right)$$

with the notation

$$\nabla_R^2 = \frac{\partial^2}{\partial R_1^2} + \frac{\partial^2}{\partial R_2^2} + \frac{\partial^2}{\partial R_3^2},$$
$$\nabla_r^2 = \frac{\partial^2}{\partial r_1^2} + \frac{\partial^2}{\partial r_3^2} + \frac{\partial^2}{\partial r_3^2}.$$

Note here that since the Hamiltonian is invariant under translations of both the 2nd and 3rd coordinates of the center of mass and there are no boundary conditions to constrain solutions in these directions. The center of mass momentum parallel to the surface will

therefore be conserved. The wavefunction can then be written as

$$\psi\left(R+\frac{r}{2}, R-\frac{r}{2}\right) = e^{iq_2R_2+iq_3R_3}\phi(R_1, r). \tag{2.9}$$

Throughout this chapter, we will work in the center of momentum frame parallel to the surface so that $q_2 = q_3 = 0$, and the source distribution appearing in the Bethe-Peierls boundary condition will depend only on the perpendicular distance of the center of mass from the surface and not the parallel coordinates,

$$\mathcal{A}(R) = \mathcal{A}(R_1). \tag{2.10}$$

Any translational motion of the center of mass parallel to the surface can be recovered after we find a solution by appending any plane wave solutions in the parallel center of mass coordinates to the wavefunctions we show here. One additional important fact about the source distribution is that since it represents the local strength of the interaction between the particles, it must be zero in any region where the particles are forbidden from being and therefore

$$\mathcal{A}(R_1) \equiv 0, \quad R_1 < 0. \tag{2.11}$$

The operator ∇_r^2 acting on the wavefunction in the region described by (2.6) gives zero almost everywhere. But precisely at $r = 0$, where we have collapsed all of the interaction via our limiting procedure, the wavefunction fails to exist as an ordinary function and the action of the Laplacian is not well-defined. However, if we extend the Laplacian in the sense of distributions, then we have that [56]

$$\nabla_r^2\left(\frac{1}{|r|}\right) = -4\pi\delta(r),$$

and so we infer that on the set $r = 0$ we should include a source term in the Schrödinger

equation to cancel this contribution for the distributional Laplacian.

$$\left(-\frac{\hbar^2}{m}\left(\frac{1}{4}\nabla_R^2+\nabla_r^2\right)-\frac{\hbar^2k^2}{2m}\right)\,\psi\left(R+\frac{r}{2},R-\frac{r}{2}\right)=\frac{8\pi\hbar^2}{m}\mathcal{A}(R_1)\delta(r). \tag{2.12}$$

Since the function $\mathcal{A}$ describes the strength of the zero-range interaction, represented by the source term in our Schrödinger equation, we call it the source distribution. The solution of this equation will satisfy the first term in the Bethe-Peierls condition (Eq. 2.6)) by construction; however, for arbitrary $\mathcal{A}$ it will not necessarily satisfy the second term, involving the scattering length. To find sufficient conditions under which the full Bethe-Peierls boundary condition will be satisfied, we will first need to find a formal solution to Eq. (2.12).

In Appendix A we derive the Green's function for our Schrödinger equation and enforce the homogeneous Neumann boundary conditions. The result for the wavefunction is

$$\psi\left(R+\frac{r}{2},R-\frac{r}{2}\right)=\psi_1\left(R+\frac{r}{2},R-\frac{r}{2}\right)+\psi_2\left(R+\frac{r}{2},R-\frac{r}{2}\right) \tag{2.13}$$

where

$$\begin{aligned}\psi_1\left(R+\frac{r}{2},R-\frac{r}{2}\right)\equiv\frac{\mathcal{N}k}{\pi}\int_0^\infty\Bigg[&\frac{K_1(k\sqrt{2R_1^2+\frac{1}{2}((r_1+2x')^2+r_3^2+r_3^2)})}{\sqrt{2R_1^2+\frac{1}{2}((r_1+2x')^2+r_3^2+r_3^2)}}\\&+\frac{K_1(k\sqrt{2R_1^2+\frac{1}{2}((r_1-2x')^2+r_3^2+r_3^2)})}{\sqrt{2R_1^2+\frac{1}{2}((r_1-2x')^2+r_3^2+r_3^2)}}\\&+\frac{K_1(k\sqrt{2(R_1+x')^2+\frac{1}{2}(r_1^2+r_3^2+r_3^2)})}{\sqrt{2(R_1+x')^2+\frac{1}{2}(r_1^2+r_3^2+r_3^2)}}\Bigg]\mathcal{A}(x')\;dx',\end{aligned} \tag{2.14}$$

$$\psi_2\left(R+\frac{r}{2},R-\frac{r}{2}\right)\equiv\frac{\mathcal{N}k}{\pi}\int_0^\infty\frac{K_1(k\sqrt{2(R_1-x')^2+\frac{1}{2}(r_1^2+r_3^2+r_3^2)})}{\sqrt{2(R_1-x')^2+\frac{1}{2}(r_1^2+r_2^2+r_3^2)}}\mathcal{A}(x')\,dx', \tag{2.15}$$

and K_1 is the modified Bessel function of the second kind of order 1. Shortly, the fact that this modified Bessel function has a singularity when its argument approaches zero will be relevant (see Appendix G for relevant properties of this special function).

This formal solution will serve as the starting point for much of our further analysis. It will allow us to derive an integral equation for the unknown source distribution, $\mathcal{A}$ in the next section, and also facilitate our investigation of the momentum distributions of the system in Chapter 3.

2.3 Integral Equation for the Source Distribution

Having found a formal solution to Eq. 2.12 that satisfies the Neumann boundary conditions, it remains to enforce that it also satisfies the Bethe-Peierls condition Eq. 2.6. We must therefore expand our wavefunction for small r, including any singular and r-independent terms.

Lemma 2.1.

$$\psi\left(R+\frac{r}{2},R-\frac{r}{2}\right)=\frac{\mathcal{N}}{|r|}\mathcal{A}(R_1)+\frac{\mathcal{N}k}{\pi}\Lambda(R_1)+\mathcal{O}(|r|),\quad r\to 0,$$

where

$$\Lambda(R_1)\equiv\int_0^\infty\left[2\frac{K_1(k\sqrt{2(R_1^2+x'^2)})}{\sqrt{2(R_1^2+x'^2)}}+\frac{K_1(k\sqrt{2(R_1+x')^2})}{\sqrt{2(R_1+x'^2)}}\right]\mathcal{A}(x')\ dx' + \fint_0^\infty\frac{K_1(k\sqrt{2(R_1-x')^2}}{\sqrt{2(R_1-x')^2}}\mathcal{A}(x')\ dx',$$

and

$$\fint_0^\infty \frac{K_1(k\sqrt{2(R_1-x')^2}}{\sqrt{2(R_1-x')^2}}\mathcal{A}(x')\,dx' = \lim_{\epsilon\to 0}\left[\frac{k}{\pi}\int_0^{R_1-\epsilon}\frac{K_1(k\sqrt{2(R_1-x')^2}}{\sqrt{2(R_1-x')^2}}\mathcal{A}(x')\,dx' + \frac{k}{\pi}\int_{R_1+\epsilon}^\infty \frac{K_1(k\sqrt{2(R_1-x')^2}}{\sqrt{2(R_1-x')^2}}\mathcal{A}(x')\,dx' - \frac{\mathcal{A}(R_1)}{\pi\epsilon}\right]$$

Proof. The ψ_1 term in Eq. 2.13 can be dealt with simply because each term is bounded above by an integrable function as $r \to 0$ and therefore the dominated convergence theorem allows us to interchange the limit and the integral. To see this, note that $\frac{K_1(x)}{x}$ is a monotonically decreasing function of x. Therefore, for all α, δ

$$\frac{K_1\left(\sqrt{(x+\delta)^2+\alpha^2}\right)}{\sqrt{(x+\delta)^2+\alpha^2}} \le \frac{K_1\left(\sqrt{x^2+\alpha^2}\right)}{\sqrt{x^2+\alpha^2}},$$
$$\frac{K_1\left(\sqrt{(x+\delta)^2+\alpha^2}\right)}{\sqrt{(x+\delta)^2+\alpha^2}} \le \frac{K_1\left(\sqrt{(x+\delta)^2}\right)}{\sqrt{(x+\delta)^2}},$$

and the expressions on the right-hand side above are integrable over $\mathbb{R}$, provided that $\alpha > 0$ and $\delta > 0$ respectively. Applying these estimates to ψ_1 gives us

$$\lim_{r\to 0}\psi_1\left(R+\frac{r}{2}, R-\frac{r}{2}\right) = \frac{\mathcal{N}k}{\pi}\int_0^\infty \left[2\frac{K_1(k\sqrt{2(R_1^2+x'^2)})}{\sqrt{2(R_1^2+x'^2)}} + \frac{K_1(k\sqrt{2(R_1+x')^2})}{\sqrt{2(R_1+x'^2)}}\right]\mathcal{A}(x')\;dx'.$$

By contrast, the integrand in ψ_2 has a non-integrable singularity when $r = 0$ and $x' \to$

R_1. So, we will decompose the integration interval $[0, \infty)$ into three pieces,

$$\psi_2\left(R + \frac{r}{2}, R - \frac{r}{2}\right)$$
$$= \frac{\mathcal{N}k}{\pi}\left[\int_{-\infty}^{R_1-\epsilon} + \int_{R_1-\epsilon}^{R_1+\epsilon} + \int_{R_1+\epsilon}^{\infty}\right] \frac{K_1\left(k\sqrt{2(R_1 - x')^2 + \frac{1}{2}r^2}\right)}{\sqrt{2(R_1 - x')^2 + \frac{1}{2}r^2}} \mathcal{A}(x') \ dx'.$$

The same dominated convergence argument applies to the intervals $[0, R_1 - \epsilon)$ and $[R_1 + \epsilon, \infty)$ and so we can move the limit inside the integral there. For the contribution to ψ_2,-

$$\frac{\mathcal{N}k}{\pi} \int_{R_1-\epsilon}^{R_1+\epsilon} \frac{K_1\left(k\sqrt{2(R_1 - x')^2 + \frac{1}{2}r^2}\right)}{\sqrt{2(R_1 - x')^2 + \frac{1}{2}r^2}} \mathcal{A}(x') \ dx', \tag{2.16}$$

when $k\epsilon << 1$ and $kr << 1$, an acceptable approximation to 2.16 is to Taylor expand $\mathcal{A}(x')$ about R_1 and also replace the modified Bessel function with its expansion for small arguments (see Appendix G),

$$\int_{R_1-\epsilon}^{R_1+\epsilon} \frac{K_1(k\sqrt{2(R_1 - x')^2 + \frac{1}{2}r^2})}{\sqrt{2(R_1 - x')^2 + \frac{1}{2}r^2}} \mathcal{A}(x') \ dx' = \frac{\mathcal{A}(R_1)}{k} \int_{R_1-\epsilon}^{R_1+\epsilon} \frac{1}{2(R_1 - x')^2 + \frac{1}{2}|r|^2} \ dx'$$
$$= \frac{2\mathcal{A}(R_1)}{k|r|} \arctan\left(\frac{2\epsilon}{|r|}\right) + \mathcal{O}(\epsilon).$$

With ϵ fixed and $r \to 0$ this reduces to

$$\frac{k}{\pi} \int_{R_1-\epsilon}^{R_1+\epsilon} \frac{K_1(k\sqrt{2(R_1 - x')^2 + \frac{1}{2}r^2})}{\sqrt{2(R_1 - x')^2 + \frac{1}{2}r^2}} \mathcal{A}(x') \ dx' = \mathcal{A}(R_1)\left(\frac{1}{|r|} - \frac{1}{\pi\epsilon}\right) + \mathcal{O}(\epsilon) + \mathcal{O}(r).$$

Recombining the three partitioned intervals for ψ_2 we have that

$$\psi_2\left(R+\frac{r}{2},R-\frac{r}{2}\right)=\mathcal{N}\lim_{\epsilon\to 0}\left[\frac{k}{\pi}\int_0^{R_1-\epsilon}\frac{K_1(k\sqrt{2(R_1-x')^2})}{\sqrt{2(R_1-x')^2}}\mathcal{A}(x')\ dx'\right.$$
$$\left.+\frac{k}{\pi}\int_{R_1+\epsilon}^{\infty}\frac{K_1(k\sqrt{2(R_1-x')^2})}{\sqrt{2(R_1-x')^2}}\mathcal{A}(x')\ dx'-\frac{\mathcal{A}(R_1)}{\pi\epsilon}\right]$$
$$+\mathcal{N}\frac{\mathcal{A}(R_1)}{|r|},$$

and we introduce the notation

$$⨍_0^{\infty}\frac{K_1(k\sqrt{2(R_1-x')^2})}{\sqrt{2(R_1-x')^2}}\mathcal{A}(x')\ dx'\equiv\lim_{\epsilon\to 0}\left[\int_0^{R_1-\epsilon}\frac{K_1(k\sqrt{2(R_1-x')^2})}{\sqrt{2(R_1-x')^2}}\mathcal{A}(x')\ dx'\right.$$
$$+\int_{R_1+\epsilon}^{\infty}\frac{K_1(k\sqrt{2(R_1-x')^2})}{\sqrt{2(R_1-x')^2}}\mathcal{A}(x')\ dx'$$
$$\left.-\frac{\mathcal{A}(R_1)}{k\epsilon}\right].$$

This is an example of a Hadamard Finite Part integral, which is a generalization of the Cauchy Principal Value integral and a regularized version of what would ordinarily be a linearly divergent integral. For functions with no singularities, the Hadamard Finite Part simply reduces to an ordinary integral. Note that this regularization did not arise by starting from a divergent integral and then 'by hand' replacing it with a regularized counterpart; rather, we started from a well-defined convergent integral and discovered that the appropriate limit as $r\to 0$ involves the Hadamard Finite Part.

Combining the results for ψ_1 and ψ_2, we have, as desired,

$$\begin{aligned}\psi\left(R+\frac{r}{2},R-\frac{r}{2}\right) = \frac{\mathcal{N}k}{\pi}\int_0^\infty \Bigg[2\frac{K_1(k\sqrt{2(R_1^2+x'^2)})}{\sqrt{2(R_1^2+x'^2)}} \\ + \frac{K_1(k\sqrt{2(R_1+x')^2})}{\sqrt{2(R_1+x'^2)}}\Bigg]\mathcal{A}(x')\,dx' \\ + \frac{\mathcal{N}k}{\pi}\fint_0^\infty \frac{K_1(k\sqrt{2(R_1-x')^2}}{\sqrt{2(R_1-x')^2}}\mathcal{A}(x')\,dx' \\ + \frac{\mathcal{N}\mathcal{A}(R_1)}{|r|} + \mathcal{O}(r), \quad r\to 0,\end{aligned}$$

□

If we compare the result of Lemma 2.1 with the Bethe-Peierls condition, 2.6, it must simultaneously be true that

$$\begin{aligned}\psi\left(R+\frac{r}{2},R-\frac{r}{2}\right) &= \frac{\mathcal{N}\mathcal{A}(R_1)}{|r|} + \frac{\mathcal{N}k}{\pi}\Lambda(R_1) + \mathcal{O}(|r|), \quad r\to 0, \\ \psi\left(R+\frac{r}{2},R-\frac{r}{2}\right) &= \mathcal{N}\mathcal{A}\left(R_1\right)\left(\frac{1}{|r|}-\frac{1}{a}\right) + O(|r|), \;\; r\to 0.\end{aligned}$$

The terms that diverge as $r\to 0$ match exactly, but we must require that the r-independent terms also match so that our solution satisfied the Bethe-Peierls condition. Therefore we must have

$$\frac{\mathcal{A}(R_1)}{a} = -\frac{k\Lambda(R_1)}{\pi} \tag{2.17}$$

If we substitute in the definition of Λ, we can write the relation more succinctly by making a slight change of notation $\beta\equiv\sqrt{2}k$ and by symmetrically extending the function $\mathcal{A}$ such that,

$$A(x)\equiv\begin{cases}\mathcal{A}(x) & x\geq 0, \\ \mathcal{A}(-x) & x<0.\end{cases} \tag{2.18}$$

Finally, then we have the integral equation

$$\boxed{\neq\!\!\!\!\!\int_{-\infty}^{\infty}\left[\frac{K_1(\beta|R_1-x'|)}{|R_1-x'|}+\frac{K_1(\beta\sqrt{R_1^2+x'^2})}{\sqrt{R_1^2+x'^2}}\right]A(x')\ dx'=-\frac{2\pi}{\beta a}A(R_1).} \tag{2.19}$$

This integral equation, which we refer to as the position-space integral equation because its solution can be used to calculate the position-space representation of the wavefunction, is a significant milestone for this problem because it is a single relationship that when satisfied guarantees that our solution, Eq 2.13, satisfies the Schrödinger equation, the homogeneous Neumann boundary conditions, and the Bethe-Peierls boundary condition.

Because this integral equation for the source distribution contains a Hadamard finite part, it is classified as a second kind hypersingular integral equation [57]. Such integral equations arise somewhat regularly in many fields that deal with scattering and radiation, including fracture dynamics [58], acoustics [59], and electrodynamics [60], but are not particularly well-studied beyond numerical solutions.

For the remainder of this chapter, we will give analytical solutions of this integral equation in several special cases

- At distances close to the surface, $(\beta R_1 << 1)$,
- At unitarity ($a = \pm\infty$), and
- At the free breakup threshold ($\beta = 0$, a finite).

We will finish by deriving and carrying out a numerical solution to find the binding energies at arbitrary scattering length.

2.3.1 Solution near the surface

Our first task is to investigate the behavior of the source distribution near the surface of the plane. We expect from experience with the Efimov effect that this behavior will be important for future analysis. Using the results of Appendix B, we find that at small values

of R_1, the asymptotic expansion for A begins

$$A(R_1) \sim \alpha_0^+ R_1^{is_0} + \alpha_0^- R_1^{-is_0} + \mathcal{O}(R_1^{s_1}), \quad R_1 \to 0, \tag{2.20}$$

where s_0 is the only positive real solution to the transcendental equation

$$s_0 \sinh\left(\frac{\pi s_0}{2}\right) - 1 = 0. \tag{2.21}$$

$A(R_1)$ therefore fails to be analytic at $R_1 = 0$, which we can see by differentiating term-by-term,

$$A'(R_1) \sim is_0 \left(\alpha_0^+ R_1^{is_0 - 1} - \alpha_0^- R_1^{-is0-1}\right),$$

which clearly diverges as $R_1 \to 0$. The non-analytic behavior of A will have consequences for later analysis, both as we seek a solution to our integral equation and for further asymptotic results in a later chapter. From this expansion and the proportionality between A and the wavefunction given by the Bethe-Peierls boundary condition, Eq. 2.6, we can calculate the probability current in the R_1 direction as two particles approach the surface ($R_1 \to 0$). It is given by

$$\psi^* \, \partial_{R_1} \psi - \psi \, \partial_{R_1} \psi^* \propto -\frac{2s_0}{R_1} \left(|\alpha_0^-|^2 - |\alpha_0^+|^2\right), \quad R_1 \to 0. \tag{2.22}$$

The current is therefore singular as $R_1 \to 0$, probability will escape through the plane, and the model will fail to be self-adjoint, unless we impose the condition

$$|\alpha_0^-|^2 = |\alpha_0^+|^2,$$

so that Eq. 2.22 is then zero. If we rewrite the coefficients in the asymptotic expansion, Eq. 2.20, in terms of a real amplitude $|\alpha|$ and real phases ϕ_+ and ϕ_-

$$\alpha_0^+ \equiv |\alpha| e^{i\phi_+},$$
$$\alpha_0^- \equiv |\alpha| e^{i\phi_-},$$

then we can rearrange the asymptotic expansion Eq. 2.20 so that it is written in terms of the new length scale, x_0,

$$A(R_1) = 2|\alpha|\, e^{\frac{i(\phi_- + \phi_+)}{2}}\, \sin\left(s_0 \log\left(\frac{R_1}{x_0}\right)\right) + \mathcal{O}(x), \tag{2.23}$$

where

$$x_0 \equiv exp\left(-\frac{\pi + \phi_+ - \phi_-}{2s_0}\right). \tag{2.24}$$

It is well-known in the Efimov effect that there is a three-body parameter, entering as a similar length scale, that is required for the model to be self-adjoint but not fixed within the zero-range approximation [61, 62], and so the appearance of the surface parameter, x_0, is not entirely unexpected. The Efimov three-body parameter specifies the relative phase between incoming and outgoing waves during a collision of three particles, just as our surface parameter, x_0, specifies the relative phase of incoming and outgoing waves when two particles collide with the surface. In our model, x_0 is a free parameter, but we expect that just as the details of the three-body interaction specify the Efimov three-body parameter, the details of the interactions between our particles and the surface specify x_0 in a physical system. We cannot show this in our model; however, because we have replaced the details of the surface interaction with the Neumann boundary condition.

The choice of a particular surface parameter corresponds to a self-adjoint extension of our Hamiltonian. Because more than one choice of x_0 is possible (in fact, infinitely many are possible), the Hamiltonian is not essentially self-adjoint and the value of observables

will depend on the particular self-adjoint extension that we choose. This is not a significant barrier for our analysis; however, because we can give results for the scattering lengths and binding energies in terms of β_0, which will be defined later (Eq 2.35) and is determined solely by x_0. In addition, we will show that the choice of x_0 affects only the overall scale of the bound states that we will find, and the ratio of adjacent binding energies is independent of x_0. We also note that x_0 does not appear explicitly in our integral equation Eq. 2.19 and so when we find a family of solutions in Section 2.3.2, every member will not necessarily be a solution to any particular self-adjoint extension and we must determine which solutions belong to which self-adjoint extension.

Note, however, that not every choice for x_0 leads to a unique self-adjoint extension. In fact, the rescaling

$$x_0 \to x_0 e^{\frac{n\pi}{s_0}}, \quad n \in \mathbb{Z} \tag{2.25}$$

alters the relation Eq. 2.23 at most by an overall factor of -1, which is an irrelevant change of global phase for the wavefunction. There is, therefore, an equivalence relation on the possible choices for x_0 whereby two choices are equivalent if they are related by the transformation Eq. 2.25. The same behavior has been observed as a limit cycle in the renormalization group flow of effective field theories describing the Efimov effect [63, 64, 65].

In our future analysis, we will regularly refer back to the asymptotic behavior Eq. 2.20 as well as the length scale x_0 because they allow us to connect the particle-surface interaction to other aspects of the problem.

2.3.2 Solution at unitarity ($a = \pm\infty$)

When the scattering length diverges, the right-hand side of our integral equation Eq. 2.19 becomes zero and we find that A satisfies

$$\fint_0^\infty \left[\frac{K_1(\beta|R_1 - x'|)}{|R_1 - x'|} + \frac{K_1(\beta(R_1 + x'))}{R_1 + x'} + 2\frac{K_1(\beta\sqrt{R_1^2 + x'^2})}{\sqrt{R_1^2 + x'^2}} \right] A(x') \; dx' = 0. \tag{2.26}$$

Lemma 2.2. *The solutions of Eq. 2.26 are given by*

$$A(R_1) \propto K_{is_0}\left(\beta_0 R_1 e^{-\frac{n\pi}{s_0}}\right), \quad n \in \mathbb{Z}, \quad n \in \mathbb{Z},$$

with

$$\beta_0 \equiv \frac{2}{x_0} e^{-\frac{1}{s_0}\arg(\Gamma(1-is_0))}$$

Proof. In light of both the solution of the radial equation for the Efimov trimer [66], and the expression for the wavefunction given by Tan [30], we attempt the ansatz

$$A(R_1) \propto K_{is}(\beta R_1), \tag{2.27}$$

with s a complex number that will be determined later. We must have that $-1 < \mathrm{Im}(s) < 1$, otherwise $A(R_1)$ will have a non-integrable singularity as $R_1 \to 0$ and the wavefunction will not exist anywhere according to Eq. 2.13.

We substitute the ansatz, Eq. 2.27, into the left-hand side of the integral equation, 2.26, and apply the following identities

$$\int_0^\infty x^{\mu-1}(x+b)^{-\mu} K_\mu(x+b) K_\nu(x)\, dx = \frac{\sqrt{\pi}\,\Gamma(\mu+\nu)\Gamma(\mu-\nu)}{2^\mu \Gamma(\mu+\frac{1}{2})} \frac{K_\nu(b)}{b^\mu}, \tag{2.28}$$

$$\int_0^\infty x^{\mu-1}|x-b|^{-\mu} K_\mu(|x-b|) K_\nu(x)\, dx = \frac{\Gamma(\frac{1}{2}-\mu)\Gamma(\mu+\nu)\Gamma(\mu-\nu)\cos\pi\nu}{\sqrt{\pi}(2b)^\mu} K_\nu(b). \tag{2.29}$$

$$\int_0^\infty 2\frac{K_1(\beta\sqrt{R_1^2+x'^2})}{\sqrt{R_1^2+x'^2}} K_{is}(\beta x')\, dx' = \frac{\pi\ \mathrm{sech}(\frac{\pi s}{2})}{\beta R_1} K_{is}(\beta R_1) \tag{2.30}$$

Eqs. 2.28 and 2.29 are Eq. 6.582 and a corrected version of Eq. 6.583 from Gradshteyn and Ryzhik's *Table of Integrals, Series, and Products, 8th Edition* [67]. We show in Appendix C how we have corrected their Eq. 6.583. We have also calculated Eq. 2.30 by the same Fourier tranform methods as shown in Appendix C. Applying these identities to our case of $\mu = 1,\ \nu = is,\ b = R_1$ and summing the three contributions, we find that s must satisfy

$$\operatorname{sech}\left(\frac{\pi s}{2}\right) - s\tanh\left(\frac{\pi s}{2}\right) = 0, \tag{2.31}$$

for our ansatz to satisfy the integral equation. There is only a single pair of real solutions, $s = \pm s_0$, with $s_0 \approx 0.7201977502$. Because the modified Bessel functions of the second kind, K_ν, are symmetric when $\nu \to -\nu$, the positive and negative solutions to Eq. 2.31 correspond to the same A, and so we consider only the positive value. There are additional complex solutions to Eq. 2.31, but they all have $|\mathrm{Im}(s)| > 1$ and thus would lead to a divergent expression for the wavefunction when substituted into Eq. 2.13. Therefore we conclude that at unitarity,

$$A(R_1) \propto K_{is_0}(\beta R_1), \tag{2.32}$$

consistent both with the analysis in Appendix B and the wavefunction found by Tan [30].

At this point, we have made no restriction on the allowed values of β for solutions at unitarity. It therefore seems that β is arbitrary and a continuous scaling symmetry exists, allowing for a bound state at any value of β. However, we must determine which values of β lead to solutions consistent with our earlier choice of self-adjoint extension via the surface parameter, x_0.

If we perform an expansion of the solution Eq. 2.32 as small R_1, we find that

$$A(R_1) \sim \left(2^{-1-is_0}\beta^{is_0}\Gamma(-is_0)\right)\ x^{is_0} + \left(2^{-1+is_0}\beta^{-is_0}\Gamma(is_0)\right)\ x^{-is_0} + \mathcal{O}(x), \quad x \to 0. \tag{2.33}$$

Comparing this to the small distance expansion for A in terms of x_0, Eq. 2.23, the two agree only if

$$\beta = \frac{2}{x_0} e^{-\frac{1}{s_0}\arg\left(\Gamma(1-is_0)\right)}. \tag{2.34}$$

Therefore, β is not arbitrary in our solution, but rather is fixed by x_0. However, recall that in Section 2.3.1 we showed that each x_0 is one representative from a set of equivalent x_0, $\left\{x_0 e^{\frac{n\pi}{s_0}} \;\middle|\; n \in \mathbb{Z}\right\}$, all of which lead to the same self-adjoint extension and identical

physics. We call the β determined by the representative x_0,

$$\beta_0 \equiv \frac{2}{x_0} e^{-\frac{1}{s_0}\arg\left(\Gamma(1-is_0)\right)}. \tag{2.35}$$

By iterating through all of the equivalent values of x_0, we find a family of allowable solutions at unitarity for this self-adjoint extension,

$$A(R_1) \propto K_{is_0}\left(\beta_0 R_1 e^{-\frac{n\pi}{s_0}}\right), \quad n \in \mathbb{Z}. \tag{2.36}$$

□

The binding energies at unitarity therefore form a geometric sequence,

$$\frac{E_{n+1}}{E_n} = e^{2\pi/s_0}. \tag{2.37}$$

Notice that this ratio is independent of x_0 and thus independent of which self-adjoint extension we choose. Knowing the solution of our integral equation, we can completely characterize the collective bound states at unitarity and extract any useful quantities, for example the contacts or the spatial distribution of the particles. The exact solution at unitarity also gives a robust check for comparison with our later numerical results.

2.3.3 Solution at zero binding energy

Next, we investigate the possibility that for some finite value of the scattering length, the lowest-lying collective bound state may become unbound, and its binding energy go to zero. When taking the limit $\beta \to 0$ with a remaining finite in Eq. 2.19, the kernel of the integral equation simplifies greatly, since for any fixed values of R_1 and x', the arguments of the Bessel functions become small. We can write the reduced integral equation as

$$⨍_0^\infty \left(\frac{1}{(R_1 - x')^2} + \frac{2}{R_1^2 + x'^2} + \frac{1}{(R_1 + x')^2}\right) A(x')\, dx' = -\frac{2\pi}{a} A(R_1). \tag{2.38}$$

Because the kernel of the reduced integral equation is now a homogeneous function of degree -2, we expect a Mellin-type representation of $A(R_1)$ will be useful and may reveal scaling behavior,

$$X(\nu) \equiv \int_0^\infty A(x) \left(\frac{x}{|a|}\right)^{-\nu-1} dx, \tag{2.39}$$

$$A(x) = \frac{1}{2\pi i} \int_{c-i\infty}^{c+i\infty} X(\nu) \left(\frac{x}{|a|}\right)^{\nu} d\nu, \tag{2.40}$$

where $c < 0$ so that we perform the inversion integral within the domain of analyticity of $X(\nu)$ [68]. Plugging this expression into Eq. 2.38 and doing the integral over x' we have that

$$\begin{aligned} \frac{\pi}{2\pi i} \int_{c-i\infty}^{c+i\infty} \left(\sec\left(\frac{\pi\nu}{2}\right) + \nu \tan\left(\frac{\pi\nu}{2}\right)\right) X(\nu) \frac{x'^{\nu-1}}{|a|^\nu} \, d\nu \\ = -\frac{2\pi}{a} \frac{1}{2\pi i} \int_{c-i\infty}^{c+i\infty} X(\nu) \left(\frac{x'}{|a|}\right)^{\nu} d\nu. \end{aligned}$$

So long as $X(\nu)$ has no poles between $\mathrm{Re}(\nu) = c$ and $\mathrm{Re}(\nu) = c-1$, we are free to displace the contour to the left on the right-hand side of the above equation. Since $A(x)$ must at least be decaying for large x, we take c to be a small negative value, say $-1 < c < 0$ to avoid crossing any poles that might arise due to this large x behavior [69]. We then relabel $\nu \to \nu - 1$ to write

$$\begin{aligned} \int_{c-i\infty}^{c+i\infty} \left(\sec\left(\frac{\pi\nu}{2}\right) + \nu \tan\left(\frac{\pi\nu}{2}\right)\right) X(\nu) \frac{x'^{\nu-1}}{|a|^\nu} \, d\nu \\ = -\frac{2}{a} \int_{c-i\infty}^{c+i\infty} X(\nu-1) \left(\frac{x'}{|a|}\right)^{\nu-1} d\nu, \end{aligned}$$

which is satisfied for negative scattering lengths when we have

$$\frac{1}{2}\left[\sec\left(\frac{\pi\nu}{2}\right) + \nu \tan\left(\frac{\pi\nu}{2}\right)\right] X(\nu) = X(\nu-1), \qquad a < 0. \tag{2.41}$$

To solve this functional relation, we apply an idea pioneered by Gogolin, Mora, and Egger [23]. We use a well-known result of complex analysis, Hadamard's strengthening of the Weierstrass Factorization Theorem [70, 71], which says that any meromorphic function can be written as an product of factors where each pole and each zero of the function contributes exactly one factor to the product. We will use this result to write

$$\frac{1}{2}\left(\sec\left(\frac{\pi\nu}{2}\right)+\nu\tan\left(\frac{\pi\nu}{2}\right)\right)=-\frac{1}{2}\prod_{p=0}^{\infty}\frac{(2p+1)^2}{|u_p|^2}\frac{u_p^2-\nu^2}{b_p^2-\nu^2}, \tag{2.42}$$

with $b_p \equiv 2p+1$ and the u_p are the complex solutions (sorted by ascending absolute value) to the transcendental equation

$$z(u) \equiv 1 + u\sin\frac{\pi u}{2} = 0,$$

The details of constructing 2.42 are given in Appendix F. This factorization is helpful because it replaces the trigonometric factor in Eq. 2.41 with a product of polynomials in ν. We can then solve a well-known functional relation for each polynomial factor separately and then multiply the solutions for all factors together to find X.

Solving the functional relation Eq. 2.41 for X requires that we be able to solve three more elementary functional relations:

$$f_p(\nu-1) = (u_p^2-\nu^2)f_p(\nu), \tag{2.43}$$

$$g_p(\nu-1) = (\nu^2-u_p^2)g_p(\nu), \tag{2.44}$$

$$h_p(\nu-1) = \frac{1}{b_p^2-\nu^2}h_p(\nu). \tag{2.45}$$

Eqs. 2.43 and 2.44 are functional relations for factors coming from the numerator of Eq. 2.42, while Eq. 2.45 corresponds to relations involving the denominator of 2.42. We can

write the corresponding solutions as:

$$f_p(\nu) = \frac{\Gamma(u_p - \nu)}{\Gamma(1 + u_p + \nu)} \tag{2.46}$$

$$g_p(\nu) = \Gamma(-u_p - \nu)\Gamma(u_p - \nu) \tag{2.47}$$

$$h_p(\nu) = \frac{\Gamma(1 + b_p + \nu)}{\Gamma(b_p - \nu)} \tag{2.48}$$

We will use the partial solutions, f_p, g_p, h_p to construct the solution, X, of Eq. 2.41. There is one functional relation involving each u_p and each b_p in Eq. 2.42. For each factor involving u_p in Eq. 2.42, we must make a choice of whether to include a factor f_p or a factor g_p (and the associated minus sign) in X. We must include at least one factor of g_p in X to fulfil the functional relation, but could potentially include further pairs of g_p, because the pair of minus signs will have no effect on whether our product satisfies Eq. 2.41. Our choice must be consistent, however, with the earlier choices to take $-1 < c < 0$ and that $X(\nu)$ should have no singularities between $\mathrm{Re}(\nu) = c$ and $\mathrm{Re}(\nu) = c - 1$. The f_p have no poles for $\mathrm{Re}(\nu) < 0$; however, the g_p have poles at $\nu = -u_p + n$ with $n \in \mathbb{N}$. For each p, the pole of g_p at $\nu_p = -u_p + \lfloor u_p \rfloor$ will satisfy $-1 < \mathrm{Re}(\nu_p) < 0$ and the pole at $\nu_{p-1} = -u_p + \lfloor u_p - 1 \rfloor$ will satisfy $-2 < \mathrm{Re}(\nu_{p-1}) < -1$. The two poles are a distance of 1 apart along the real axis and none of the u_p are integers. Therefore, unless $\lfloor u_p - 1 \rfloor \notin \mathbb{N}$, there can be no strip of width 1 within $-2 < \mathrm{Re}(\nu) < 0$ where g_p has no poles. But, $\lfloor u_p - 1 \rfloor \notin \mathbb{N}$ is satisfied only for $p = 0$. Therefore for all u_p with $p > 0$ we include a factor f_p in X, but for $p = 0$ we use g_p to accommodate the minus sign in the Weierstrass product.

$X(\nu)$ can then be written as

$$X(\nu) = g_0(\nu)h_0(\nu)2^{\nu+\frac{1}{2}}|u_0|^{2\nu+1}\prod_{p=1}^{\infty}\lambda_p f_p(\nu)h_p(\nu).$$

where the λ_p must be chosen so that the infinite product converges. All of our functional

relations are homogeneous, therefore we have complete freedom to choose the λ_p. We must have, then,

$$\lim_{p\to\infty} \lambda_p f_p(\nu) h_p(\nu) = 1.$$

Considering the behavior of f_p and h_p at large p,

$$f_p(\nu)h_p(\nu) = \frac{b_p^{2\nu+1}}{u_p^{2\nu+1}} + \mathcal{O}\left(\frac{1}{p^2}\right),$$

and therefore we satisfy the necessary condition for convergence if we choose

$$\lambda_p = \frac{u_p^{2\nu+1}}{b_p^{2\nu+1}}$$

Combining these elements, our solution is then

$$X(\nu) = g_0(\nu)h_0(\nu)2^{\nu+\frac{1}{2}}|u_0|^{2\nu+1}\prod_{p=1}^{\infty}\frac{u_p^{2\nu+1}}{(2p+1)^{2\nu+1}}f_p(\nu)h_p(\nu).$$

From the general properties of the Mellin transform which relate the residues of $X(\nu)$ to the asymptotic expansion of $A(x)$ for small or large x [69], we find that

$$A(R_1) \sim \frac{\text{Res}(X(\nu), is_0)}{|a|^{-is_0}}R_1^{is_0} + \frac{\text{Res}(X(\nu), -is_0)}{|a|^{is_0}}R_1^{-is_0} + \mathcal{O}(R_1), \quad R_1 \to 0. \tag{2.49}$$

When $\nu \to is_0$ all of the factors in $X(\nu)$ are regular, except for $g_0(\nu)$, which is proportional to $\Gamma(is_0 - \nu)$. So, we can find the residue according to

$$\begin{aligned}\text{Res}(X(\nu), is_0) = &-\frac{\Gamma(-2is_0)\Gamma(2+is_0)}{\Gamma(1-is_0)}2^{\nu+\frac{1}{2}}|u_0|^{2\nu+1} \\ &\times\prod_{p=1}^{\infty}\frac{(2p+1)^{-2\nu-1}}{u_p^{-2\nu-1}}\frac{\Gamma(u_p - is_0)\Gamma(1+b_p+is_0)}{\Gamma(b_p-is_0)\Gamma(1+u_p+is_0)}.\end{aligned} \tag{2.50}$$

We have already checked the necessary condition for convergence of our infinite product, and now we must develop an approximate representation of the u_p to check sufficiency.

The main difficulty is that we have no algebraic representation of the u_p, and to overcome this we will use the Newton-Raphson method to find an approximate algebraic form for the u_p. This method finds a root by starting at an initial guess, linearizing the function we are finding a root of about that initial guess, and then computing where the linearized function is zero. The linearized zero becomes the new guess for the location of the true root and the process repeats. When u is large, $1 + u \sin \frac{\pi u}{2} = 0$ only when the sine function is small, and therefore $u \approx 2p$, $p \in \mathbb{Z}$. We use this as an initial guess, and in Apprendix E we prove the following necessary results:

- Within each interval $u \in [2p-1, 2p+1],\ p \in \mathbb{N}^+$, z(u) has exactly 1 zero
- The Newton-Raphson method with initial guess $u_{p,0} = 2p$ applied to $z(u) = 0$ converges to the unique zero of z(u) in $[2p-1, 2p+1],\ \forall p \in \mathbb{N}^+$
- Every real, positive zero of z(u), u_p, is given by

$$\begin{aligned} u_p &= 2p - \frac{z(2p)}{z'(2p)} + \mathcal{O}(p^{-3}) \\ &= 2p - \frac{(-1)^p}{\pi p} + \mathcal{O}(p^{-3}), \end{aligned} \tag{2.51}$$

  and

$$|u_p - 2p| = |\epsilon_p| \leq \frac{2}{\pi p}. \tag{2.52}$$

To check the convergence, consider

$$\begin{aligned} \left| \prod_{p=1}^{\infty} \frac{(2p+1)^{-2is_0-1}}{u_p^{-2is_0-1}} \frac{\Gamma(u_p - is_0)\Gamma(2+2p+is_0)}{\Gamma(1+2p-is_0)\Gamma(1+u_p+is_0)} \right| &= \prod_{p=1}^{\infty} \frac{u_p}{2p+1} \left| \frac{2p+1+is_0}{u_p+is_0} \right| \\ &\leq \sqrt{\prod_{p=1}^{\infty} \left(1 + \frac{s_0^2}{(2p+1)^2}\right)} \\ &= \left(\frac{\cosh\left(\frac{\pi s_0}{2}\right)}{1+s_0^2} \right)^{\frac{1}{2}}, \end{aligned}$$

which is finite and therefore the product converges.

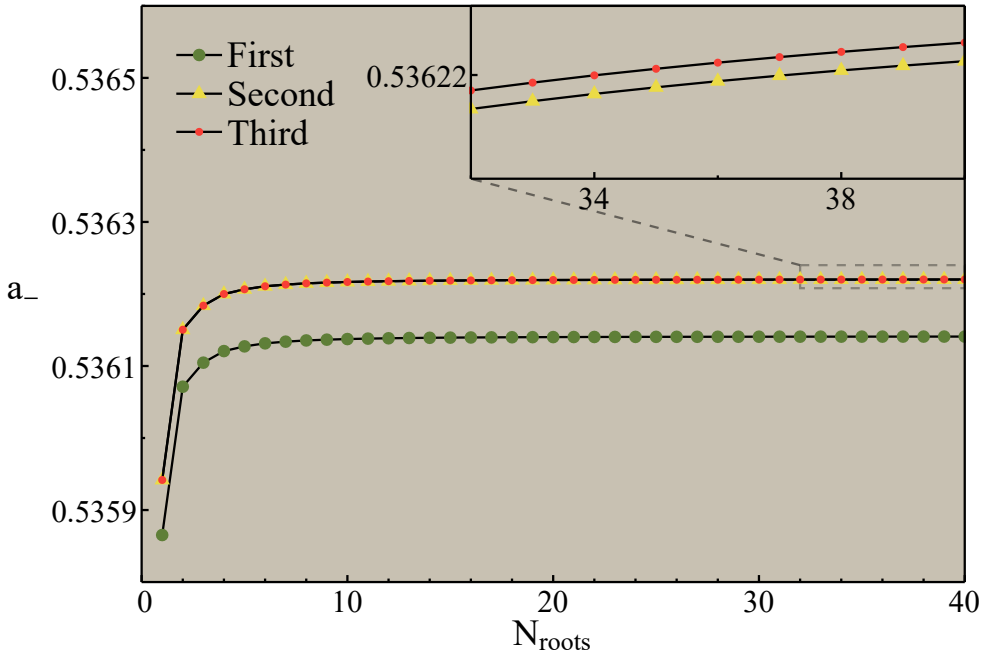

Figure 2.3: Numerical estimate of the critical negative scattering length as a function of the number of roots included in the product at each iteration of the Newton-Raphson method. The product converges rapidly as the number of roots increases. First, second, and third refer to the number of iterations of the Newton-Raphson method used to approximate each root after the initial guess. At the scale of this plot, further iterates are visually indistinguishable for the third iteration.

Table 2.1: The calculated critical negative scattering length at each iteration of the Newton-Raphson approximation to the set of roots. As the number of iterations increases, the calculated critical negative scattering length converges rapidly to more than 10 digits of precision at 5 iterations.

Iterations	Critical Scattering Length
0	-0.5371773089
1	-0.5361410951
2	-0.5362202918
3	-0.5362203454
4	-0.5362203454
5	-0.5362203454

Returning then to the residue, Eq. 2.50, we apply the Newton-Raphson technique with initial guess $u_p \approx 2p$ to calculate the location of the first M roots. We use these approximate roots to calculate a finite approximation of Eq. 2.50, increasing M until the result converges to at least 10 digits of precision. Generally this requires including roughly the first 10,000 factors of Eq. 2.50. The convergence of this process is shown in Figure 2.3.

Next, we compute the next Newton-Raphson iteration of each root and repeat the process until our final estimate of the critical scattering length has converged to at least 10 digits of precision. Table 2.1 shows the calculated critical scattering length from the initial Newton-Raphson guess through five iterations, which is sufficient for our desired precision.

Substituting the fully converged value into the asymptotic expansion Eq. 2.49 and comparing with Eq. 2.23, we find that

$$x_0 = \exp\left(\frac{1}{s_0}\arctan\left(\frac{\cos\left(\arg\left(\mathrm{Res}(X(\nu), is_0)\right) - s_0\log|a|\right)}{\sin\left(\arg\left(\mathrm{Res}(X(\nu), is_0)\right) - s_0\log|a|\right)}\right) - \frac{n\pi}{s_0}\right) \tag{2.53}$$

$$\approx 0.7111864418|a|, \tag{2.54}$$

and finally using Eq. 2.35 to re-express the critical scattering length at which the collective binding energy vanishes in terms of the binding wavenumber at unitarity, β_0,

$$\frac{1}{|a|} \approx 0.5362203454\ \beta_0. \tag{2.55}$$

Recall from Section 2.3.2 that there is an infinite sequence of bound states at unitarity with binding wavenumbers

$$\beta = \beta_0 e^{\frac{n\pi}{s_0}}, \quad n \in \mathbb{Z},$$

and therefore there is an infinite sequence of critical negative scattering lengths at which each of these bound states disappears into the continuum of two free atoms.

The solution at zero energy is somewhat more cumbersome to use than that at unitarity. Still, with enough effort we can extract any quantity of interest about the collective bound states at threshold. Having a precise value for the critical negative scattering length also helps greatly with the numerical solution we will carry out later because it defines the window in which a single bound state exists. Knowing these values precisely also allows for a detailed comparison with experiment, which can facilitate measurement of new quantities, since the corrections to the universal results are themselves typically related to a few well-known parameters (for example, the Efimov width, the s-wave effective range, etc.).

2.4 Numerical Solution at Arbitrary Scattering Length

2.4.1 Recasting the integral equation with a sequence of integral transforms

Although we have successfully found analytical solutions in some important limiting cases, at arbitrary scattering length we must construct a solution numerically. However, the kernel of the integral equation presents complications for any attempt to discretize the problem and seek a numerical solution. Most obviously, there is a quadratic singularity in the kernel and so any choice of quadrature points must be made carefully so that the naive divergences are cancelled appropriately to compute the regularized integral. But the point $x' = R_1$ also involves a logarithmic singularity, further complicating the choice of quadrature points. Rather than develop a more sophisticated rule to handle this unusual scenario, we will instead rewrite this integral equation via a series of integral transforms. The result will convert this equation to one that, although still unusual, contains only simple poles at fixed

values so that a simple numerical scheme suffices to achieve very high accuracy.

Lemma 2.3. *Applying the integral transform*

$$A(x) = \frac{\beta}{\pi^2} \int_0^\infty \widetilde{f}(s) \cosh\left(\frac{\pi s}{2}\right) K_{is}(\beta x)\, ds, \tag{2.56}$$

the integral equation Eq. 2.19 is transformed to

$$\left(1 - \frac{1}{s \sinh \frac{\pi s}{2}}\right) \widetilde{f}(s) = \frac{1}{\beta a} \int_{-\infty}^\infty \widetilde{f}(s')\, \mathit{sech}\left(\frac{\pi(s-s')}{2}\right)\, ds'. \tag{2.57}$$

Remark. *The primary benefit of this transform is that the kernel of Eq. 2.57 is smooth and exponentially decaying.*

Proof. To remove the quadratic divergence in the integrand, we first make a Fourier transform according to

$$A(x) = \frac{1}{2\pi} \int_{-\infty}^\infty \widetilde{A}(k') e^{ik'x}\, dk'.$$

substituting this into (2.19) and integrating requires the results

$$\begin{aligned}
&\int_{-\infty}^\infty \frac{K_1(\beta\sqrt{x'^2 + R_1^2})}{\sqrt{x'^2 + x^2}} e^{ik'x'}\, dx' = \frac{\pi}{\beta|x|} e^{-\sqrt{k'^2+\beta^2}|x|}, \\
&\int_{-\infty}^\infty \frac{K_1(\beta|x - x'|)}{|x - x'|} e^{ik'x'}\, dx' = -\frac{\pi}{\beta}\sqrt{k'^2 + \beta^2} e^{ik'x}, \\
&\int_{-\infty}^\infty \frac{e^{-\sqrt{k'^2+\beta^2}|x|}}{|x|} e^{-ikx}\, dx = -\ln\left(k^2 + k'^2 + \beta^2\right),
\end{aligned}$$

and leads to the representation of our integral equation in momentum space

$$\frac{1}{2\pi} \int_{-\infty}^\infty \ln\left(k'^2 + k^2 + \beta^2\right) \widetilde{A}(k')\, dk' = \left(\frac{2}{a} - \sqrt{k^2 + \beta^2}\right) \widetilde{A}(k). \tag{2.58}$$

Next, we make a one-to-one change of variables and relabel the unknown function accord-

ing to

$$k \equiv \beta \sinh\theta,$$
$$\widetilde{A}(k) \equiv \frac{f(\text{arcsinh}(\frac{k}{\beta}))}{\sqrt{1+\frac{k^2}{\beta^2}}}.$$

This gives an integral equation for $f(\theta)$,

$$\frac{1}{2\pi}\int_{-\infty}^{\infty} \ln\left(\sinh^2\theta' + \sinh^2\theta + 1\right) f(\theta')\, d\theta' = \left(\frac{2}{\beta a \cosh\theta} - 1\right) f(\theta). \tag{2.59}$$

Trading the term $\widetilde{A}(k)\sqrt{k^2+\beta^2}$ for a product term $\frac{2}{\beta a \cosh\theta} f(\theta)$ has the advantage that the function depending explicitly on θ is smooth and exponentially decaying, and so its Fourier transform, which becomes the kernel of a convolution, will be smooth and exponentially decaying as well. With that in mind, along with the identity that

$$\log\left(1+\sinh^2\theta+\sinh^2\theta'\right) = \log\left(\cosh\left(\theta-\theta'\right)\right) + \log\left(\cosh\left(\theta+\theta'\right)\right),$$

we make use of the convolution and cross-correlation theorems to again apply a Fourier transform according to

$$f(\theta) = \frac{1}{2\pi}\int_{-\infty}^{\infty} e^{is\theta}\widetilde{f}(s)\, ds.$$

The result is

$$\widetilde{f}(s) - \frac{1}{2s\sinh\frac{\pi s}{2}}\widetilde{f}(s) - \frac{1}{2s\sinh\frac{\pi s}{2}}\widetilde{f}(-s) = \frac{1}{\beta a}\int_{-\infty}^{\infty}\widetilde{f}(s')\,\text{sech}\left(\frac{\pi(s-s')}{2}\right)\, ds'.$$

Because $A(x)$ is a real and even function of x, $\widetilde{A}(k)$ is also real and even. Thus, $f(\theta)$ is real and even by extension and so is $\widetilde{f}(s)$, therefore,

$$\left(1 - \frac{1}{s\sinh\frac{\pi s}{2}}\right)\widetilde{f}(s) = \frac{1}{\beta a}\int_{-\infty}^{\infty}\widetilde{f}(s')\,\text{sech}\left(\frac{\pi(s-s')}{2}\right)\, ds'. \tag{2.60}$$

The composition of this Fourier transform, change of variables, and then a second Fourier transform can be written as a single transformation applied to the function $A(x)$ as,

$$\widetilde{f}(s) = 4s \sinh\left(\frac{\pi s}{2}\right) \int_0^\infty A(x) K_{is}(\beta x)\, \frac{dx}{x}. \tag{2.61}$$

This transform and bears a strong resemblance to the Kontorovich-Lebedev transform, first developed to solve certain scattering problems in electrodynamics [72, 73]. □

Distribution contributions to the transformed solution

We extract the large-s behavior Eq. 2.60 by considering the ansatz $f(s) \sim e^{-\alpha s},\ s >> s_0$ and splitting the integral into two pieces with $s_0 << s_1 << s$. We have

$$\begin{aligned}\int_{-\infty}^{\infty} \widetilde{f}(s')\ \text{sech}\left(\frac{\pi(s-s')}{2}\right)\ ds' = &\int_{-\infty}^{s_1} \widetilde{f}(s')\ \text{sech}\left(\frac{\pi(s-s')}{2}\right)\ ds' \\ &+ \int_{s_1}^{\infty} \widetilde{f}(s')\ \text{sech}\left(\frac{\pi(s-s')}{2}\right)\ ds',\end{aligned}$$

where in the second term we can replace $\widetilde{f}(s')$ with the ansatz expression and for the first we note that since $s' < s$ we can write

$$\text{sech}\left(\frac{\pi(s-s')}{2}\right) = 2\sum_{n=0}^{\infty}(-1)^n e^{-(2n+1)\frac{\pi(s-s')}{2}}.$$

Supposing that the integrals over s' are finite, we can neglect all but the $n = 0$ term in the sum for asymptotically large s. The first term is then asymptotically

$$\int_{-\infty}^{s_1} \widetilde{f}(s')\ \text{sech}\left(\frac{\pi(s-s')}{2}\right)\ ds' = \mathcal{O}(e^{-\frac{\pi s}{2}}).$$

So long as the remaining integral term is asymptotically dominant compared to $e^{-\frac{\pi s}{2}}$, we are free to neglect this contribution. And similarly we are free to add

$$\int_{-\infty}^{s_1} e^{-\alpha s'} \operatorname{sech}\left(\frac{\pi(s-s')}{2}\right)\, ds' = \mathcal{O}(e^{-\frac{\pi s}{2}}),$$

without changing the leading order asymptotic behavior so that we find

$$\widetilde{f}(s) \approx \frac{1}{\beta a}\int_{-\infty}^{\infty} e^{-\alpha s'} \operatorname{sech}\left(\frac{\pi(s-s')}{2}\right)\, ds' = \frac{2}{\beta a \cos(\alpha)} e^{-\alpha s}, \quad s \to \infty.$$

This is consistent with our assumptions regarding dominant terms provided that $\alpha < \frac{\pi}{2}$, and consistent with our initial ansatz provided that $\alpha = \arccos\left(\frac{2}{\beta a}\right)$. These conditions can simultanesouly be true when $\beta a > 2$; therefore, we have that

$$\widetilde{f}(s) \sim \exp\left(-\arccos\left(\frac{2}{\beta a}\right)s\right), \quad \beta a > 2. \tag{2.62}$$

As βa approaches 2 we expect the exponential decay of $\widetilde{f}(s)$ to become weaker until it disappears precisely at $\beta a = 2$.

Recalling that $A(x) \propto K_{is_0}(\beta x)$ at unitarity, we can find the corresponding solutions by following the above sequence of transformations,

$$A(x) \propto K_{is_0}(\beta x), \tag{2.63a}$$

$$\widetilde{A}(k) \propto \frac{\pi \operatorname{sech}\left(\frac{\pi s_0}{2}\right)}{\sqrt{k^2+\beta^2}} \cos\left(s_0 \operatorname{arcsinh}\left(\frac{k}{\beta}\right)\right), \tag{2.63b}$$

$$f(\theta) \propto \frac{\pi \operatorname{sech}\left(\frac{\pi s_0}{2}\right)}{\beta} \cos(s_0\theta), \tag{2.63c}$$

$$\widetilde{f}(s) \propto \frac{\pi^2 \operatorname{sech}\left(\frac{\pi s_0}{2}\right)}{\beta}\Big(\delta(s-s_0)+\delta(s+s_0)\Big). \tag{2.63d}$$

These delta function solutions for $\widetilde{f}(s)$ are somewhat unexpected, but upon further analysis, the solution to Eq. (2.60) must not be an ordinary function at unitarity. Consider that since

the surface parameter is fixed by the short-range physics, Eq. 2.35 shows that β_0 is finite and therefore for $a \to \pm\infty$, $\beta a \to \beta_0 a \to \pm\infty$. If we search for a solution near unitarity then the right-hand side of Eq. 2.60 goes to zero, so $\widetilde{f}(s) = 0$ almost everywhere. And in addition, any expansion about $\beta a \sim \pm\infty$ would never be able to balance factors of $\frac{1}{\beta a}$ on both sides of the equation, and so $\widetilde{f}(s) = 0$ would be the only continuous solution near unitarity as well. Clearly, the trivial solution for $\widetilde{f}(s)$ does not correspond to the solution for $A(R_1)$ that we found in Section 2.3.2 and so we should expect solutions that are not ordinary functions.

To investigate the lack of smoothness of $\widetilde{f}(s)$ away from unitarity, we must trace its signature through the series of integral transformations. To start, the wavefunction must satisfy the free Schrödinger equation and thus be $C^2\left(\mathbb{R}^6\right)$ at least when the two atoms are not coincident with each other or with the surface. According to the Bethe-Peierls boundary condition, the wavefunction is proportional to $A(x)$ in a certain region of the configuration space. We therefore conclude that $A(x) \in C^2(\mathbb{R} \setminus \{0\})$. The asymptotic expansion Eq. 2.23 however specifies the behavior of $A(x)$ near the origin, where the function fails even to be continuously differentiable, $A'(x) \sim \frac{1}{x^{1 \pm i s_0}}$.

Given the duality between smoothness and decay for Fourier transforms, we expect that the signature of the lack of differentiability manifests in the large-k behavior of $\widetilde{A}(k)$. By replacing $A(x)$ with its Mellin transform in the definition of $\widetilde{A}(k)$ we have

$$\begin{aligned}\widetilde{A}(k) &= \int_{-\infty}^{\infty} A(x) e^{-ikx}\, dx \\ &= \int_0^{\infty} \frac{1}{2\pi i} \int_{c-i\infty}^{c+i\infty} \phi(s) x^{-s}\, ds\ \left(e^{-ikx} + e^{ikx}\right)\, dx,\end{aligned}$$

with $0 < c < 1$ so that the Mellin transform of $A(x)$ exists in the ordinary sense. Evaluating the integral over x

$$\widetilde{A}(k) = \frac{1}{2\pi i} \int_{c-i\infty}^{c+i\infty} -2|k|^{s-1} \sin\left(\frac{\pi s}{2}\right) \phi(s) \Gamma(1-s)\, ds.$$

Since all of the dependence on k is sequestered in one explicit factor, we can generate an asymptotic expansion of the result by shifting the contour to the left in the complex s plane [69]. The only contributions will arise from the poles of $\phi(s)$, and the first set arise at $s = \pm i s_0$, corresponding to the asymptotic expansion of $A(x)$ at small x:

$$\begin{aligned}\widetilde{A}(k) &= 2s_0 \sinh\left(\frac{\pi s_0}{2}\right)|k|^{-1+is_0}\Gamma(-is_0)\,\text{Res}(\phi(s), is_0) \\ &\quad + 2s_0 \sinh\left(\frac{\pi s_0}{2}\right)|k|^{-1-is_0}\Gamma(is_0)\,\text{Res}(\phi(s), -is_0) + \mathcal{O}(k^{-2}) \\ &= 2|k|^{-1+is_0}\Gamma(-is_0)\alpha_0^- + 2|k|^{-1-is_0}\Gamma(is_0)\alpha_0^+ + \mathcal{O}(k^{-2}).\end{aligned}$$

Then, combining this relation with Eq. 2.23 and Eq. 2.35 we have

$$\widetilde{A}(k) \sim -\sqrt{\frac{2}{s_0 \sinh(\pi s_0)}}\frac{1}{|k|}\cos\left(s_0 \log\left(\frac{2|k|}{\beta_0}\right)\right) + \mathcal{O}(k^{-2}), \quad |k| \to \infty. \tag{2.64}$$

And after the change of variables,

$$f(\theta) \sim -\frac{1}{\beta}\sqrt{\frac{2}{s_0 \sinh(\pi s_0)}}\cos\left(|s_0\,\theta| + \Phi\right) + \mathcal{O}(e^{-|\theta|}), \quad |\theta| \to \infty. \tag{2.65}$$

Here, it is convenient to define the angle

$$\Phi \equiv s_0 \log\left(\frac{\beta}{\beta_0}\right). \tag{2.66}$$

Unlike in the k-space, the sub-leading terms in θ decrease faster than any polynomial. Thus the only term which indicates that $\widetilde{f}(s)$ fails to be $C^\infty(\mathbb{R})$, is the first; all others decay sufficiently quickly that they correspond only to smooth behavior. We can find how this non-decaying behavior of f corresponds to terms within $\widetilde{f}$ that are tempered distributions

but not L^2 functions:

$$\int_{-\infty}^{\infty} \cos\left(|s_0\,\theta| + \Phi\right) e^{-is\theta}\, d\theta \\ = \pi \cos\left(\Phi\right)\Big(\delta(s-s_0) + \delta(s+s_0)\Big) + P\frac{2s_0}{s^2 - s_0^2}\sin\left(\Phi\right),$$

where P denotes that the term should be understood as a principal value distribution. And, therefore, not just at unitarity, but regardless of scattering length we have that

$$\widetilde{f}(s) \sim \pi\cos\left(\Phi\right)\delta(s \pm s_0) \pm P\frac{\sin\left(\Phi\right)}{s \mp s_0}, \quad s \to \pm s_0.$$

We now make a choice of normalization, namely that

$$\widetilde{f}(s) = \pi\delta(s-s_0) + P\frac{\tan\left(\Phi\right)}{s-s_0} + \mathcal{O}(1), \quad s \to s_0, \tag{2.67}$$

and then explicitly separate the delta functions from our solution via

$$\widetilde{f}(s) = \pi\Big(\delta(s-s_0) + \delta(s+s_0)\Big) + \widetilde{f}_0(s).$$

Further we use the evenness of $\widetilde{f}(s)$ to rewrite the relation as an integral over only $s > 0$. This recasts Eq. 2.60 into a non-homogeneous equation:

$$\left(1 - \frac{1}{s\sinh\frac{\pi s}{2}}\right)\widetilde{f}_0(s) = \frac{1}{\beta a}\fint_0^{\infty} \widetilde{f}_0(s')S(s,s')\,ds' + \frac{\pi}{\beta a}S(s,s_0), \tag{2.68}$$

where,

$$S(s,s') \equiv \text{sech}\left(\frac{\pi(s-s')}{2}\right) + \text{sech}\left(\frac{\pi(s+s')}{2}\right) \tag{2.69}$$

Having accounted explicitly for the distributions within our solution, the remaining f_0 will be an ordinary function that we can find by solving Eq. 2.68 numerically. First though, we find that this representation easily allows us to give another approximate solution.

2.4.2 Perturbative solution near unitarity

For $\beta a >> 1$, the right-hand side of Eq. 2.68 appears to become negligible, and so we can attempt an iterative solution. First, write a trial solution as a power series,

$$\widetilde{f}_0(s) = \sum_{n=0}^{\infty} \widetilde{f}_{0,n}(s) \left(\frac{1}{\beta a}\right)^n .$$

Substituting this expansion into Eq. 2.68 and equating like powers of βa leads to the recurrence relation

$$\left(1 - \frac{1}{s \sinh \frac{\pi s}{2}}\right) \widetilde{f}_{0,n}(s) = \fint_0^{\infty} \widetilde{f}_{0,n-1}(s') S(s,s')\, ds' + \pi\, \delta_{1,n}\, S(s,s_0).$$

Writing out the first few solutions, this leads to

$$\begin{aligned}
&\widetilde{f}_{0,0}(s) = 0, \\
&\widetilde{f}_{0,1}(s) = \pi \left(1 - \frac{1}{s \sinh \frac{\pi s}{2}}\right)^{-1} S(s,s_0), \\
&\widetilde{f}_{0,2}(s) = \pi \left(1 - \frac{1}{s \sinh \frac{\pi s}{2}}\right)^{-1} \fint_0^{\infty} \left(1 - \frac{1}{s' \sinh \frac{\pi s'}{2}}\right)^{-1} S(s',s_0) S(s,s')\, ds'.
\end{aligned}$$

We can further expand $\widetilde{f}_{0,1}(s)$ near s_0 and compare with Eq. 2.67 to extract,

$$\tan(\Phi) \approx \frac{s_0}{\beta_0}(\beta - \beta_0) \approx \frac{1}{\beta a} \frac{2\pi s_0 \left(1 + \operatorname{sech}(\pi s_0)\right)}{2 + \pi s_0^2 \cosh\left(\frac{\pi s_0}{2}\right)},$$

for which the approximate solution that reduces to β_0 when $a \to \pm\infty$ is

$$\beta = \beta_0 + \frac{2\pi \left(1 + \operatorname{sech}(\pi s_0)\right)}{2 + \pi s_0^2 \cosh\left(\frac{\pi s_0}{2}\right)} \frac{1}{a} + \mathcal{O}\left(\frac{1}{a^2}\right) \tag{2.70}$$

We have, then, extended the the solution at unitarity that we found in Section 2.3.2 to a solution in a neighborhood of unitarity, which also provides a check for our later

numerical calculation of the derivative of the binding energy with respect to the scattering length. Once we have defined the interparticle contact for this system as the major result of Chapter 3, we can also use this approximate solution to find the interparticle contact near unitarity.

2.4.3 Details of the numerical scheme

Eq. 2.68 is the expression of our integral equation which we will discretize and evaluate numerically. Compared to our original representation in terms of the function A, we have made several improvements. First, the kernel of this integral equation is smooth and does not depend on either the binding wavenumber β or the scattering length a. This allows for all matrices involved in the numerical solution to be pre-computed, greatly decreasing the computation time per unit of output. Second, we have traded a Hadamard regularized integral of a kernel with both quadratic and logarithmic singularities for a Cauchy principal value integral of a function which has only simple poles at $s = \pm s_0$. The principal value is easier to implement because we can choose quadrature points symmetrically about the locations of the poles to cancel the divergent contributions. Finally, since β and a occur in this equation only through the non-dimensional combination βa, we do not need to specify a value of a and then search for the appropriate β. Instead, we can simply specify a value of the product βa and then extract the corresponding values of β and a by finding the residue at $s = s_0$.

We approximate the integral via a simple rectangular rule using an equally spaced grid of points arranged symmetrically about the pole at $s = s_0$. Let

$$p_n \equiv \left(n - \frac{1}{2}\right)\frac{s_0}{N}$$
$$\widetilde{f}_n \equiv \widetilde{f}_0(p_n),$$

with $N \in \mathbb{N}, n \in \mathbb{N}$. Our approximation for Eq. 2.68 is the infinite system of linear

equations for $\widetilde{f}_n$

$$\begin{aligned}\left(1-\frac{1}{p_n \sinh\frac{\pi p_n}{2}}\right)\widetilde{f}_n &= \frac{1}{\beta a}\sum_{n'=1}^{\infty}\widetilde{f}_{n'}S(p_n,p'_n)\Delta p'_n + \frac{\pi}{\beta a}S(p_n,s_0)\\ &= \frac{s_0}{N\beta a}\sum_{n'=1}^{\infty}\widetilde{f}_{n'}S(p_n,p'_n) + \frac{\pi}{\beta a}S(p_n,s_0),\end{aligned} \tag{2.71}$$

which approaches our original integral equation as $N \to \infty$. Computationally, we solve the truncated system with $n, n' \leq M$,

$$\sum_{n'=1}^{M} A_{nn'}\widetilde{f}_{n'} = b_n,$$

$$\begin{aligned}A_{nn'} &= \left(1-\frac{1}{p_n \sinh\frac{\pi p_n}{2}}\right)\delta_{nn'} - \frac{s_0}{N\beta a}S(p_n,p'_n),\\ b_n &= \frac{\pi}{\beta a}S(p_n,s_0),\end{aligned}$$

increasing M until the $\widetilde{f}_n$ converge to the desired precision for a given N, then repeating this procedure for each larger N until there is no change in output up to the desired precision. Two representative examples of the output of this process are shown below: Figure 2.4 when $\beta a = 10$ and Figure 2.5 when $\beta a = -10^{-6}$. We see that indeed $\widetilde{f}(s)$ has a simple pole at $s = s_0$ in all cases. For positive βa, the f_n decrease exponentially, whereas when βa is negative, f_n becomes oscillatory with the amplitude and frequency of oscillation increasing as $\beta a \to 0$.

For a given value of βa, once we have computed the $\widetilde{f}_n$, we can extract the appropriate β and a using the asymptotics derived earlier. In particular, suppose that we discretize the

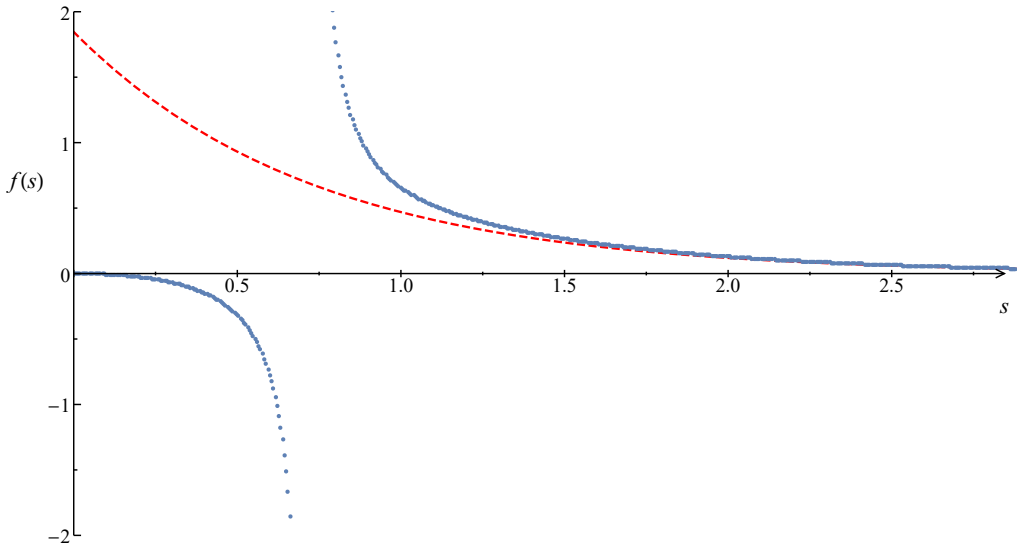

Figure 2.4: Numerical solution of Eq. 2.71 at $\beta a = 10$ (blue dots). The pole at $s = s_0$ is clearly visible, and the decay at large s is consistent with the asymptotic ansatz of Eq. 2.62 (dashed red line). Both axes are dimensionless.

integral in an identical manner, but let $p_n \to s_0$, then

$$\lim_{s\to s_0}\left(1-\frac{1}{s\sinh\frac{\pi s}{2}}\right)\widetilde{f}_0(s) = \frac{d}{ds}\left(1-\frac{1}{s\sinh\frac{\pi s}{2}}\right)\Bigg|_{s=s_0}(s-s_0)\left(\frac{\tan(\Phi)}{s-s_0}\right)$$
$$= \tan(\Phi)\left(\frac{1}{s_0}+\frac{\pi s_0}{2}\cosh\left(\frac{\pi s_0}{2}\right)\right),$$

and therefore

$$\tan(\Phi)\left(\frac{1}{s_0}+\frac{\pi s_0}{2}\cosh\left(\frac{\pi s_0}{2}\right)\right) = \frac{s_0}{N\beta a}\sum_{n'=1}^{\infty}\widetilde{f}_{n'}S(s_0,p'_n)+\frac{\pi}{\beta a}S(s_0,s_0). \qquad (2.72)$$

For any particular solution, we can verify we have extracted the appropriate value of $\tan\Phi$ by comparing the result from Eq. 2.72 with the linear interpolation of $(s-s_0)\widetilde{f}_n$ near $s \approx s_0$. In our solutions, the two values agree to beyond the pre-set precision goal, as shown in Figure 2.6. Since the right-hand side depends only on the known product, βa, we

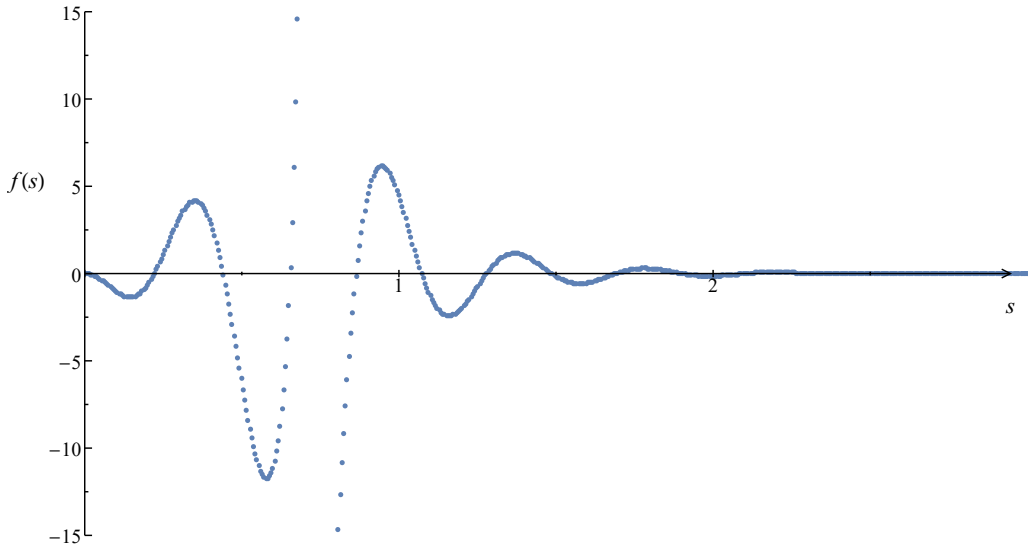

Figure 2.5: Numerical solution of 2.71 at $\beta a = -10^{-6}$ (blue dots). The pole at $s = s_0$ is clearly visible, and the oscillations are characteristic of solutions that are close to the free particle threshold, where a single bound state disappears into the continuum of two particles unbound from the surface.

can solve for $\tan(\Phi)$ and, recalling the definition of Φ from Eq. 2.66, extract β via

$$\beta = \beta_0 \exp\left(\frac{\arctan(\tan(\Phi))}{s_0}\right) = \beta_0\, e^{\left(\frac{\Phi_0 + k\pi}{s_0}\right)}.$$

For a given $\tan(\Phi)$ and βa, there are then an infinite sequence of allowed values of β indexed by the principle value of the arctangent, $\Phi_0 \in [-\pi, \pi]$, and $k \in \mathbb{Z}$. For each β we can find a corresponding value of a related by

$$\beta \to \beta e^{\frac{k\pi}{s_0}}, \quad a \to a e^{-\frac{k\pi}{s_0}}, \tag{2.73}$$

such that 2.72 is satisfied. Therefore, each value of βa for which our procedure converges to a sequence of $\widetilde{f}_n$ corresponds to an infinite sequence of solutions $A_k(x)$ to Eq. 2.19, each with its own unique value of β. The binding wavenumber and scattering length for

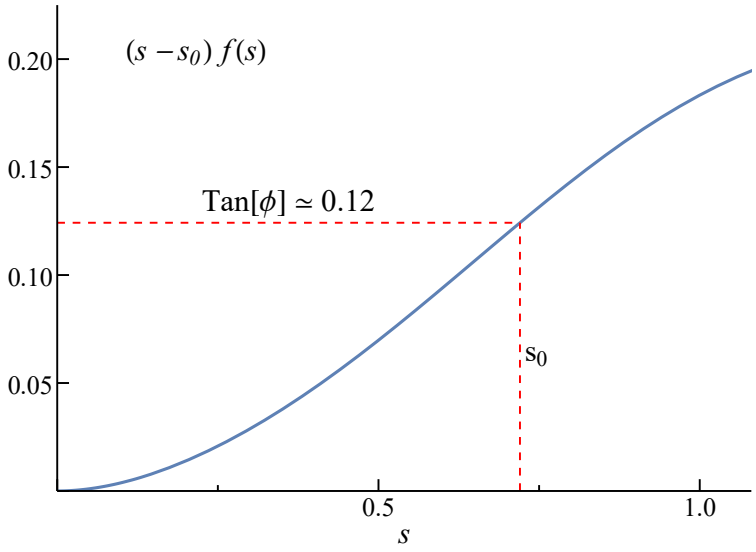

Figure 2.6: $(s - s_0)\widetilde{f}(s)$ for $\beta a = 10$. The interpolated value of $\tan\Phi$ shown here agrees with the value extracted from 2.72 to the pre-specified precision goal.

any one of these solutions is related to that of all other solutions for the same value of βa by the discrete scaling transform 2.73.

This procedure quickly yields accurate calculations of the $\widetilde{f}_n$ when $\widetilde{f}(s)$ is rapidly decaying; that is, βa is not too close to 2, according to Eq. 2.62. However, as $\beta a \to 2$, the number of points needed to accurately solve for the $\widetilde{f}_n$ becomes prohibitively large. Instead when βa is close to 2 we extend the number of points considered from M to $K > M$, and then for $M < n' < K$ we apply the asymptotic result of 2.62,

$$\widetilde{f}_{n'} \approx \widetilde{f}_M \exp\left(-\arccos\left(\frac{2}{\beta a}\right)(p_{n'} - p_M)\right), \quad n' > M. \tag{2.74}$$

Therefore,

$$\sum_{n'=M+1}^{K} \widetilde{f}_{n'} S(p_n, p'_n)$$
$$\approx \sum_{n'=M+1}^{K} \widetilde{f}_M \exp\left(-\arccos\left(\frac{2}{\beta a}\right)(p_{n'} - p_M)\right) \operatorname{sech}\left(\frac{\pi(p_n - p'_n)}{2}\right).$$

So then when βa nears 2 we instead solve the linear system

$$\left(1 - \frac{1}{p_n \sinh\frac{\pi p_n}{2}}\right)\widetilde{f}_n = \frac{s_0}{N\beta a}\sum_{n'=1}^{M} \widetilde{f}_{n'} S(p_n, p'_n) + \frac{\pi}{\beta a} S(p_n, s_0)$$
$$+ \frac{s_0}{N\beta a}\sum_{n'=M+1}^{K} \widetilde{f}_M \exp\left(-\arccos\left(\frac{2}{\beta a}\right)(p_{n'} - p_M)\right) \operatorname{sech}\left(\frac{\pi(p_n - p'_n)}{2}\right), \quad (2.75)$$

and extract the values of β and a via solving

$$\tan(\Phi)\left(\frac{1}{s_0} + \frac{\pi s_0}{2}\cosh\left(\frac{\pi s_0}{2}\right)\right) = \frac{s_0}{N\beta a}\sum_{n'=1}^{M} \widetilde{f}_{n'} S(s_0, p'_n) + \frac{\pi}{\beta a} S(s_0, s_0)$$
$$+ \frac{s_0}{N\beta a}\sum_{n'=M+1}^{K} \widetilde{f}_M \exp\left(-\arccos\left(\frac{2}{\beta a}\right)(p_{n'} - p_M)\right) \operatorname{sech}\left(\frac{\pi(s_0 - p'_n)}{2}\right). \quad (2.76)$$

A representative example of the output for this extended process is shown in Figure 2.7, along with a comparison to the exponential ansatz Eq. 2.74.

Using this scheme we can, on a desktop computer, arbitrarily choose a particular value of the bound state at unitarity, β_0, and by sweeping through many values of βa determine the evolution of the binding energy of this single bound state as the scattering length is changed. Using about 1 day's worth of computing time we have computed over 100,000 points along this curve to at least 10 digits of precision, which are displayed in Figure 2.8. This improves by several orders of magnitude both the number of points and precision of each point that can be calculated, compared to the most recent analogous calculations for the Efimov effect [74]. Our findings show a smooth crossover through unitarity with,

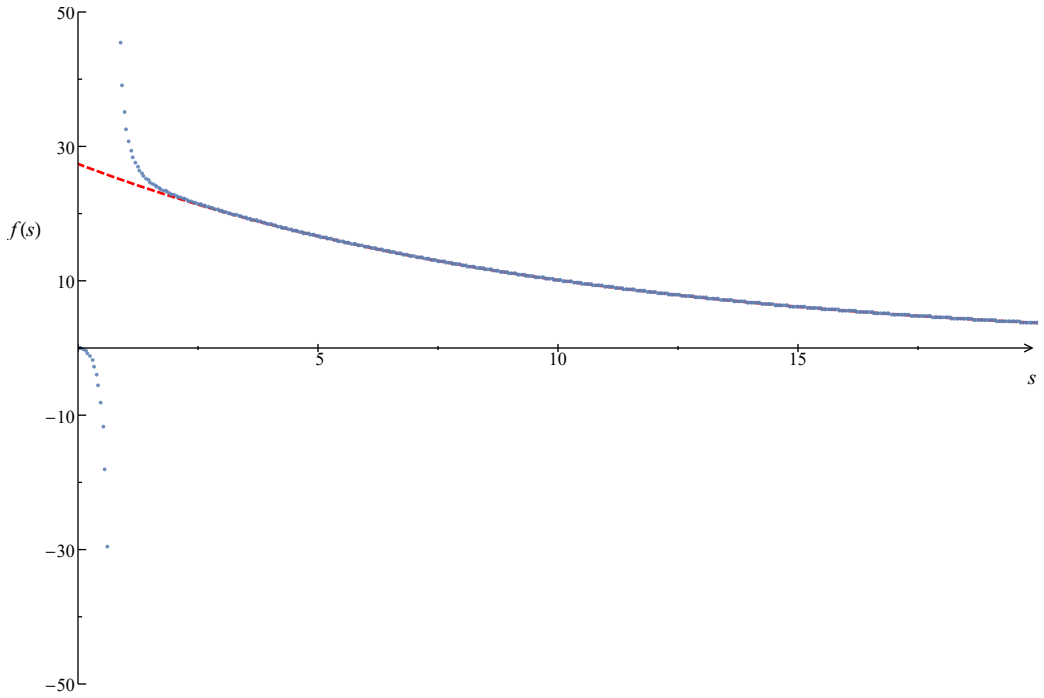

Figure 2.7: Numerical solution of Eq. 2.71 at $\beta a = 2.01$ (blue dots). The pole at $s = s_0$ is clearly visible, and the decay at large s is consistent with the asymptotic ansatz of Eq. 2.62 (dashed red line). Both axes are dimensionless.

as expected, a decreasing binding energy (compared to unitarity) for positive scattering length due to the effectively attractive interaction, and a binding energy approaching 0 for negative scattering length. We find that as $\beta a \to 2^+$, the binding energy approaches that of the shallow dimer (see Section 1.4) until, at $\beta a = 2$, our bound state disappears into the continuum of dimer states unbound from the surface. We have computed the critical scattering length at which this occurs, a_+, to be $\frac{1}{a_+} = 4.010047279\beta_0$. As the scattering length is tuned away from unitarity on the negative side, the bound state becomes less and less tightly bound with its binding energy approaching 0 at an increasingly steep slope. The bound state finally intersects the continuum of two free atoms, both unbound from the surface, at the critical negative scattering length $\frac{1}{a_-} = -0.5362203455\beta_0$. Note that this

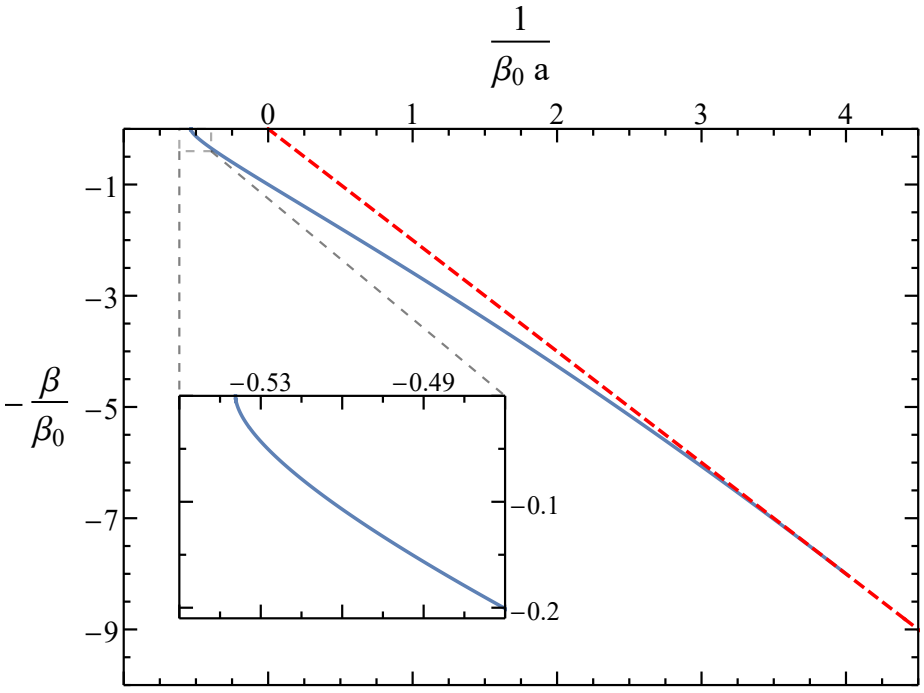

Figure 2.8: The binding wavenumber of the collective bound state specified by $\beta = \beta_0$ at unitarity as a function of the inverse scattering length. In the positive scattering length direction, the binding energy decreases until the state becomes metastable due to crossing into the continuum of shallow dimers unbound from the surface (dashed red line). In the negative scattering length direction, the collective state becomes less and less weakly bound until it disassociates into the continuum of free particles unbound from the surface.

numerical result is consistent with the result derived earlier in Eq. 2.55.

2.4.4 Numerical calculation of the derivative of the binding energy with respect to the scattering length

We anticipate that to compute any contacts associated with this system, we will need to find the derivative of the binding energy with respect to the inverse of the scattering length. Although we could compute this directly via a finite difference approximation from our previous numerical results, the precision would be substantially reduced. Instead, taking the already computed numerical values of β, a, and $\widetilde{f}_n$ as given, we find a new linear system which we solve first for the derivative of each $\widetilde{f}_n$ with respect to the inverse of the scattering length, and then similarly for the derivative of β.

Using the notation

$$\alpha_{s_0} \equiv \left(\frac{1}{s_0} + \frac{\pi s_0}{2}\cosh\left(\frac{\pi s_0}{2}\right)\right)^{-1},$$
$$p(\Phi) \equiv s_0 \sec^2\Phi + \tan(\Phi),$$

we find when taking the derivative of 2.71 and rearranging that

$$\frac{\partial \widetilde{f}_n}{\partial\left(\frac{1}{a}\right)} + \widetilde{f}_n \frac{s_0\alpha_{s_0}}{N\beta a\, p(\Phi)} \sum_{n'=1}^{\infty} \frac{\partial \widetilde{f}_{n'}}{\partial\left(\frac{1}{a}\right)} S(s_0, p_{n'})$$
$$- \frac{s_0}{N\beta a}\left(1 - \frac{1}{p_n \sinh\frac{\pi p_n}{2}}\right)^{-1} \sum_{n'=1}^{\infty} \frac{\partial \widetilde{f}_{n'}}{\partial\left(\frac{1}{a}\right)} S(p_n, p_{n'}) = a\widetilde{f}_n\left(1 - \frac{\tan(\Phi)}{p(\Phi)}\right). \qquad (2.77)$$

We write this relation in matrix form as

$$\sum_{n'=1}^{\infty} B_{n,n'}\, df_{n'} = c_n,$$

where,

$$B_{n,n'} \equiv \delta_{n,n'} - \frac{s_0}{N\beta a}\left(1 - \frac{1}{p_n \sinh\frac{\pi p_n}{2}}\right)^{-1} S(p_n, p_{n'}) + \widetilde{f}_n \frac{s_0\alpha_{s_0}}{N\beta a\, p(\Phi)} S(s_0, p_{n'})$$
$$c_n \equiv a\widetilde{f}_n\left(1 - \frac{\tan(\Phi)}{p(\Phi)}\right)$$
$$df_n \equiv \frac{\partial \widetilde{f}_n}{\partial\left(\frac{1}{a}\right)},$$

and we solve in an analogous way to Eq. 2.71. Once we determine the df_n, we take the derivative of Eq. 2.72 and solve for the derivative of β to find

$$\frac{\partial\beta}{\partial\left(\frac{1}{a}\right)} = \frac{\beta a\tan(\Phi)}{p(\Phi)} + \frac{s_0\alpha_{s_0}}{Na\, p(\Phi)}\sum_{n'=1}^{\infty}\frac{\partial\widetilde{f}_{n'}}{\partial\left(\frac{1}{a}\right)} S(s_0, p_{n'}). \tag{2.78}$$

Our numerical results for the derivative of the binding wavenumber are consistent with the perturbative result near unitarity,

$$\begin{aligned}\frac{d\beta}{d\left(\frac{1}{a}\right)} &= \frac{2\pi\left(1 + \operatorname{sech}(\pi s_0)\right)}{2 + \pi s_0^2\cosh\left(\frac{\pi s_0}{2}\right)} \\ &\approx 1.58.\end{aligned} \tag{2.79}$$

They also show that the derivative β at the critical negative scattering length diverges (see Figure 2.9); although, the divergence is weak enough that $\beta\frac{d\beta}{d\left(\frac{1}{a}\right)}$ approaches 0 and so the derivative of the energy is zero. And finally, they suggest that as the collective bound state approaches the dimer threshold, both the wavenumber and its derivative with respect to the scattering length approach the values of the shallow dimer as shown in Figures 2.8 and 2.9.

$$\begin{aligned}\beta_{dimer} &= \frac{2}{a}, \\ \frac{d\beta_{dimer}}{d\left(\frac{1}{a}\right)} &= 2.\end{aligned}$$

This provides evidence that the bound state between the particles and the surface is decay-

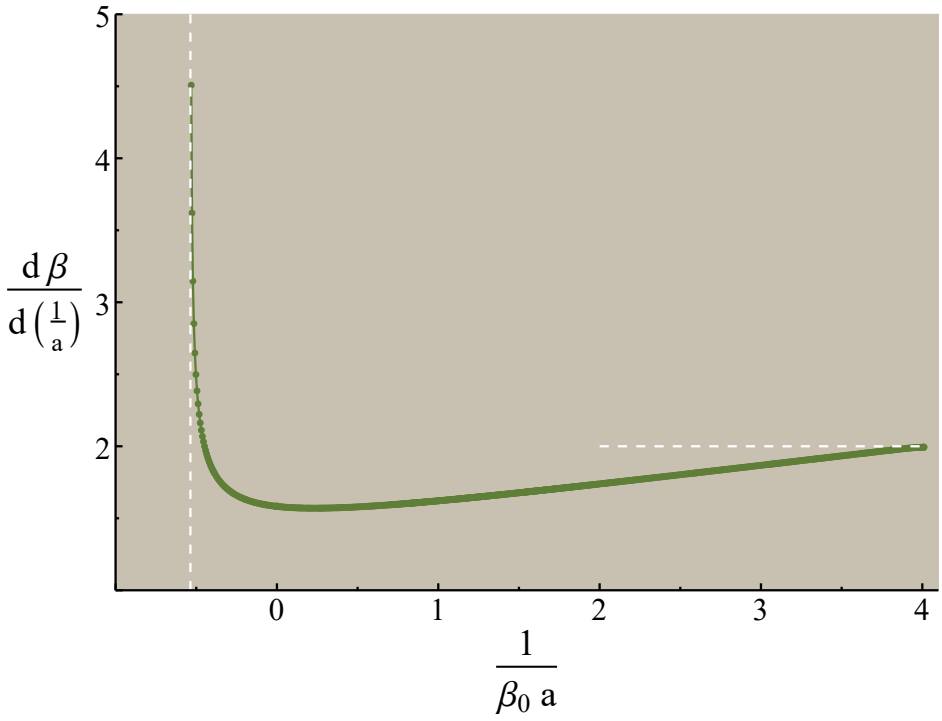

Figure 2.9: Results of the numerical calculation of the derivative of the binding wavenumber, β, with respect to the inverse of the scattering length. Calculated points are shown in green and connected by a linear interpolation. The vertical dashed line marks the position of the critical negative scattering length. The horizontal dashed line marks the value $\frac{d\beta}{d\left(\frac{1}{a}\right)} = 2$

ing via an outgoing dimer at this point and not via any other channel.

2.5 Exact Relation Between the Derivatives of the Collective Binding Energy

As our numerical results demonstrate, the binding energy of the collective bound state is determined solely by the scattering length, a, and the binding wavenumber at unitarity, β_0. As a result, we can write the binding energy in terms of the binding energy at unitarity times a dimensionless function. And there is only a single dimensionless combination of these two parameters, $\beta_0 a$. Therefore,

$$E = \frac{\hbar^2\beta^2}{4m} = \frac{\hbar^2\beta_0^2}{4m}\zeta(\beta_0 a). \tag{2.80}$$

Taking derivatives, then, we have

$$\frac{\partial E}{\partial\left(\frac{1}{a}\right)} = -\frac{\hbar^2 a^2\beta_0^3}{4m}\zeta'(\beta_0 a) \tag{2.81}$$

$$\begin{aligned}\frac{\partial E}{\partial\beta_0} &= \frac{\hbar^2\beta_0}{2m}\zeta(\beta_0 a) + \frac{\hbar^2 a\beta_0^2}{4m}\zeta'(\beta_0 a)\\ &= \frac{2}{\beta_0}E + \frac{\hbar^2 a\beta_0^2}{4m}\zeta'(\beta_0 a),\end{aligned}$$

and eliminating ζ' we can write these relations as

$$\beta_0\frac{\partial E}{\partial\beta_0} + \frac{1}{a}\frac{\partial E}{\partial\left(\frac{1}{a}\right)} = 2E \tag{2.82}$$

Therefore, from our numerical calculations of the binding wavenumber and the derivative of the binding wavenumber with respect to the inverse scattering length, we can use this relation to find the derivative of the binding energy with respect to the parameter β_0, which is set by the short-range physics.

Consider the following limiting cases:

1. Unitarity ($a \to \pm\infty$)

2. The dimer threshold ($\beta a \to 2$)

3. The breakup threshold ($\beta a \to 0$)

At unitarity, the scattering length diverges, but the derivative of the energy with respect to the inverse scattering length remains finite. Therefore we have that

$$\frac{\partial E}{\partial \beta_0} = -\frac{\hbar^2 \beta_0}{2m},$$

which is consistent with the definition that at unitarity the energy is given by $E = -\frac{\hbar^2 \beta_0^2}{4m}$

At the dimer threshold, the curve for the binding energy of the collective bound state intersects with that of the shallow dimer. It is well-known that

$$E_{dimer} = -\frac{\hbar^2}{m a_+^2}$$

and we have already presented that our numerical results suggest a value for the derivative of

$$\frac{\partial E}{\partial \left(\frac{1}{a}\right)} = -\frac{2\hbar^2}{m a_+}.$$

We can then substitute this results into Eq. 2.82 to find that

$$\frac{\partial E}{\partial \beta_0} \to 0, \quad \beta a \to 2.$$

Finally, at the breakup threshold we showed that the derivative of the wavenumber appears to diverge at this point, but slowly enough that the derivative of the energy approaches zero. By definition, the energy itself approaches zero at the point, and therefore

$$\frac{\partial E}{\partial \beta_0} \to 0, \quad \beta a \to 0.$$

This somewhat distinguishes our system from the Efimov effect. In that case, the three-body contact is not zero at the breakup threshold and provides the leading-order contribution to the rate of three-body recombination. However, because the derivative of the energy with respect to the three-body parameter is zero at the free particle threshold in our case, we suspect that any associated contact is also zero. The rate of recombination in the vicinity of this point for a gas of particles may potentially be suppressed, with the leading order contribution coming either from finite-range corrections or collisions involving more particles near the surface.

Following our work on the momentum distribution of the system in the next chapter, we will return to this relation so that we can relate the contacts in our system to each other.

2.6 Conclusion

Within this chapter, we have given an extensive description of the universal interaction between two particles and a surface tuned to resonance. We have shown how the interaction can be modeled by requiring that the normal derivative of the wavefunction be zero at the surface and that this simple model has some surprising consequences. In particular, we have found a sequence of shallow bound states where both particles are bound to the surface and to each other. Each of these states exists within a window of scattering lengths that is a function only of the surface parameter, x_0, which sets the relative phase induced when a pair of particles interacts with the surface. We have also found a discrete scale invariance with scaling factor $e^{\pi/s_0} \approx 78.4$ (about 4 times the scaling factor observed in the Efimov effect), which implies that these bound states can be extremely large – much larger than the characteristic size of the underlying potentials.

The calculations shown in this chapter should be useful in both few- and many- body realizations of atoms interacting with a resonantly tuned surface, for example the potential created by a double evanescent wave mirror. We suspect that resonances associated with the breakup of these collective bound states into either two free atoms or a free dimer can be

observed; although, the scaling factor is prohibitively large and so it may not be possible to observe more than one such resonance without other experimental advances. We also hope that the precision of the calculations given here will allow for comparisons that determine even small deviations indicative of interesting few- or many-body physics.

The work of this thesis forms a basis for addressing some open questions within the field, in the same way that similar early work on the Efimov effect led to several future studies. For example, the system described here has two further notable advantages for studying zero-range models and strongly interacting systems beyond the scattering length approximation, compared to the Efimov effect:

- These two-particle states do not themselves cause three particles to come into close contact, so the states may be much longer lived.
- The surface potential is experimentally constructed, thus it can also be varied to investigate parameters beyond the scattering length.

The three-body correlations created within the Efimov effect naturally lead to the particles sometimes closely approaching each other, especially for the more deeply bound trimers. In a cold atomic gas, this induces recombination events where two atoms enter a deeply bound molecular state while the third atom is ejected at high speed, which leads to heating and evaporation of the gas. By contrast, our states cause two atoms and the surface to sometimes be in close proximity, but because the surface cannot carry energy or momentum away from the system, recombination events that do not involve a third particle are kinematically forbidden. Thus, these bound states may be much longer lived on average than Efimov trimers and play an even more notable role in systems where they appear. Further, we showed that the parameter x_0 is determined by the relative phase induced by two particles interacting with the surface, which implies that by modifying the surface potential, we can modify x_0. This is an interesting opportunity, because in the Efimov effect, the three-body parameter is set by the Van der Waals interaction; we are stuck with what nature

has provided. Here, though, we may be able to test predictions regarding the universality and effect of the three-body parameter by varying the characteristic length of the surface interaction.

It is also interesting to consider the problem of three identical bosons interacting with such a surface, since both the conditions for our universal states as well as for Efimov trimers are met. Whether both families of states coexist is an open question, and there will almost certainly be points in the spectrum where the energy of the two states would be identical, and thus we expect an avoided crossing with hybridized states.

In the next chapter, we continue discussing the interaction between two particles and a surface; however, we shift focus to present a new method for determining how the short-range correlations in the system are related to its large momentum behavior and to changes in the system's energy as the scattering length and surface parameter are varied.

CHAPTER 3

CONTACTS AND THE ASYMPTOTIC EXPANSION OF THE SINGLE-PARTICLE MOMENTUM DISTRIBUTION AT ARBITRARY SCATTERING LENGTH

Following Tan's invention of a microscopic parameter called the contact (see Section 1.6 for a more thorough introduction) and demonstration that this parameter plus the scattering length (which describes the low-energy scattering, see Section 1.2) determines the internal energy, the change in internal energy due to changes in the inter-particle interaction, and the pressure, of a two-component Fermi gas [24, 25, 26], several authors have sought to extend these insights to systems of bosonic particles [10, 28]. For two-component Fermi systems the Pauli exclusion principle suppresses the contributions of three-body interactions to the these properties. However, bosonic systems require a more careful analysis because the probability of finding three particles interacting may be greatly enhanced compared to the fermionic case. In particular, it has been shown, using both renormalization group techniques with the operator product expansion and combined asymptotic and numerical techniques at unitarity, that for systems of unconfined bosons with zero-range interactions (see Section 1.3 for a definition of zero-range models), analogous relations to those developed by Tan still hold. There are, however, both sub-leading modifications and new relations that arise from the three-body physics [27, 28, 75].

Here, we apply the same physical intuition to our system of two particles interacting resonantly with a plane. Instead of interactions among three or more particles, we have interactions between two particles and a surface. Because our system exhibits a similar discrete scale invariance (see Eqs. 2.25, 2.55, and 2.73) and log-periodic oscillations (see Eq. 2.23) as that seen in the Efimov trimer, we suspect that the short-range correlations created by inter-particle and particle-surface interactions can be observed in the number of

particles, $n(k_\parallel)$, travelling with large momentna, $\hbar k_\parallel$, parallel to the surface. Specifically, we will show that

$$n(k_\parallel) = \frac{C_2}{k_\parallel^3} + \frac{C_3 L(k_\parallel)}{k_\parallel^4} + o(k_\parallel^{-4}), \quad k_\parallel \to \infty. \tag{3.1}$$

We call C_2 the two-particle contact because we will show it is proportional to the probability of finding the particles within a small distance of each other. Further, we will demonstrate that the function L exhibits log-periodic oscillations and that C_3 is proportional to the probability of finding the two particles near the surface, confirming that this sub-leading term is a hallmark of the three-body-like interaction between the particles and the surface.

We will accomplish this goal starting with 2 inputs, the formal solution for the wavefunction given in Eq. 2.13 and the asymptotic form of the source distribution found in Appendix B. In Section 3.1 we begin by proving several lemmas so that we can find the momentum space representation of the wavefunction and then give an expression for the distribution of particle momenta parallel to the surface. We then employ a double Mellin transform to asymptotically expand this distribution in Section 3.2, keeping all relevant terms through next-to-leading order and demonstrating the asymptotic form Eq. 3.1. Having found this expression involving the two-particle and particle-surface contacts, we finish in Sections 3.4 and 3.5 showing how the two-particle contact is related to the derivative of the binding energy with respect to the scattering length and the probability of finding two particles in close proximity.

Although our general goal is similar to several prior works in that we are seeking an asymptotic expansion of a momentum distribution, our methods differ substantially. The calculations performed in Refs. [27, 76, 77, 37] all utilize the operator product expansion applied to an effective field theory. This technique is extremely powerful and allows for the numerical computation of experimentally relevant parameters. However, although a calculation of the contacts for a particular state is in principle possible, it has not been demon-

strated using this technique; whereas, our technique combined with either the analytical or numerical results of Chapter 2 for a particular scattering length makes it straight-forward to compute the contacts. In addition, the relevant effective field theory for a particular problem, including the necessary counter-terms to properly renormalize, are not always known or easy to determine. We therefore wish to generate alternative procedures that serve as an independent theoretical check and are understandable to practitioners without a background in effective field theory.

Our calculations are more closely aligned with Refs. [75, 78, 79, 80] where an integral representation of a momentum distribution was given and expanded. We improve on them, though, by considering arbitrary scattering lengths (rather than focusing primarily on the unitarity limit) and giving exact calculations of all state-independent universal numbers involved in the expansion through next-to-leading order. This enables us to show the physical origin of each coefficient in the expansion, even without computing it explicitly. Our approach is also systematically improvable and can find higher-order contributions without requiring any modifications.

3.1 Expression for the Wavefunction in Momentum Space and the Parallel Momentum Distribution

We begin by defining our notation before proceeding to give an expression for the wavefunction in momentum space, in preparation for calculating the parallel momentum distribution. Let $x = (x_1, x_2, x_3) \in \mathbb{R}^3$ and $y = (y_1, y_2, y_3) \in \mathbb{R}^3$ be coordinate vectors for particles 1 and 2. Recall from the previous chapter that the particles are confined to the space $x_1 > 0$, $y_1 > 0$, but rather than the wavefunction vanishing at $x_1 = 0$ or $y_1 = 0$, instead its normal derivative is zero due to a resonant interaction with a flat surface spanning the $2 - 3$ plane. Their conjugate Fourier variables are $q = (q_1, q_2, q_3)$ and $k = (k_1, k_2, k_3)$, respectively. In addition, we utilize the slightly unusual scaling of center of mass and relative coordinates given by $R = \frac{x+y}{2} = (R_1, R_2, R_3),\ r = \frac{x-y}{2} = (r_1, r_2, r_3)$ to minimize

carrying additional numerical factors. By convention, the 1-direction will always correspond to motion perpendicular to the flat surface, whereas, the 2-direction and 3-direction always run parallel to the surface.

We define the Fourier transform of the square-integrable function g,

$$\tilde{g}(q,k) = \int_{\mathbb{R}^6} g(x,y) e^{-iq\cdot x - ik\cdot y} dx dy,$$

where the scalar product $q \cdot x := q_1 x_1 + q_2 x_2 + q_3 x_3$, and $|q| := \sqrt{q \cdot q}$. Also, we define the characteristic function

$$\chi_{\{x_1>0\}}(x) = \begin{cases} 1, & \text{if } x \in \{(x_1,x_2,x_3) : x_1 > 0\} \\ 0, & \text{otherwise} \end{cases}$$

and similarly for $\chi_{\{y_1>0\}}(y)$.

Because the particles cannot penetrate the surface as discussed before Eq. 2.8, the wavefunction is taken to be of the form

$$\Psi(x,y) = \psi(x,y)\chi_{\{x_1>0\}}(x)\chi_{\{y_1>0\}}(y). \tag{3.2}$$

The first two sections of this chapter will establish the lemma,

Lemma 3.1. *The distribution of particle momenta parallel to surface is given by*

$$\begin{aligned} n(k_2,k_3) &\equiv \frac{1}{(2\pi)^4} \int_{\mathbb{R}^4} |\widetilde{\Psi}(q,k)|^2 \, d^3q \, dk_1 \\ &= \frac{2^7\pi^2 L^2 \eta^2}{\beta^2} \int_{\mathbb{R}^2} \frac{\tilde{A}(q_1+k_1)\tilde{A}(q_1-k_1) + \tilde{A}(q_1+k_1)\tilde{A}(q_1+k_1)}{\left((q_1+k_1)^2 + (q_1-k_1)^2 + (2k_2)^2 + (2k_3)^2 + \beta^2\right)^2} \, dq_1 \, dk_1, \end{aligned}$$

where β is the binding wavenumber, and $\widetilde{A}$ is the Fourier transform of the source distribution defined in Eqs. 2.18 and 2.12.

Remark. *We note that the right-hand side of the above equation is a function of k_2, k_3*

because only the k_1 dependence has been integrated out.

Proof. The proof will take up the remainder of this section.

We would like to calculate the Fourier transform of the wavefunction and the associated single-particle momentum distribution; however, the characteristic functions in Eq. 3.2 complicate a direct calculation significantly. It will instead be more efficient to compute the Fourier transform of $\psi(x, y)$ defined in Eq. 3.2,

$$\widetilde{\psi}(q, k) = \int_{\mathbb{R}^6} \psi(x, y) e^{-iq\cdot x - ik\cdot y} d^3x d^3y, \tag{3.3}$$

due to the following lemma:

Lemma 3.2.

$$\int_{\mathbb{R}^4} |\widetilde{\Psi}(q, k)|^2 \, d^3q \, dk_1 = \frac{1}{4} \int_{\mathbb{R}^4} |\widetilde{\psi}(q, k)|^2 \, d^3q \, dk_1.$$

Proof. Let

$$F(k) \equiv \frac{1}{(2\pi)^3} \int_{\mathbb{R}^3} |\widetilde{\Psi}(q, k)|^2 \, d^3q \tag{3.4}$$

$$f(k) \equiv \frac{1}{(2\pi)^3} \int_{\mathbb{R}^3} |\widetilde{\psi}(q, k)|^2 \, d^3q \tag{3.5}$$

and recall for later use that that our formal solution for the wavefunction is equivalent to

$$\begin{aligned} \psi(R + r, R - r) = \eta \int_{-\infty}^{\infty} \Bigg[& \frac{K_1(\beta\sqrt{(R_1 - x')^2 + r_1^2 + r_2^2 + r_3^2})}{\sqrt{(R_1 - x')^2 + r_1^2 + r_2^2 + r_3^2}} \\ & + \frac{K_1(\beta\sqrt{R_1^2 + (r_1 - x')^2 + r_2^2 + r_3^2})}{\sqrt{R_1^2 + (r_1 + x')^2 + r_2^2 + r_3^2}} \Bigg] A(x') \, dx', \end{aligned} \tag{3.6}$$

Substituting the expression Eq. (3.2) into the definition of $F(k)$, we have

$$\begin{aligned} F(k) = \frac{1}{(2\pi)^3} \int_{\mathbb{R}^3} \Bigg[& \int_{\mathbb{R}^6} \psi(x, y) \chi_{\{x_1 > 0\}}(x) \chi_{\{y_1 > 0\}}(y) e^{-iq\cdot x - ik\cdot y} \, d^3x \, d^3y \\ & \times \int_{\mathbb{R}^6} \psi(x', y') \chi_{\{x_1' > 0\}}(x') \chi_{\{y_1' > 0\}}(y') e^{iq\cdot x' + ik\cdot y'} \, d^3x' \, d^3y' \Bigg] \, d^3q. \end{aligned} \tag{3.7}$$

Exchanging the order of integration and doing the integrals over q and then x' in Eq. 3.7 gives

$$F(k) = \int_{\mathbb{R}^3} \int_{\mathbb{R}^6} \psi(x,y)\chi_{\{x_1>0\}}(x)\chi_{\{y_1>0\}}(y)e^{-ik\cdot y} \\ \times\psi(x,y')\chi_{\{x_1>0\}}(x)\chi_{\{y_1'>0\}}(y')e^{ik\cdot y'}\ d^3x\ d^3y\ d^3y',$$

which is symmetric in x_1 since Eq. 3.6 is invariant under interchange of R_1 and r_1. Thus, the characteristic functions in x_1 can be removed by compensating with the appropriate factor,

$$F(k) = \frac{1}{2}\int_{\mathbb{R}^3} \int_{\mathbb{R}^6} \psi(x,y)\chi_{\{y_1>0\}}(y)e^{-ik\cdot y}\psi(x,y')\chi_{\{y_1'>0\}}(y')e^{ik\cdot y'}\ d^3x\ d^3y\ d^3y'.$$

Continuing by applying the convolution theorem, we need the distributional Fourier transform

$$\int_{-\infty}^{\infty} \chi_{\{y_1'>0\}}(y')e^{ik_1y_1'}\ dy_1' = \pi\delta(k_1) - \frac{i}{k_1},$$

and then we decompose

$$F(k) = F_1(k) + F_2(k) + F_3(k) + F_4(k).$$

There are 4 terms to consider:

$$F_1(k) \equiv \frac{1}{8}\int_{\mathbb{R}^2} \int_{\mathbb{R}^5} \left[\int_{-\infty}^{\infty} \left(\int_{-\infty}^{\infty} \psi(x,y)e^{-il_1y_1}\ dy_1 \right) \delta(l_1-k_1)\ dl_1 e^{-ik_{2,3}\cdot y_{2,3}} \right. \\ \left. \times \int_{-\infty}^{\infty} \left(\int_{-\infty}^{\infty} \psi(x,y')e^{im_1y_1'}\ dy_1' \right) \delta(m_1-k_1)\ dm_1 e^{ik_{2,3}\cdot y_{2,3}'} \right] d^3x\ d^2y\ d^2y'$$

$$F_2(k) \equiv \frac{1}{8\pi} \int_{\mathbb{R}^2} \int_{\mathbb{R}^5} \left[\int_{-\infty}^{\infty} \left(\int_{-\infty}^{\infty} \psi(x,y) e^{-il_1 y_1} \, dy_1 \right) \delta(l_1 - k_1) \, dl_1 e^{-ik_{2,3} \cdot y_{2,3}} \right.$$
$$\left. \times \int_{-\infty}^{\infty} \left(\int_{-\infty}^{\infty} \psi(x,y') e^{im_1 y_1'} \, dy_1' \right) \frac{i}{k_1 - m_1} \, dm_1 e^{ik_{2,3} \cdot y_{2,3}'} \right] d^3x \, d^2y \, d^2y'.$$

$$F_3(k) \equiv \frac{1}{8\pi} \int_{\mathbb{R}^2} \int_{\mathbb{R}^5} \left[\int_{-\infty}^{\infty} \left(\int_{-\infty}^{\infty} \psi(x,y) e^{-il_1 y_1} \, dy_1 \right) \frac{-i}{k_1 - l_1} \, dl_1 e^{-ik_{2,3} \cdot y_{2,3}} \right.$$
$$\left. \times \int_{-\infty}^{\infty} \left(\int_{-\infty}^{\infty} \psi(x,y') e^{im_1 y_1'} \, dy_1' \right) \delta(m_1 - k_1) \, dm_1 e^{ik_{2,3} \cdot y_{2,3}'} \right] d^3x \, d^2y \, d^2y'.$$

$$F_4(k) \equiv \frac{1}{8\pi^2} \int_{\mathbb{R}^2} \int_{\mathbb{R}^5} \left[\int_{-\infty}^{\infty} \left(\int_{-\infty}^{\infty} \psi(x,y) e^{il_1 y_1} \, dy_1 \right) \frac{1}{k_1 - l_1} \, dl_1 e^{ik_{2,3} \cdot y_{2,3}} \right.$$
$$\left. \times \int_{-\infty}^{\infty} \left(\int_{-\infty}^{\infty} \psi(x,y') e^{im_1 y_1'} \, dy_1' \right) \frac{1}{k_1 - m_1} \, dm_1 e^{ik_{2,3} \cdot y_{2,3}'} \right] d^3x \, d^2y \, d^2y'$$

$F_1(k)$ contains two delta functions and therefore

$$F_1(k) = \frac{1}{8} \int_{\mathbb{R}^3} \int_{\mathbb{R}^6} \psi(x,y) e^{-ik \cdot x} \psi(x,y') e^{ik \cdot y} \, d^3x \, d^3y \, d^3y'$$
$$= \frac{1}{8} \frac{1}{(2\pi)^3} \int_{\mathbb{R}^3} |\widetilde{\psi}(q,k)|^2 \, d^3q.$$

The next two terms each contain a single delta function:

$$F_2(k) = \frac{i}{8\pi} \int_{\mathbb{R}^6} \psi(x,y) e^{-ik \cdot y} \, d^3y \int_{-\infty}^{\infty} \left(\int_{\mathbb{R}^3} \psi(x,y') e^{im \cdot y'} \, d^3y' \left(\frac{1}{k_1 - m_1} \right) \right) dm_1 \, d^3x,$$
$$F_3(k) = \frac{-i}{8\pi} \int_{\mathbb{R}^3} \int_{-\infty}^{\infty} \left(\int_{\mathbb{R}^3} \psi(x,y) e^{-il \cdot y} \, d^3y \left(\frac{1}{k_1 - l_1} \right) \right) dl_1 \int_{\mathbb{R}^3} \psi(x,y') e^{ik \cdot y'} \, d^3y' \, d^3x.$$

Relabeling the dummy variables in F_3, $l_1 \to m_1$, $y' \to y$, $y \to y'$ makes clear that these two terms are almost identical. The only difference is the sign in the exponential. However, since $\psi(-x,-y) = \psi(x,y)$, if we let the dummy variables $y \to -y,\ y' \to -y',\ x \to -x$, the two terms cancel exactly.

The final term has no delta functions:

$$\begin{aligned} F_4(k) &= \frac{1}{8}\frac{1}{(2\pi)^3}\int_{\mathbb{R}^3}\left[\frac{1}{\pi}\int_{-\infty}^{\infty}\widetilde{\psi}(q,(l_1,k_2,k_3))\left(\frac{1}{k_1-l_1}\right)\,dl_1\right. \\ &\qquad\left.\times\frac{1}{\pi}\int_{-\infty}^{\infty}\widetilde{\psi}(q,(m_1,k_2,k_3))\left(\frac{1}{k_1-m_1}\right)\,dm_1\right]\,d^3q \\ &= \frac{1}{8}\frac{1}{(2\pi)^3}\int_{\mathbb{R}^3}H\widetilde{\psi}(q,k_1,k_2,k_3)^2\,d^3q, \end{aligned}$$

where $H\widetilde{\psi}(q,k_1,k_2,k_3)$ is the Hilbert transform defined as

$$Hf(a,t,b,c) \equiv \frac{1}{\pi}\int_{-\infty}^{\infty}\frac{f(a,\tau,b,c)}{t-\tau}\,d\tau.$$

All 4 terms combined will then give

$$F(k) = \frac{1}{8}\frac{1}{(2\pi)^3}\left[\int_{\mathbb{R}^3}|\widetilde{\psi}(q,k)|^2\,d^3q + \int_{\mathbb{R}^3}H\widetilde{\psi}(q,k_1,k_2,k_3)^2\,d^3q\right] \tag{3.8}$$

If we further integrate out the k_1 dependence, we can make a major simplification because it is a well-known property of Hilbert transforms (Theorem 8.1.7 of Ref. [81]) that

$$\int_{-\infty}^{\infty}f(a,t,b,c)^2\,dt = \int_{-\infty}^{\infty}Hf(a,\tau,b,c)^2\,d\tau,$$

and therefore this second term in $F(k)$ above is equal to the first. Therefore,

$$\begin{aligned} \int_{-\infty}^{\infty}F(k)\,dk_1 &= \frac{1}{4}\frac{1}{(2\pi)^3}\int_{-\infty}^{\infty}\int_{\mathbb{R}^3}|\widetilde{\psi}(q,k)|^2\,d^3q\,dk_1 \\ &= \frac{1}{4}\int_{-\infty}^{\infty}f(k)\,dk_1, \end{aligned}$$

which completes the proof in light of Eqs. 3.4 and 3.5. □

With Lemma 3.2 we have shown that

$$n(k_2, k_3) = \frac{1}{4}\frac{1}{(2\pi)^4}\int_{-\infty}^{\infty}\int_{\mathbb{R}^3} |\widetilde{\psi}(q,k)|^2 \, d^3q \, dk_1. \tag{3.9}$$

To then complete the proof of Lemma 3.1 it remains to show that

Lemma 3.3.

$$\begin{aligned}
&\frac{1}{4}\frac{1}{(2\pi)^4}\int_{-\infty}^{\infty}\int_{\mathbb{R}^3} |\widetilde{\psi}(q,k)|^2 \, d^3q \, dk_1 \\
&= \frac{2^7\pi^2 L^2\eta^2}{\beta^2}\int_{-\infty}^{\infty}\int_{-\infty}^{\infty} \frac{\tilde{A}(q_1+k_1)\tilde{A}(q_1-k_1) + \tilde{A}(q_1+k_1)\tilde{A}(q_1+k_1)}{\left((q_1+k_1)^2 + (q_1-k_1)^2 + (2k_2)^2 + (2k_3)^2 + \beta^2\right)^2} \, dq_1 \, dk_1.
\end{aligned}$$

Proof. We begin with an expression for the wavefunction equivalent to Eq. 2.13 from the previous chapter,

$$\begin{aligned}
\psi(R+r, R-r) = \eta\int_{-\infty}^{\infty}\Bigg[&\frac{K_1(\beta\sqrt{(R_1-x')^2 + r_1^2 + r_2^2 + r_3^2})}{\sqrt{(R_1-x')^2 + r_1^2 + r_2^2 + r_3^2}} \\
&+ \frac{K_1(\beta\sqrt{R_1^2 + (r_1-x')^2 + r_2^2 + r_3^2})}{\sqrt{R_1^2 + (r_1+x')^2 + r_2^2 + r_3^2}}\Bigg] A(x') \, dx'.
\end{aligned} \tag{3.10}$$

This expression does not depend of R_2 or R_3 because the motion of the center of mass parallel to the surface is completely unconstrained. To this point, we have been working in the center-of-momentum frame, which implies that $q_2 + k_2 = 0$, $q_3 + k_3 = 0$, so that no plane wave factors would appear in our solution. However, after returning them the wavefunction will have to be normalized in the sense that

$$\begin{aligned}
&\int_{\mathbb{R}^6} \psi^*(x,y) e^{i(k_2+q_2)R_2 + i(k_3+q_3)R_3} \psi(x,y) e^{i(k_2'+q_2')R_2 + i(k_3'+q_3')R_3} \, d^3x \, d^3y \\
&= (2\pi)^2\delta(q_2+k_2-q_2'-k_2')\delta(q_3+k_3-q_3'-k_3').
\end{aligned} \tag{3.11}$$

To overcome this normalization difficulty, we will temporarily imagine that the center of mass coordinates R_2 and R_3 are not unconstrained, but instead lie in a box of side-length L, with periodic boundary conditions. We then require that the wavefunction be normalized

within one unit-cell, which has the effect of constraining the domain of integration over R_2 and R_3. Once we arrive at an expression for the momentum distribution, we will be able to take the limit that $L \to \infty$. If we then account for the normalization constant, all dependence on the length L will disappear. This procedure leads to a unique result because the Fourier transform is a one-to-one map from the space of tempered distributions to itself.

For this section, we will rewrite A in terms of its Fourier transform

$$A(x') = \int_{-\infty}^{\infty} \tilde{A}(l) e^{ilx'} \, \frac{dl}{2\pi} \, , \tag{3.12}$$

then in the first term make the shift $x' \to x' + R_1$ and in the second term $x' \to x' + r_1$, which results in the expression:

$$\psi(R+r, R-r) = \frac{\eta}{2\pi} \int_{-\infty}^{\infty} \int_{-\infty}^{\infty} \left[\frac{K_1(\beta\sqrt{x'^2 + r_1^2 + r_2^2 + r_3^2})}{\sqrt{x'^2 + r_1^2 + r_2^2 + r_3^2}} e^{il(x'+R_1)} \right.$$
$$\left. + \frac{K_1(\beta\sqrt{x'^2 + R_1^2 + r_2^2 + r_3^2})}{\sqrt{x'^2 + R_1^2 + r_2^2 + r_3^2}} e^{il(x'+r_1)} \right] \tilde{A}(l) \, dx' \, dl.$$

This requires us to compute the Fourier transform

$$\int_{-\infty}^{\infty} \frac{K_1(\beta\sqrt{x^2 + \alpha^2})}{\sqrt{x^2 + \alpha^2}} e^{ilx} \, dx = \frac{\pi}{\beta\sqrt{\alpha^2}} e^{-\sqrt{\beta^2 + l^2}\sqrt{\alpha^2}}, \tag{3.13}$$

which we then apply to our previous expression for the wavefunction, yielding

$$\psi(R+r, R-r) = \frac{\eta}{2\beta} \int_{-\infty}^{\infty} \left[\frac{e^{-\sqrt{l^2+\beta^2}}\sqrt{r_1^2 + r_2^2 + r_3^2}}{\sqrt{r_1^2 + r_2^2 + r_3^2}} e^{ilR_1} + \frac{e^{-\sqrt{l^2+\beta^2}}\sqrt{R_1^2 + r_2^2 + r_3^2}}{\sqrt{R_1^2 + r_2^2 + r_3^2}} e^{ilr_1} \right] \tilde{A}(l) \, dl.$$

Now we take the Fourier transform in the 6 dimensional configuration space:

$$\widetilde{\psi}(q,k) = \widetilde{\psi}_1(q,k) + \widetilde{\psi}_2(q,k),$$

with

$$\psi_1\left(\frac{P+p}{2},\frac{P-p}{2}\right) \equiv \frac{4\eta}{\beta}\int_{\mathbb{R}^6}\int_{-\infty}^{\infty} \frac{e^{-\sqrt{l^2+\beta^2}\sqrt{r_1^2+r_2^2+r_3^2}}}{\sqrt{r_1^2+r_2^2+r_3^2}}\tilde{A}(l)e^{-iP\cdot R-ip\cdot r+ilR_1}\,dl\,d^3r\,d^3R,$$
$$\psi_2\left(\frac{P+p}{2},\frac{P-p}{2}\right) \equiv \frac{4\eta}{\beta}\int_{\mathbb{R}^6}\int_{-\infty}^{\infty} \frac{e^{-\sqrt{l^2+\beta^2}\sqrt{R_1^2+r_2^2+r_3^2}}}{\sqrt{R_1^2+r_2^2+r_3^2}}\tilde{A}(l)e^{-iP\cdot R-ip\cdot r+ilr_1}\,dl\,d^3r\,d^3R,$$

and $P \equiv q+k = (P_1,P_2,P_3),\ p \equiv q-k = (p_1,p_2,p_3)$.

Considering ψ_1, the integral over R_1 immediately yields a delta function because it is the Fourier transform of a plane wave that is then being integrated against a smooth, rapidly-decaying function,

$$\int_{\mathbb{R}} e^{-i(l-P_1)R_1}\,dR_1 = 2\pi\delta(l-P_1).$$

For the R_2 and R_3 directions, we are confined to a periodic box so we instead have

$$\int_{-\frac{L}{2}}^{\frac{L}{2}} e^{-iP_jR_j}\,dR_j = \frac{2}{P_j}\sin\left(\frac{P_jL}{2}\right).$$

Therefore we find

$$\widetilde{\psi}_1\left(\frac{P+p}{2},\frac{P-p}{2}\right)$$
$$= \frac{32\pi\eta}{\beta}\sigma_L(P_2,P_3)\int_{\mathbb{R}^3}\int_{-\infty}^{\infty} \frac{e^{-\sqrt{l^2+\beta^2}\sqrt{r_1^2+r_2^2+r_3^2}}}{\sqrt{r_1^2+r_2^2+r_3^2}}\delta(l-P_1)\tilde{A}(l)\,dl\,e^{-ip\cdot r}\,d^3r,$$

with

$$\sigma_L(P_2,P_3) = \frac{\sin\left(\frac{P_2L}{2}\right)}{P_2}\frac{\sin\left(\frac{P_3L}{2}\right)}{P_3}.$$

This allows us to perform the integration over l, which just replaces l with P_1

$$\widetilde{\psi}_1\left(\frac{P+p}{2},\frac{P-p}{2}\right) = \frac{32\pi\eta}{\beta}\sigma_L(P_2,P_3)\tilde{A}(P_1)\int_{\mathbb{R}^3} \frac{e^{-\sqrt{P_1^2+\beta^2}\sqrt{r_1^2+r_2^2+r_3^2}}}{\sqrt{r_1^2+r_2^2+r_3^2}}\,e^{-ip\cdot r}\,d^3r.$$

The remaining integrals can then be completed easily using spherical coordinates

$$\widetilde{\psi}_1\left(\frac{P+p}{2},\frac{P-p}{2}\right)=\frac{128\pi^2\eta}{\beta}\sigma(P_2,P_3)\frac{\tilde{A}(P_1)}{P_1^2+p^2+\beta^2}. \tag{3.14}$$

The calculation for $\psi_2(q,k)$ proceeds analogously but with the roles of P_1 and p_1 reversed and therefore:

$$\begin{aligned}|\psi\left(q,k\right)|^2&=|\psi_1(q,k)+\psi_2(q,k)|^2\\&=\frac{2^{14}\pi^4\eta^2}{\beta^2}\sigma_L^2(P_2,P_3)\frac{|\tilde{A}(q_1+k_1)+\tilde{A}(q_1-k_1)|^2}{\left((q_1+k_1)^2+(q-k)^2+\beta^2\right)^2}.\end{aligned}$$

At this point, we can take the large L limit. All of the dependence on L is contained within the function σ and the normalization constant η. We will compute the limit in an unconventional way. Note that the inverse Fourier transform of σ^2 exists in the ordinary sense for finite L and is given by

$$\frac{1}{(2\pi)^2}\int_{\mathbb{R}^2}\sigma_L^2(P_2,P_3)e^{iP_2R_2+iP_3R_3}\,dP_2\,dP_3=\frac{1}{64}\prod_{j=2,3}\left(|L-R_j|-2|R_j|+|L+R_j|\right). \tag{3.15}$$

In the limit of $L\to\infty$, this approaches pointwise

$$\frac{1}{64}\prod_{j=2,3}\left(|L-R_j|-2|R_j|+|L+R_j|\right)\sim\frac{L^2}{16},\quad L\to\infty.$$

Therefore the sequence of Fourier transforms of σ_L^2 approaches the constant function and so

$$\sigma_L^2(P_2,P_3)\to\frac{\pi^2L^2}{4}\delta(P_2)\delta(P_3),\quad L\to\infty. \tag{3.16}$$

This results in our final expression for the momentum distribution of the bound state be-

tween the surface and the two particles,

$$|\psi\left(q,k\right)|^2 = \frac{2^{12}\pi^6\eta^2L^2}{\beta^2}\delta(P_2)\delta(P_3)\frac{|\tilde{A}(q_1+k_1)+\tilde{A}(q_1-k_1)|^2}{\left((q_1+k_1)^2+(q-k)^2+\beta^2\right)^2}. \tag{3.17}$$

We show in Appendix D that η^2L^2 is in fact independent of L.

Recall that A is an even function and therefore its Fourier transform $\widetilde{A}$ is also even. The above expression is then symmetric in the momenta of the two particles, and therefore it does not matter which one we choose to integrate over when finding the single-particle momentum distribution. Carrying out the integrals over q_2, q_3 using sifting property of the delta function and recalling the definition Eq. 3.5,

$$f(k) = \frac{2^9\pi^3\eta^2L^2}{\beta^2}\int_{-\infty}^{\infty}\frac{|\tilde{A}(q_1+k_1)+\tilde{A}(q_1-k_1)|^2}{\left((q_1+k_1)^2+(q_1-k_1)^2+(2k_2)^2+(2k_3)^2+\beta^2\right)^2}\,dq_1 \tag{3.18}$$

There are two types of terms in the numerator, squared terms and cross terms. The cross terms clearly have the same value and so can be combined. For the squared terms, note that by taking $q_1 \to -q_1$ and using the fact that $\tilde{A}(k)$ is even we map one squared term to the other, and therefore these also have the same value. We can therefore represent our distribution as

$$f(k) = \frac{2^{10}\pi^3\eta^2L^2}{\beta^2}\int_{-\infty}^{\infty}\frac{\tilde{A}(q_1+k_1)\tilde{A}(q_1-k_1)+\tilde{A}(q_1+k_1)\tilde{A}(q_1+k_1)}{\left((q_1+k_1)^2+(q_1-k_1)^2+(2k_2)^2+(2k_3)^2+\beta^2\right)^2}\,dq_1. \tag{3.19}$$

□

Combining Lemma 3.2 and Lemma 3.3 will then prove Lemma 3.1.

$$\begin{aligned} n(k_2,k_3) &= \frac{1}{4}\frac{1}{2\pi}\int_{\mathbb{R}} f(k)\,dk_1 \\ &= \frac{2^7\pi^2L^2\eta^2}{\beta^2}\int_{\mathbb{R}^2}\frac{\tilde{A}(q_1+k_1)\tilde{A}(q_1-k_1)+\tilde{A}(q_1+k_1)\tilde{A}(q_1+k_1)}{\left((q_1+k_1)^2+(q_1-k_1)^2+(2k_2)^2+(2k_3)^2+\beta^2\right)^2}\,dq_1\,dk_1 \end{aligned}$$

□

3.2 Asymptotic Expansion of the Parallel Momentum Distribution

Now we proceed to the asymptotic expansion of $n(k_2, k_3)$, by decomposing it into two terms. For each, we will perform a separate expansion.

Lemma 3.4.

$$n(k_2, k_3) = \frac{2^6 \pi^3 L^2 \eta^2}{\beta^2} \left(I_1(\gamma) + I_2(\gamma) \right) \tag{3.20}$$

with

$$\begin{aligned}
I_1(\gamma) &\equiv \frac{1}{\gamma} \int_{-\infty}^{\infty} \int_{-\infty}^{\infty} A(x) A(x') |x + x'| K_1 \left(\gamma |x + x'| \right) \, dx' \, dx \\
I_2(\gamma) &\equiv \frac{4}{\gamma^2} \int_0^{\infty} \int_0^{\infty} \int_0^{\infty} A(x) A(x') J(\gamma, \theta, x, x') d\theta \, dx' \, dx \\
J(\gamma, \theta, x, x') &\equiv \text{sech}\, \theta \left(\gamma x' + \text{sech}\, \theta \right) e^{-\gamma \, x' \cosh \theta} \cos \left(\gamma x \sinh \theta \right)
\end{aligned}$$

and

$$\gamma^2 \equiv 4k_2^2 + 4k_3^2 + \beta^2$$

Proof. Without loss of generality, we assume that the global phase of the wavefunction has been chosen such that the wavefunction and therefore A are purely real functions. Beginning from the result of Lemma 3.1, replacing $\widetilde{A}$ with its Fourier transform, and making the change of variables to $P_1 = q_1 + k_1, \; p_1 = q_1 - k_1$ we have that

$$n(k_2, k_3) = \frac{2^6 \pi^2 L^2 \eta^2}{\beta^2} \int_{-\infty}^{\infty} \int_{-\infty}^{\infty} A(x) A(x') \left(L_1(\gamma, x, x') + L_2(\gamma, x, x') \right) \, dx' \, dx \tag{3.21}$$

with

$$\begin{aligned}
L_1(\gamma, x, x') &\equiv \int_{-\infty}^{\infty} \int_{-\infty}^{\infty} \frac{e^{-iP_1(x+x')}}{\left(P_1^2 + p_1^2 + \gamma^2 \right)^2} \, dP_1 \, dp_1 \\
L_2(\gamma, x, x') &\equiv \int_{-\infty}^{\infty} \int_{-\infty}^{\infty} \frac{e^{-iP_1 x - ip_1 x'}}{\left(P_1^2 + p_1^2 + \gamma^2 \right)^2} \, dP_1 \, dp_1.
\end{aligned}$$

The integrals in L_1 can both be performed immediately resulting in

$$L_1(\gamma, x, x') = \frac{\pi|x + x'|}{\gamma} K_1\left(\gamma|x + x'|\right). \tag{3.22}$$

Plugging this back into Eq. 3.21 gives the desired $I_1(\gamma)$.

For L_2 only one integral can be carried out immediately. Using the identity that

$$\int_{-\infty}^{\infty} \frac{e^{-ip_1 x'}}{\left(P_1^2 + p_1^2 + \gamma^2\right)^2}\, dp_1 = \frac{\pi\left(1 + |x'|\sqrt{P_1^2 + \gamma^2}\right)}{2\left(P_1^2 + \gamma^2\right)^{\frac{3}{2}}} e^{-|x'|\sqrt{P_1^2+\gamma^2}}, \tag{3.23}$$

and then making the change of variables $P_1 = \gamma \sinh\theta$ we find that

$$L_2(\gamma, x, x') = \int_{-\infty}^{\infty} \frac{\pi \text{ sech } \theta\left(\gamma|x'| + \text{sech } \theta\right)}{4\gamma^2} e^{-\gamma(|x'|\cosh\theta + ix\sinh\theta)} d\theta. \tag{3.24}$$

Returning this expression to 3.21 we see that since both A and L_2 are even in x', we can rewrite the result as an integral over only positive x'. Next, we can separate the integral over negative x values, let $x \to -x$ and recombine with the original integral over positive x to find

$$\begin{aligned}
&\int_{-\infty}^{\infty}\int_{-\infty}^{\infty} A(x)A(x')L_2(\gamma, x, x')\, dx'\, dx \\
&= \frac{2\pi}{\gamma^2}\int_0^{\infty}\int_0^{\infty}\int_{-\infty}^{\infty} A(x)A(x')\text{ sech }\theta\left(\gamma x' + \text{sech }\theta\right) e^{-\gamma x'\cosh\theta}\cos\left(\gamma x\sinh\theta\right) d\theta\, dx'\, dx,
\end{aligned}$$

which is then also even in θ and therefore

$$= \frac{4\pi}{\gamma^2}\int_0^{\infty}\int_0^{\infty}\int_0^{\infty} A(x)A(x')\text{ sech }\theta\left(\gamma x' + \text{sech }\theta\right) e^{-\gamma x'\cosh\theta}\cos\left(\gamma x\sinh\theta\right) d\theta\, dx'\, dx. \tag{3.25}$$

Substituting this expression into Eq. 3.21 yields the desired $I_2(\gamma)$. □

We are interested in the expansion of $n(k_2, k_3)$ as the magnitude of the parallel momentum becomes large, and we can implement this by looking at the asymptotic behavior of I_1

and I_2 as γ becomes large. To that end, we can now proceed with the expansion of I_1.

3.2.1 Asymptotic expansion of I_1 for large parallel momentum

Recall that

$$I_1(\gamma) = \frac{1}{\gamma} \int_{-\infty}^{\infty} \int_{-\infty}^{\infty} A(x)A(x')|x + x'|K_1\left(\gamma|x + x'|\right)\, dx'\, dx. \tag{3.26}$$

There are 2 primary difficulties that must be overcome in the expansion of this expression:

- The function $A(x)$ is not differentiable at $x = 0$ and therefore any scheme that relies on approximating $A(x)$ using a Taylor-like series will fail when the argument becomes small; the error terms are unbounded.
- As $\gamma \to \infty$ we would like to replace the kernel $|x + x'|K_1\left(\gamma|x + x'|\right)$ with its own asymptotic expansion for large arguments (see Appendix G). However, the line $x = -x'$ remains the dominant region of contribution as $\gamma \to \infty$ and this asymptotic replacement cannot be made there.

Therefore we will turn to a Mellin transform technique to avoid both of these problems. We can summarize the primary steps as

1. Replace $A(x)$ and $A(x')$ with their Mellin transforms $\phi(s)$ and $\phi(t)$.
2. Carry out the integrals over x and x', which is equivalent to computing the double Mellin transform of $|x + x'|K_1\left(\gamma|x + x'|\right)$. This will concentrate the γ dependence into a single simple term.
3. Displace the s and t contours to the left in the complex s and t planes, picking up the residues of any poles encountered. The remaining integrals will be asymptotically small compared to the sum of residues, which represent a complete asymptotic expansion of the double integral.

We are now ready to prove the following lemma:

Lemma 3.5.

$$\begin{aligned} I_1(\gamma) = \frac{2\pi}{\gamma^3}\int_0^\infty |A(x)|^2\,dx + \frac{\alpha_0^+\alpha_0^-}{\gamma^4}M(is_0,-is_0) \\ + \gamma^{2is_0-4}\left(\alpha_0^-\right)^2 M(is_0,is_0) \\ + \gamma^{-2is_0-4}\left(\alpha_0^+\right)^2 M(-is_0,-is_0) + o\left(\gamma^{-4}\right), \quad \gamma\to\infty \end{aligned}$$

$$\begin{aligned} M(s,t) \equiv 2\pi^{\frac{3}{2}} i^{t+1}\frac{\tan\left(\frac{\pi s}{2}\right)\Gamma(1-s)\Gamma\left(\frac{1}{2}(s+t-1)\right)}{\Gamma(t)\Gamma\left(\frac{1}{2}(s+t-2)\right)} \\ \times\left(i^{s+1}\csc\left(\frac{\pi}{2}(s+t)\right)+\sec\left(\frac{\pi t}{2}\right)\right) \end{aligned}$$

Proof. We define the inverse Mellin transform of A by

$$A(x) = \frac{1}{2\pi i}\int_{c_s-i\infty}^{c_s+i\infty}\phi(s)x^{-s}\,ds, \tag{3.27}$$

where c_s is a real number that must be chosen so that the vertical line $\mathrm{Re}(s) = c_s$ lies completely within the fundamental strip of ϕ. The fundamental strip is determined by the values of $\mathrm{Re}(s)$ for which the Mellin transform

$$\phi(s) = \int_0^\infty A(x)x^{s-1}\,dx \tag{3.28}$$

exists in the ordinary sense. Let σ^+ and σ^- be the largest (respectively, smallest) values of $\mathrm{Re}(s)$ such that the Mellin transform exists as an ordinary integral. As we argued after Eq. 2.8, we must have $A \in L^2(\mathbb{R})$ for the wavefunction to represent a state bound to the surface and so the right boundary of the fundamental strip satisfies at least $\mathrm{Re}(\sigma^+) \geq \frac{1}{2}$. Further, we showed in Appendix B that $A(x) = \mathcal{O}(1),\ x\to 0$ and so the left boundary of the fundamental strip will be at $\sigma^- \leq 0$. Therefore, at worst we may chose $0 < c_s < \frac{1}{2}$ and be guaranteed that our vertical contour is within the fundamental strip of ϕ. We will need

to keep this choice in mind during the following calculations to ensure that they are valid for these values of c_s.

We first insert the definition of the Mellin transform Eq. 3.27 into the definition of I_1 Eq. 3.26. Exchanging the order of integration, we must then carry out the double integral

$$D(\gamma, s, t) \equiv (2\pi i)^2 \int_{-\infty}^{\infty} \int_{-\infty}^{\infty} |x + x'| K_1 \left(\gamma |x + x'|\right) |x|^{-s} |x'|^{-t} \, dx' \, dx. \tag{3.29}$$

Lemma 3.6. *For* $0 < \mathrm{Re}(s) < 1$, $0 < \mathrm{Re}(t) < 1$, *and* $\mathrm{Re}(s + t) > 1$,

$$D(\gamma, s, t) = \gamma^{s+t-3} M(s, t),$$

where $M(s, t)$ *is defined in Lemma 3.5.*

Proof. Here, we use a trick that applies to many integrals involving Bessel functions. Often, expressions involving Bessel functions have Fourier transforms that can be expressed in terms of more elementary functions. To wit,

$$|x + x'| K_1 \left(\gamma |x + x'|\right) = \frac{1}{2\pi} \int_{-\infty}^{\infty} \frac{\pi \gamma}{(k^2 + \gamma^2)^{\frac{3}{2}}} e^{ik(x+x')} \, dk.$$

Inserting this into Eq. 3.29 allows us to use the identities

$$\int_{-\infty}^{\infty} |x|^{-s} e^{ikx} \, dx = 2|k|^{s-1} \Gamma(1 - s) \sin\left(\frac{\pi s}{2}\right), \quad 0 < \mathrm{Re}(s) < 1,$$

and

$$\int_{-\infty}^{\infty} \frac{|k|^{s-1}}{(k^2 + \gamma^2)^{\frac{3}{2}}} e^{ikx'} \, dk = \left[\frac{2}{\sqrt{\pi}} \gamma^{s-3} \, \Gamma\left(\frac{3}{2} - \frac{s}{2}\right) \Gamma\left(\frac{s}{2}\right) {}_1F_2\left(\frac{s}{2}; \frac{1}{2}, \frac{s}{2} - \frac{1}{2}; \frac{x'^2 \gamma^2}{4}\right) \right.$$
$$\left. - 2|x'|^{3-s} \Gamma(s - 3) \sin\left(\frac{\pi s}{2}\right) {}_1F_2\left(\frac{3}{2}; 2 - \frac{s}{2}, \frac{5}{2} - \frac{s}{2}; \frac{x'^2 \gamma^2}{4}\right) \right]$$

to write

$$
\begin{aligned}
&D(\gamma, s, t) \\
&= \gamma\ (\cos(\pi s) - 1)\,\Gamma(1-s)\Gamma(s-3) \int_{-\infty}^{\infty} {}_1F_2\left(\frac{3}{2}; 2 - \frac{s}{2}, \frac{5}{2} - \frac{s}{2}; \frac{x'^2\gamma^2}{4}\right) |x'|^{3-s-t}\, dx' \\
&- 2^{s-1}\pi^{\frac{3}{2}}\gamma^{s-2}\Gamma\left(\frac{1}{2} - \frac{s}{2}\right) \sec\left(\frac{\pi s}{2}\right) \int_{-\infty}^{\infty} {}_1F_2\left(\frac{s}{2}; \frac{1}{2}, \frac{s}{2} - \frac{1}{2}; \frac{x'^2\gamma^2}{4}\right) |x'|^{-t}\, dx',
\end{aligned}
$$

where ${}_1F_2$ is the generalized hypergeometric function.

One simplification is immediate: the integrals are even in x' and can thus be rewritten to range only over positive x'. They are then plainly the Mellin transforms of generalized hypergeometric functions which reduce to relatively simple expressions involving the Gamma function:

$$
\begin{aligned}
D(\gamma, s, t) &= 2i^{t+1}\pi^{\frac{3}{2}}\gamma^{s+t-3} \frac{\tan\left(\frac{\pi s}{2}\right)\Gamma(1-s)\Gamma\left(\frac{1}{2}(s+t-1)\right)}{\Gamma(t)\Gamma\left(\frac{1}{2}(s+t-2)\right)} \\
&\quad \times \left(i^{s+1}\csc\left(\frac{\pi}{2}(s+t)\right) + \sec\left(\frac{\pi t}{2}\right)\right) \\
&= \gamma^{s+t-3} M(s,t)
\end{aligned}
$$

so long as $0 < \mathrm{Re}(t) < 1$ and $\mathrm{Re}(s) + \mathrm{Re}(t) > 1$. □

Remark. *Our previous estimates that we can choose* $0 < c_s < \frac{1}{2}$ *and* $0 < c_t < \frac{1}{2}$ *are then not quite adequate to apply Lemma 3.6.*

We must further assume (without proof) that $A(x) = \mathcal{O}\left(x^{-\frac{1}{2}-\epsilon}\right),\ x \to \infty$ for some $\epsilon > 0$ so that we may choose c_s, c_t such that $c_s + c_t > 1$ and apply Lemma 3.6. In practice, we find that this assumption is always satisfied. When the binding wavenumber $\beta > 0$, we expect that $A(x)$ decreases exponentially at large x, and our solution at unitarity in Section 2.3.2 is a typical example. We may worry about power-law decay for $\beta = 0$; however, since we have found an expression for the Mellin transform, X, of A at $\beta = 0$ in Section 2.3.3, we can check that there are no poles of $X(\nu)$ between $-2 < \mathrm{Re}(\nu) < 0$ and therefore

$A(x) = \mathcal{O}(x^{-1}),\ x \to \infty$ even when $\beta = 0$. Therefore, although we have no general proof, we believe that our decay assumption is always satisfied and so we can choose c_s, c_t such that $c_s + c_t > 1$ and apply the result of Lemma 3.6.

Substituting this result into Eq. 3.26 we have

$$I_1(\gamma) = \frac{1}{(2\pi i)^2} \int_{c_t - i\infty}^{c_t + i\infty} \int_{c_s - i\infty}^{c_s + i\infty} \phi(s)\phi(t)\gamma^{s+t-4} M(s,t)\, ds\, dt. \tag{3.30}$$

Remark. *All of the dependence of I_1 on γ has been segregated into the factor γ^{s+t-3} and thus by considering different s or t contours in the complex plane, we are potentially changing the order of the double integral in γ in an explicit and well-controlled way.*

To generate an asymptotic expansion of I_1 for large γ, we need to displace the s and t contours to the left in the complex plane so that the real part of the exponent of γ^{s+t-3} becomes smaller and smaller. Of course the contour cannot be displaced at will while preserving the value of the double integral. Any time we cross a pole we must use the residue theorem to preserve the overall value of the integral. The poles, then, determine the asymptotic expansion in γ while the double integral is constantly being displaced so that its value is asymptotically small and can be neglected.

Recall that by prior assumption we begin with $0 < c_s < 1$, $0 < c_t < 1$, and $c_s + c_t > 1$. We will be careful to first displace the contour in the complex-s plane, and then in the complex-t plane so that we do not accidentally cross a pole and then cross back across the same pole.

The first pole we encounter as we move the s-contour of Eq. 3.30 is a pole of $M(s,t)$ at $s = 1 - t$ with

$$\text{Res}(M(1-t,t)) = 2\pi.$$

Therefore

$$I_1(\gamma) = \frac{2\pi}{\gamma^3}\frac{1}{2\pi i}\int_{c_t-i\infty}^{c_t+i\infty} \phi(1-t)\phi(t)\, dt + \frac{1}{(2\pi i)^2}\int_{c_t-i\infty}^{c_t+i\infty}\int_{1-c_t-\epsilon-i\infty}^{1-c_t-\epsilon+i\infty} \phi(s)\phi(t)\gamma^{s+t-4}M(s,t)\, ds\, dt, \tag{3.31}$$

with $1 - c_t > \epsilon > 0$. We cannot let ϵ be larger than $1 - c_t$ or we would cross another set of poles.

Lemma 3.7.

$$\frac{1}{(2\pi i)^2}\int_{c_t-i\infty}^{c_t+i\infty}\int_{1-c_t-\epsilon-i\infty}^{1-c_t-\epsilon+i\infty} \phi(s)\phi(t)\gamma^{s+t-4}M(s,t)\, ds\, dt = o\left(\gamma^{-3}\right) \tag{3.32}$$

Proof. Let

$$\delta_1(\gamma) \equiv \frac{1}{(2\pi i)^2}\int_{c_t-i\infty}^{c_t+i\infty}\int_{1-c_t-\epsilon-i\infty}^{1-c_t-\epsilon+i\infty} \phi(s)\phi(t)\gamma^{s+t-4}M(s,t)\, ds\, dt,$$

$$|\delta_1(\gamma)| \leq \frac{1}{4\pi^2\gamma^{-3-\epsilon}}\int_{c_t-i\infty}^{c_t+i\infty}\int_{1-c_t-\epsilon-i\infty}^{1-c_t-\epsilon+i\infty} |\phi(s)\phi(t)M(s,t)|\, ds\, dt.$$

The double integral is then independent of γ and so as long it is finite, then $\delta_1(\gamma) = o(\gamma^{-3})$. It is each to check directly using the asymptotic properties of the gamma and trigonometic functions that $M(s,t)$ grows at most as

$$M(s,t) \sim \mathrm{Im}(s)^{c_t-\epsilon-\frac{1}{2}}\mathrm{Im}(t)^{\frac{1}{2}-c_t}.$$

The decay properties of ϕ along vertical lines are then strong enough to guarantee that the integrals converge. We do not give the full argument here; the interested reader may consult Section 6.2 of Ref. [69] for detailed estimates and decay properties of Mellin transforms. □

By the Plancherel-type formula for the Mellin transform then, we find from Eq. 3.31

$$I_1(\gamma) = \frac{2\pi}{\gamma^3} \int_0^\infty |A(x)|^2 \, dx + o(\gamma^{-3}).$$

As desired, this gives the leading order contribution in γ to $I_1(\gamma)$ sought for Lemma 3.5. Next, we will proceed with the next-to-leading order term.

Lemma 3.8.

$$\begin{aligned}\delta_1(\gamma) =& \frac{\alpha_0^+ \alpha_0^-}{\gamma^4} M(is_0, -is_0) + \gamma^{2is_0-4} \left(\alpha_0^-\right)^2 M(is_0, is_0) \\ &+ \gamma^{-2is_0-4} \left(\alpha_0^+\right)^2 M(-is_0, -is_0) + o\left(\gamma^{-4}\right)\end{aligned} \tag{3.33}$$

Proof. Starting from Eq. 3.31, we continue displacing the s-contour to the left from $\mathrm{Re}(s) = 1 - c_t - \epsilon > 0$. The next poles that we encounter arise from $\phi(s)$ and $\phi(t)$. These poles result from the asymptotic behavior of $A(x)$ and $A(x')$ at small argument because if

$$A(x) \sim \alpha_p x^p, \quad x \to 0,$$

then

$$\phi(s) \sim \frac{\alpha_{p^*}}{s-p}, \quad s \to p.$$

Drawing on the result of Appendix B, in our case we have that

$$A(x) \sim \alpha_0^+ x^{is_0} + \alpha_0^- x^{-is_0} + \mathcal{O}(x^{1\pm is_0}).$$

Therefore, we next encounter the poles at $s = \pm is_0$. As a reminder, $s_0 \approx 0.7202$ is the only real solution to the transcendental equation Eq. 2.31 and it defines the scaling factor $\lambda = e^{\frac{\pi}{s_0}} \approx 78.4$ for the discrete scaling symmetry present in our system of two particles interacting with a surface. Carrying forward our definition of δ_1 from Lemma 3.6, after

moving the s-contour we have

$$\begin{aligned}\delta_1(\gamma) = \quad & \frac{1}{(2\pi i)}\text{Res}(\phi(is_0))\int_{c_t-i\infty}^{c_t+i\infty}\phi(t)\gamma^{is_0+t-4}M(is_0,t)\,dt \\ & + \frac{1}{(2\pi i)}\text{Res}(\phi(-is_0))\int_{c_t-i\infty}^{c_t+i\infty}\phi(t)\gamma^{-is_0+t-4}M(-is_0,t)\,dt \\ & + \frac{1}{(2\pi i)^2}\int_{c_t-i\infty}^{c_t+i\infty}\int_{-\epsilon-i\infty}^{-\epsilon+i\infty}\phi(s)\phi(t)\gamma^{s+t-4}M(s,t)\,ds\,dt,\end{aligned}$$

where $0 < \epsilon < c_t$. Again we must be careful not to let ϵ be too large or we will cross another pole at $s = -t - 1$. In each of the first two terms above, we then move the t-contour to the left, including the residues as we cross the poles of $\phi(t)$ at $t = \pm is_0$.

$$\begin{aligned}\delta_1(\gamma) = \; & 2\gamma^{-4}\,\text{Res}(\phi(is_0))\text{Res}(\phi(-is_0))M(is_0,-is_0) \\ & + \gamma^{2is_0-4}\text{Res}(\phi(is_0))^2M(is_0,is_0) \\ & + \gamma^{-2is_0-4}\text{Res}(\phi(-is_0))^2M(-is_0,-is_0) \\ & + \frac{1}{(2\pi i)^2}\int_{c_t-i\infty}^{c_t+i\infty}\int_{-\epsilon-i\infty}^{-\epsilon+i\infty}\phi(s)\phi(t)\gamma^{s+t-4}M(s,t)\,ds\,dt,\end{aligned}$$

since M is symmetric under interchange of s and t (although this is not obvious just by inspection). For the term

$$\delta_2(\gamma) \equiv \frac{1}{(2\pi i)^2}\int_{c_t-i\infty}^{c_t+i\infty}\int_{-\epsilon-i\infty}^{-\epsilon+i\infty}\phi(s)\phi(t)\gamma^{s+t-4}M(s,t)\,ds\,dt, \tag{3.34}$$

we can show that $\delta_2(\gamma) = o\left(\gamma^{-4}\right)$ by the same argument as that we used for Lemma 3.6 provided that we recognize that we can displace the t-contour until $0 < \text{Re}(t) < \epsilon$ so that we do not cross the poles at $\text{Re}(t) = 0$, and yet $\text{Re}(s+t) < 0$. That way, $|\gamma^{s+t-4}| = \gamma^{\text{Re}(t)-\epsilon-4} = o\left(\gamma^{-4}\right)$ and the double-integral is again asymptotically negligible. Replacing

the residues of ϕ with the appropriate expansion coefficients gives the desired result

$$\begin{aligned}\delta_1(\gamma) =& \frac{2\alpha_0^+\alpha_0^-}{\gamma^4} M(is_0, -is_0) + \gamma^{2is_0-4} \left(\alpha_0^-\right)^2 M(is_0, is_0) \\ &+ \gamma^{-2is_0-4} \left(\alpha_0^+\right)^2 M(-is_0, -is_0) + o\left(\gamma^{-4}\right).\end{aligned}$$

□

Combining Eq. 3.31 with the results of Lemmas 3.7 and 3.8 then proves Lemma 3.5 and gives a complete asymptotic expansion of $I_1(\gamma)$ as $\gamma \to \infty$:

$$\begin{aligned}I_1(\gamma) = \frac{2\pi}{\gamma^3} \int_0^\infty |A(x)|^2 \, dx + \frac{2\alpha_0^+\alpha_0^-}{\gamma^4} M(is_0, -is_0) \\ + \gamma^{2is_0-4} \left(\alpha_0^-\right)^2 M(is_0, is_0) \\ + \gamma^{-2is_0-4} \left(\alpha_0^+\right)^2 M(-is_0, -is_0) + o\left(\gamma^{-4}\right), \quad \gamma \to \infty\end{aligned}$$

□

To validate this expansion numerically, we chose two functional forms for $A(x)$ and computed $I_1(\gamma)$ using numerical integration for a random selection of γ values. The relative differences between our numerical calculations and the asymptotic expansion of Lemma 3.5 are plotted in Figure 3.1. All comparisons show that the relative error decreases as γ increases, at leading and next-to-leading order, and also that the next-to-leading order corrections decrease the relative error by approximately the expected factor of γ^{-1}. This gives us confidence that our expansion is correct and includes all relevant terms through next-to-leading order.

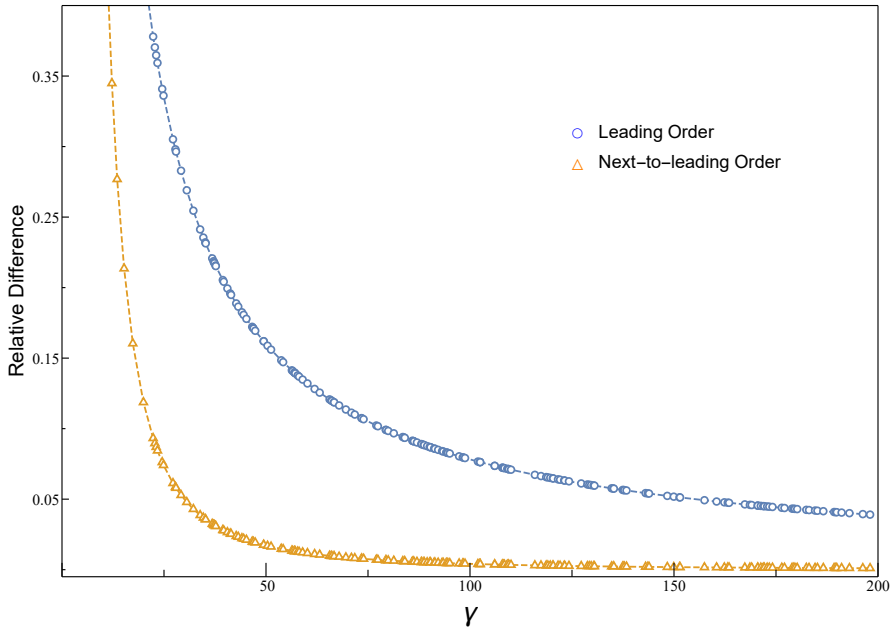

(a) $A(x) = \frac{x^{3i}+x^{-3i}}{1+x^2}$, and therefore $\alpha_0^+ = \alpha_0^- = 1$, $s_0 = 3$.

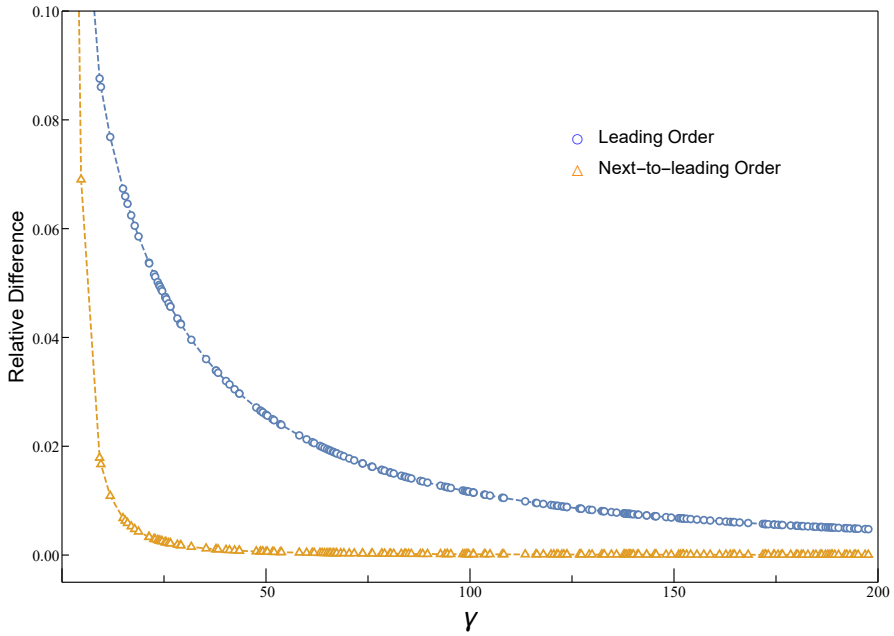

(b) $A(x) = K_{is_0}(x)$, and therefore $\alpha_0^+ = 2^{-1-is_0}\Gamma(-is_0)$, $\alpha_0^- = 2^{-1+is_0}\Gamma(is_0)$, $s_0 \approx 0.720198$.

Figure 3.1: Relative difference between numerically computed $I_1(\gamma)$ and the asymptotic expansion Eq. 3.5 through leading-order and next-to-leading order for two different choices of $A(x)$ and randomly chosen γ.

3.2.2 Asymptotic expansion of I_2 for large parallel momenta

The expansion of $I_2(\gamma)$ for large γ proceeds in a similar way to that of $I_1(\gamma)$ presented in Section 3.2.1 and so we will not show all of the details because they give no new insight.

Summarizing, then, we again replace $A(x)$ and $A(x')$ by their Mellin transforms and use the identity that

$$\begin{aligned}&\int_0^\infty \int_0^\infty \int_0^\infty \operatorname{sech}\theta\,(\gamma x' + \operatorname{sech}\theta)\, e^{-\gamma(x'\cosh\theta)} \cos(\gamma x \sinh\theta)\, x^{-s}(x')^{-t}\, dx'\, dx\, d\theta \\ &= \frac{\gamma^{s+t-2}}{\sqrt{\pi}} 2^{-t}\Gamma(1-s)\Gamma\left(\frac{1}{2}-\frac{t}{2}\right)\Gamma\left(\frac{s}{2}\right)\Gamma\left(2-\frac{s}{2}-\frac{t}{2}\right)\sin\left(\frac{\pi s}{2}\right),\end{aligned}$$

provided that $0 < \mathrm{Re}(s) < 1$ and $0 < \mathrm{Re}(t) < 1$. This motivates the definition

$$N(s,t) \equiv \frac{4}{\sqrt{\pi}} 2^{-t}\Gamma(1-s)\Gamma\left(\frac{1}{2}-\frac{t}{2}\right)\Gamma\left(\frac{s}{2}\right)\Gamma\left(2-\frac{s}{2}-\frac{t}{2}\right)\sin\left(\frac{\pi s}{2}\right),$$

and therefore we can write I_2 as

$$I_2(\gamma) = \frac{1}{(2\pi i)^2}\int_{c_t-i\infty}^{c_t+i\infty}\int_{c_s-i\infty}^{c_s+i\infty} \frac{\phi(t)\phi(s)}{\gamma^{4-s-t}} N(s,t)\, ds\, dt \tag{3.35}$$

Unlike the case of I_1, the function $N(s,t)$ has no poles in either left half-plane when $\mathrm{Re}(s) < 1$ and $\mathrm{Re}(t) < 1$. The factor $\Gamma\left(\frac{s}{2}\right)$ would contribute poles at the negative even integers, but they all become removable singularities due to the $\sin\left(\frac{\pi s}{2}\right)$ factor. Therefore, an asymptotic evaluation of this term will first encounter the poles of $\phi(s)$ and $\phi(t)$, which are related to the short-distance asymptotic expansion of $A(x)$.

As before, the first poles encountered as we shift the s and t contours to the left in the respective complex planes will occur at $s = \pm i s_0$ when the s-contour is shifted and then $t = \pm i s_0$ when the t-contour is shifted. Each pole contributes $2\pi i$ times its residue and

adding the 4 terms we find, noting $N(s,t)$ is symmetric under exchange of s and t, that

$$\begin{aligned} I_2(\gamma) = \quad & \gamma^{-4+2is_0}(\alpha_0^-)^2 N(is_0, is_0) + \gamma^{-4-2is_0}(\alpha_0^+)^2 N(-is_0, -is_0) \\ & + 2\gamma^{-4}\alpha_0^+\alpha_0^- N(is_0, -is_0) + o(\gamma^{-4}). \end{aligned} \tag{3.36}$$

We again carry out a numerical check to validate our expansion. Using the source distribution at unitarity, we numerically calculated the expression for $I_2(\gamma)$ in terms of the source distribution shown in Lemma 3.4 for several values of γ using a Monte Carlo technique. The results are plotted in Figure 3.2 and show that the average of our Monte Carlo calculations agrees very closely with the prediction from the expansion Eq. 3.36. This again suggests that we have not omitted any terms or made any invalid approximations when creating this expansion.

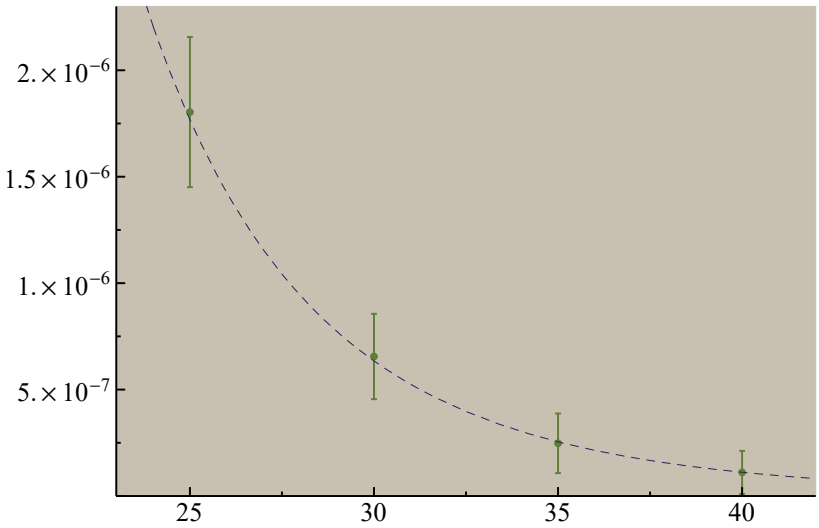

Figure 3.2: Comparison between I_2 computed numerically (green dots) and the asymptotic expansion Eq. 3.36 (blue dashed line) for the function $A(x) = K_{is_0}(x)$. The dots represent the mean of 64 MonteCarlo calculations of I_2 with error bars spanning twice the standard deviation of the samples.

3.3 Expansion for the Parallel Momentum Distribution and the Contacts

Having given asymptotic expansions for $I_1(\gamma)$ and $I_2(\gamma)$ through order γ^{-4}, we can insert these expansions in the result of Lemma 3.4 to find an expansion for the distribution of particle momenta parallel to the surface, $n(k_2, k_3)$. We will then analyze the form of this expansion and show how the two-particle and particle-surface contacts can be identified, and also how our formula qualitatively connects the two-body and particles-surface correlations to each contact.

Recall from Lemma 3.4 that

$$n(k_2, k_3) = \frac{2^6 \pi^3 L^2 \eta^2}{\beta^2} \left(I_1(\gamma) + I_2(\gamma) \right)$$

At leading order, only $I_1(\gamma)$ contributes. Because we are interested in the large momentum limit, we write the expansion in terms of the magnitude of a particle's momentum parallel to the surface,

$$k_\parallel \equiv \sqrt{k_2^2 + k_3^2}, \tag{3.37}$$

to convert

$$\frac{1}{\gamma^3} = \frac{1}{8k_\parallel^3} + \mathcal{O}\left(k_\parallel^{-5}\right) \tag{3.38}$$

and find that

$$\begin{aligned} n(k_2, k_3) &= \frac{2^7 \pi^4 L^2 \eta^2}{\beta^2 \gamma^3} \int_0^\infty |A(x)|^2 \, dx + o(\gamma^{-3}) \\ &= \frac{(2\pi)^4 L^2 \eta^2}{\beta^2 k_\parallel^3} \int_0^\infty |A(x)|^2 \, dx + o\left(k_\parallel^{-3}\right). \end{aligned}$$

Therefore by comparing with Eq. 3.1 and using the result of Appendix D we have that

$$C_2 = \frac{2\pi^2 \int_0^\infty |A(x)|^2 \, dx}{\int_{-\infty}^\infty \int_{-\infty}^\infty A(u') A(u) \left[K_0\left(\beta |u - u'|\right) + K_0\left(\beta \sqrt{u^2 + u'^2}\right) \right] du' \, du}. \tag{3.39}$$

We will turn then to the next-to-leading order terms and the particle-surface contact before remarking further on this result.

At next-to-leading order we have three contributions each from $I_1(\gamma)$ and $I_2(\gamma)$. The contribution from I_1 we have called δ_1:

$$\begin{aligned}\delta_1(\gamma) =& \frac{2\alpha_0^+\alpha_0^-}{\gamma^4} M(is_0, -is_0) + \gamma^{2is_0-4}\left(\alpha_0^-\right)^2 M(is_0, is_0) \\ &+ \gamma^{-2is_0-4}\left(\alpha_0^+\right)^2 M(-is_0, -is_0) + o\left(\gamma^{-4}\right).\end{aligned}$$

And then we have I_2,

$$\begin{aligned}I_2(\gamma) = \quad & \gamma^{-4+2is_0}(\alpha_0^-)^2 N(is_0, is_0) + \gamma^{-4-2is_0}(\alpha_0^+)^2 N(-is_0, -is_0) \\ &+ \gamma^{-4}\alpha_0^+\alpha_0^-\left(N(is_0, -is_0) + N(-is_0, is_0)\right) + o(\gamma^{-4}).\end{aligned}$$

We note that using the definition of s_0 from Eq. 2.31

$$\begin{aligned}M(is_0, -is_0) + N(is_0, -is_0) &= 4\pi\left(\text{sech}\left(\frac{\pi s_0}{2}\right) - s_0\text{tanh}\left(\frac{\pi s_0}{2}\right)\right) \\ &= 0,\end{aligned} \tag{3.40}$$

therefore, although both I_1 and I_2 give a non-oscillatory contribution at order γ^{-4}, the sum is zero for the particular value of s_0 relevant to our surface problem. This phenomenon also occurs for the Efimov effect, where no non-oscillatory terms are observed at next-to-leading order in the momentum distribution for large momenta.

For the remaining terms, note that since we assumed that A is a real function, we must have that $\alpha_0^- = (\alpha_0^+)^*$, and therefore

$$\delta_1(\gamma) + I_2(\gamma) = \gamma^{2is_0-4}(\alpha_0^-)^2\left(N(is_0, is_0) + M(is_0, is_0)\right) + \text{c.c.},$$

where c.c. stands for the complex conjugate of the prior expression. Decomposing the

complex factors into (real) phases and amplitudes, we define

$$|\alpha|e^{-i\phi_\alpha} \equiv \alpha_0^-,$$
$$|\mu|e^{-i\zeta} \equiv N(is_0, is_0) + M(is_0, is_0).$$

Recall from Eq. 2.24 that the surface parameter x_0 was introduced to make our model self-adjoint and conserve probability. The physical origin of this parameter is the short-range details of the interaction between the particles and the surface, and we showed in the previous chapter that x_0 is given by the relative phase of the first two terms in the short distance expansion of the source distribution, A. In terms of the phase we have defined above, this leads to

$$x_0^{2is_0} = e^{-2i\phi\alpha}. \tag{3.41}$$

Therefore,

$$\begin{aligned}\delta_1(\gamma) + I_2(\gamma) &= \frac{|\mu||\alpha|^2}{\gamma^4}\left((\gamma x_0)^{2is_0}e^{-i\zeta} + \text{c.c.}\right) \\ &= \frac{2|\mu||\alpha|^2}{\gamma^4}\sin\left(2s_0\log(\gamma x_0) + \left(\frac{\pi}{2} - \zeta\right)\right).\end{aligned} \tag{3.42}$$

Finally, we are ready then to substitute Eq. 3.42 into the result of Lemma 3.4 and compare our sub-leading term to the form Eq. 3.1 and we find that:

$$C_3 = \frac{(2\pi)^3 L^2\eta^2}{\beta^2}|\mu||\alpha|^2, \tag{3.43}$$
$$L(k_\parallel) = \sin\left(2s_0\log(2k_\parallel x_0) + \left(\frac{\pi}{2} - \zeta\right)\right). \tag{3.44}$$

In contrast to the Efimov effect where the analogous parameters are known only numerically [27], the numbers $|\mu|$ and ζ are not dependent on the particular collective bound state and can be computed exactly from the definitions of s_0, M, and N. We give the first few

digits below:

$$|\mu| \approx 7.730 \tag{3.45}$$

$$\zeta \approx 0.0255 \tag{3.46}$$

Together, Eqs. 3.39, 3.43, and 3.44 complete our sought after asymptotic expansion of the distribution of momenta parallel to the surface in our problem:

$$n(k_2, k_3) = \frac{C_2}{k_\parallel^3} + \frac{C_3\ L(k_\parallel)}{k_\parallel^4}$$

Interestingly, if we write our $L(k_\parallel)$ in the same way that the analogous function for the Efimov effect is written in Ref. [27], we find that the phase of the oscillations is very close to $-\pi$ (differing by only 2 parts in 1000). Despite the fact that there is no known importance to this phase, we mention it because it is a surprising coincidence, perhaps.

This expansion establishes the close connection between the short-range correlations in our system and its behavior at large momenta. When combined with the numerical scheme of Chapter 2, we have provided a method that exactly establishes the universal features of the momentum distribution and a practical method for calculating the state-dependent aspects at arbitrary scattering length. By contrast, for the Efimov effect, the universal aspects were largely treated via effective field theory techniques that, at least in part, must numerically determine the functional form and do not generally calculate the state-dependent parameters (though such calculations are in-principle possible). In addition, the state-dependent contacts have been calculated only near unitarity.

Our results also reveal a log-periodic oscillation in the system that may be measurable via time-of-flight imaging. Such log-periodic oscillations have proven challenging to measure in the past and so having additional systems that exhibit this effect may open new possibilities. Because our states are bound to the surface of the plane, it is possible that a trapping potential can be turned off even as the surface potential is left on and the

movement of particles along the surface can be imaged.

We turn now to relating the two-particle contact to changes in the energy due to changes in the scattering length and the number of small pairs of particles before returning to these result and discussing further conclusions.

3.4 The Adiabatic Derivative of the Energy

In Chapter 2, we computed the adiabatic derivative of the collective bound state energy with respect to the scattering length numerically. In this section, we give an analytic relationship between this derivative and the source distribution, $A(x)$, so that we can compare this expression with our asymptotic expansion of the single-particle parallel momentum distribution (Eq. 3.1) and establish a quantitative relationship between the two. In particular, based on the similarity to other systems with zero-range interactions, we expect that

$$\frac{dE}{d\left(-\frac{1}{a}\right)} = \frac{\alpha_E \int_0^\infty |A(x)|^2 \, dx}{\int_{-\infty}^{\infty}\int_{-\infty}^{\infty} A(x')A(x)\left[K_0\left(\beta|x-x'|\right) + K_0\left(\beta\sqrt{x^2+x'^2}\right)\right] \, dx' \, dx},$$

with α_E a constant that is independent of the source distribution. This section will show that, in fact,

$$\alpha_E = \frac{\pi\hbar^2}{m}.$$

Beginning with the Hamiltonian,

$$\hat{H} = -\frac{h^2}{2m}\left(\frac{\partial^2}{\partial x_1^2} + \frac{\partial^2}{\partial x_2^2} + \frac{\partial^2}{\partial x_3^2} + \frac{\partial^2}{\partial y_1^2} + \frac{\partial^2}{\partial y_2^2} + \frac{\partial^2}{\partial y_3^2}\right) = -\frac{h^2}{2m}\nabla^2,$$

Let $|\psi\rangle$ and $|\phi\rangle$ be normalized eigenstates of this Hamiltonian with scattering lengths a and α and eigenvalues E and E', respectively. Namely,

$$\hat{H}|\psi\rangle = E|\psi\rangle,$$
$$\hat{H}|\phi\rangle = E'|\phi\rangle.$$

Therefore, taking the adjoint of the second relation and cross-multiplying by ψ and ϕ^*,

$$\langle\phi|\hat{H}|\psi\rangle - \langle\phi|\hat{H}^\dagger|\psi\rangle = (E - E')\langle\phi|\psi\rangle.$$

Here we have avoided setting $H^\dagger = H$ as a reminder of the discussion preceding Eq. 2.24 where we found that probability is not conserved in our model unless we impose an additional boundary condition. This implies that the model is not essentially self-adjoint until we make a choice of a particular self-adjoint extension. Rewriting the left-hand side we have

$$\begin{aligned}\langle\phi|\hat{H}|\psi\rangle - \langle\phi|\hat{H}^\dagger|\psi\rangle &= \frac{-\hbar^2}{2m}\int_V \phi^*\,\nabla^2\psi - \psi\,\nabla^2\phi^*\,d^3x\,d^3y \\ &= \frac{-\hbar^2}{2m}\int_V \vec{\nabla}\cdot\left(\phi^*\,\vec{\nabla}\psi - \psi\,\vec{\nabla}\phi^*\right)\,d^3x\,d^3y,\end{aligned}$$

where $V \in \mathbb{R}^6$ is the region of configuration space where $x_1 > \delta$, $y_1 > \delta$, and $r > \epsilon$. Because the expression for the wavefunction in V is even in each coordinate, we can rewrite this as an integral over the region V' given by $|x_1| > \delta$, $|y_1| > \delta$, and $r > \epsilon$:

$$\langle\phi|\hat{H}|\psi\rangle - \langle\phi|\hat{H}^\dagger|\psi\rangle = \frac{-\hbar^2}{8m}\int_{V'} \nabla\cdot(\phi^*\nabla\psi - \psi\,\nabla\phi^*)\,d^3x\,d^3y,$$

By the divergence theorem, we can rewrite this as a flux through boundary:

$$\begin{aligned}= -\frac{\hbar^2}{8m}\Bigg[&\int_{|y_1|>\delta, r>\epsilon} (\phi^*\nabla\psi - \psi\,\nabla\phi^*)\cdot(-\hat{x_1})\,dx_2\,dx_3\,d^3y \\ &+ \int_{|x_1|>\delta, r>\epsilon} (\phi^*\nabla\psi - \psi\,\nabla\phi^*)\cdot(-\hat{y_1})\,dy_2\,dy_3\,d^3x \\ &+ \int_{|x_1|>\delta, |y_1|>\delta} (\phi^*\nabla\psi - \psi\,\nabla\phi^*)\cdot d\vec{S}\Bigg]\end{aligned}$$

$$= \frac{\hbar^2}{8m}\Bigg[\int_{|y_1|>\delta, r>\epsilon}\left(\phi^*\frac{\partial}{\partial x_1}\psi - \psi\,\frac{\partial}{\partial x_1}\phi^*\right)\,dx_2\,dx_3\,d^3y$$
$$+\int_{|x_1|>\delta, r>\epsilon}\left(\phi^*\frac{\partial}{\partial y_1}\psi - \psi\,\frac{\partial}{\partial y_1}\phi^*\right)\,dy_2\,dy_3\,d^3x$$
$$-\int_{|x_1|>\delta, |y_1|>\delta}(\phi^*\nabla\psi - \psi\,\nabla\phi^*)\cdot d\vec{S}\Bigg]$$

As $\epsilon, \frac{\delta}{\epsilon} \to 0$, the contributions from $|x_1|, |y_1| = \delta$ go to 0 independent of a and α, since the Neumann boundary condition holds independently for ψ and ϕ. The only relevant contribution then comes from the third term where $r = \epsilon$ and we can take $\delta = 0$. We make the change of variables

$$R \equiv \frac{x+y}{2} \equiv (R_1, R_2, R_3), \qquad r \equiv x - y \equiv (r_1, r_2, r_3),$$

so that

$$d\vec{S} = (-\hat{r})r^2\sin\theta\,d\theta\,d\phi\,d^3R,$$

and then substituting we have that

$$(E - E')\langle\phi|\psi\rangle = -\frac{\hbar^2}{8m}\int_{r=\epsilon}(\phi^*\nabla\psi - \psi\,\nabla\phi^*)\cdot\hat{r}\,r^2\sin\theta\,d\theta\,d\phi\,d^3R,$$

where we can use the Bethe-Peierls ansatz

$$\psi\left(R + \frac{r}{2}, R - \frac{r}{2}\right) = A(R_1)\left(\frac{1}{r} - \frac{1}{a}\right), \quad r \to 0$$
$$\phi\left(R + \frac{r}{2}, R - \frac{r}{2}\right) = B(R_1)\left(\frac{1}{r} - \frac{1}{\alpha}\right), \quad r \to 0.$$

to find that

$$\begin{aligned}(E-E')\langle\phi|\psi\rangle &= -\frac{\pi\hbar^2\epsilon^2}{m}\int_{r=\epsilon}\left(\phi^*\frac{\partial}{\partial r}\psi-\psi\,\frac{\partial}{\partial r}\phi^*\right)\,d^3R \\ &= -\frac{4\pi^3\eta^2\hbar^2}{\beta^2 m}\left(\frac{1}{\alpha}-\frac{1}{a}\right)\int_{\mathbb{R}^3}B(R_1)A(R_1)\,d^3R \\ &= -\frac{8\pi^3L^2\eta^2\hbar^2}{\beta^2 m}\left(\frac{1}{\alpha}-\frac{1}{a}\right)\int_0^\infty A(x)B(x)\,dx,\end{aligned}$$

where we have again used the fact that A and B are even functions, as in the previous chapter. In the limit then that $\alpha \to a$, $E' \to E$, $B \to A$,

$$\frac{E-E'}{1/\alpha-1/a} \to \frac{dE}{d\left(-\frac{1}{a}\right)} = \frac{8\pi^3L^2\eta^2\hbar^2}{\beta^2 m}\int_0^\infty A(x)^2\,dx.$$

Therefore we can write the adiabatic derivative of the energy with respect to the scattering length using the normalization result of Appendix D as,

$$\frac{dE}{d\left(-\frac{1}{a}\right)} = \frac{\pi\hbar^2}{m}\frac{\int_0^\infty|A(x)|^2\,dx}{\int_{-\infty}^\infty\int_{-\infty}^\infty A(x')A(x)\left[K_0\left(\beta|x-x'|\right)+K_0\left(\beta\sqrt{x^2+x'^2}\right)\right]\,dx'\,dx}. \tag{3.47}$$

Relating this back to the two-particle contact that we found in Eq. 3.3, we find that

$$\frac{dE}{d\left(-\frac{1}{a}\right)} = \frac{\hbar^2 C_2}{2\pi m}. \tag{3.48}$$

Therefore we find that as we vary the inter-particle interaction via changing the scattering length, the changes in bound state energy are completely determined by the correlation between particles at small separation, encapsulated in the two-particle contact. This validates that the contact is also an important microscopic quantity in our system.

3.5 The Probability of a Close Approach

Because the interaction is over zero-range, we expect that the change in the energy as the scattering length is varied should be related to the probability that we indeed find the two atoms in close proximity. For our system, this probability is particularly easy to calculate. The probability of finding both atoms within a small sphere of radius ϵ, which is equivalent to the average number of pairs in our system, is given by

$$P(r<\epsilon) = N_{pairs}(\epsilon) = \int_{r<\epsilon}\int_{\mathbb{R}^3} \left|\Psi\left(R+\frac{r}{2}, R-\frac{r}{2}\right)\right|^2 \, d^3R \, d^3r. \tag{3.49}$$

Recall that our wavefuction Ψ is zero whenever $x_1 < 0$ or $y_1 < 0$; however, because the functional form in the non-zero region, ψ, is even in x_1 and y_1, we can take the behavior to be non-zero everywhere, so long as we compensate with a factor of 4:

$$P(r<\epsilon) = \frac{1}{4}\int_{r<\epsilon}\int_{\mathbb{R}^3} \left|\psi\left(R+\frac{r}{2}, R-\frac{r}{2}\right)\right|^2 \, d^3R \, d^3r. \tag{3.50}$$

If we take $a >> \epsilon >> r_0$, then we can replace the wavefunction by the Bethe-Peierls ansatz in the above expression to find

$$\begin{aligned}
P(r<\epsilon) &= \frac{\pi^2|\eta|^2}{\beta^2}\int_{r<\epsilon}\int_{\mathbb{R}^3} |A(R_1)|^2 \left(\frac{1}{|r|}-\frac{1}{a}\right)^2 \, d^3R \, d^3r \\
&= \frac{4\pi^3 L^2|\eta|^2}{\beta^2}\int_{-\infty}^{\infty}|A(x)|^2\,dx \int_0^{\epsilon}\left(\frac{1}{|r|}-\frac{1}{a}\right)^2 r^2 dr \\
&= \frac{8\pi^3 L^2|\eta|^2}{\beta^2}\left(\epsilon - \frac{\epsilon^2}{a}+\frac{\epsilon^3}{3a^2}\right)\int_0^{\infty}|A(x)|^2\,dx \\
&= \frac{8\pi^3 L^2|\eta|^2\epsilon}{\beta^2}\int_0^{\infty}|A(x)|^2\,dx + \mathcal{O}(\epsilon^2).
\end{aligned}$$

Comparing this with our expression for the adiabatic derivative of the energy, Eq. 3.47,

the two are proportional with the very simple relationship

$$\frac{dE}{d\left(-\frac{1}{a}\right)} = \frac{\hbar^2}{m}\frac{dN(\epsilon)}{d\epsilon}\bigg|_{\epsilon=0}. \tag{3.51}$$

This relationship requires some comment because it may be somewhat counter-intuitive. Because the set of exactly overlapping configurations is measure zero in configuration space, of course the probability of having exactly that configuration must be zero. So we cannot meaningfully talk about the number of particles that are exactly overlapping, for instance. However, what we find is that the more the particles are concentrated in an infinitesimal region around 0 separation, the greater the change in energy when we change the scattering length, which agrees with our intuition.

3.6 Conclusion

The expansion, Eq. 3.1, along with the results Eqs. 3.39 and 3.43 fully determine the two-particle and particle-surface contacts in terms of the source distribution A. For any particular scattering length, these expressions can be used to calculate the contacts from the analytical or numerical results presented in Chapter 2. In addition, our expansion makes clear that regardless of the particular state under consideration, the two-particle contact is determined by the behavior of the source distribution throughout the region of configuration space where two-particles are close together. Our results in Sections 3.47, 3.4, and 3.5 also connect the short-range inter-particle and particle-surface correlations with the energy, the change in the energy due to changes in the microscopic parameters, and the number of small pairs found in our system. Almost everything about the state seems to be determined by what happens in a small region of configuration space where particles closely approach each other (and potentially collide).

Our result also makes clear that the parallel momentum distribution undergoes log periodic oscillations at next-to-leading order, with the phase and log-period of the oscillations

dependent on the short distance surface physics, but not the scattering length or the particular collective bound state in question. The particular state does, however, affect the overall amplitude of these oscillations, but only through the behavior of the system very near the surface. The greater the probability of finding two nearby particles close to the surface, the greater the amplitude, since the wavefunction,

$$\begin{aligned} |\Psi|^2 &\propto |A(x)|^2, \quad r \to 0 \\ &\propto |\alpha|^2, \quad r \to 0, x \to 0, \end{aligned}$$

according to Eqs. 2.6 and 2.23.

We also hope that these calculations may be useful if some systematic connection between the contact for few-body states and that for many-body states is found in the future (for example, perhaps if a gas of such states near a surface is stable).

Part II

Efimov Effect

CHAPTER 4

EFIMOV TRIMER CONTACTS AT THE THREE ATOM THRESHOLD

As we have discussed previously (see Section 1.5), a system of three bosons interacting via zero-range forces can form a three-body bound state, known as an Efimov trimer, with properties that depend on just two parameters derived from the inter-particle potential: the scattering length (which describes the low-energy scattering of two partcles, see Section 1.2) and the Efimov parameter (which specifies the phase shift due to three-particle scattering at low energy). The signature of this state has been observed experimentally in bosonic systems ranging from three atoms to millions, and a detailed understanding of its properties has helped explain resonances and log-periodic oscillations observed in many-body systems.

In this thesis, we have already investigated the importance of the contact, first defined by Tan, as a microscopic parameter that relates the short distance two-body or three-body correlations in a system to its macroscopic properties, including its internal energy, pressure, rate of transition between internal states, and response to small changes in the inter-particle potential. Because the Efimov effect has such notable three-body correlations, we would expect that the associated contact plays an important role in any many-body states strongly influenced by the presence of the Efimov effect. Calculating the contact of a state, though, remains a difficult challenge. The most common approach in the literature is to first find the wavefunction of a system and from there extract the contacts. However, the wavefunction can rarely be found analytically, which limits the availability of analytical calculations of the contact. For example, the only point at which the wavefunction of the Efimov trimer is known in closed form is at the unitarity limit (scattering length, $a \to \pm\infty$) and thus the two-body contact of the Efimov trimer is known analytically only at unitarity [75]. However, this limit is not the only interesting point for Efimov physics. Another exceptional set

of points is the three atom threshold, which is reached at a set of critical negative scattering lengths where the least-bound Efimov trimer disappears into the continuum of three free particles. Experimentally, these points have been used to identify Efimov trimer resonances and measure their scaling ratio due to the easily observable peak in the three-body loss rate [82, 83]. The three-body loss rate itself of course depends on how particles are correlated at short distances, where three particles approach each other, and thus has been shown to be proportional to the three-body contact of the state [28]. We therefore hope that a precise calculation of the two- and three-body contacts of the Efimov trimer at the three-atom threshold will be useful when investigating these important points.

In this chapter we will demonstrate that the Efimov trimer state can be characterized by solving a particular singular integral equation, similar in form to that of Chapter 2. We will construct the solution to a transformed version of this integral equation when the binding energy of the trimer is zero. We find a solution to the three-boson problem at zero binding energy and negative scattering using the main idea of Ref. [23], although we begin from a more general starting point. By analyzing this solution and its governing equation, we show how to find an analytical expression for the trimer two-body contact in terms of the binding wavenumber at unitarity (the so-called three-body parameter) and use this expression to also find the trimer three-body contact at the three atom threshold.

4.1 A Singular Integral Equation for the Efimov Trimer

Consider a system of 3 bosonic particles with positions denoted $x, y, z \in \mathbb{R}^3$, respectively. If the inter-particle potential, with characteristic length scale r_0, decreases at large separation faster than an inverse quadratic potential, then for energies where the characteristic wavenumber, k, of the system is small (and therefore the characteristic size is large) such that $kr_0 << 1$ and the thermal de Broglie wavelength is large such that $\Lambda >> r_0$, then we expect that the system properties should depend only weakly on the particular shape of the inter-particle potential. It should then be possible to categorize potentials into equivalence

classes such that their properties are approximately the same below the appropriate scale.

For the case of two interacting particles, the interacting Schrödinger Equation can be replaced by the free Schrödinger equation supplemented with the Bethe-Peierls boundary condition, Eq. 1.14, which results in a model that depends only on the scattering length of the underlying potential. Rather than developing approximate results based on a specific choice of potential, we instead work in this model where the scattering length is the only relevant two-body parameter at all scales, with the understanding that the results will only be physically meaningful at scales large compared to that of the potential.

In the case of three particles, the same procedure applies modulo the complication that the space of possible models is larger and requires that both the scattering length and an additional three-body parameter be specified. This three-body parameter specifies the behavior of the wavefuntion in the region of configuration space where all three particles are interacting [27].

We implement the Bethe-Peierls boundary condition in the same manner as we have previously. In particular, our system of 3 identical bosons obeys the free Schrödinger equation so long as no pair of particles is coincident,

$$-\frac{\hbar^2}{2m}\left(\nabla^2 - E\right)\psi(x,y,z) = 0, \tag{4.1}$$

with $x, y, z \in \mathbb{R}^3$ the positions of the three identical bosons,

$$\nabla^2 = \sum_{i=1}^{3} \frac{\partial^2}{\partial x_i^2} + \frac{\partial^2}{\partial y_i^2} + \frac{\partial^2}{\partial z_i^2},$$

and $|x-y| > 0$, $|x-z| > 0$, $|y-z| > 0$. We can describe this system using any of the

three equivalent sets of Jacobi coordinates defined by

$$
\begin{aligned}
R &= \frac{1}{3}(x+y+z) \\
s_1 &= y-z, \quad t_1 = \frac{y+z}{2} - x \\
s_2 &= z-x, \quad t_2 = \frac{z+x}{2} - y \\
s_3 &= x-y, \quad t_3 = \frac{x+y}{2} - z
\end{aligned}
$$

where R is the center of mass of the system, each of the s_i is the separation between one pair of particles, and the t_i are the position of the third particle relative to the center of mass of the first two. The Laplacian in the Jacobi coordinates labeled by j becomes

$$
\nabla^2 = \sum_{i=1}^{3} \frac{1}{3}\frac{\partial^2}{\partial R_{j,i}^2} + \frac{3}{2}\frac{\partial^2}{\partial t_{j,i}^2} + 2\frac{\partial^2}{\partial s_{j,i}^2}.
$$

As we have done in the two-body case, we augment the free Schrödinger equation with a non-homogeneous term that is relevant only when at least two of the atoms are coincident:

$$
-\left(\nabla^2 - 2\kappa^2\right)\phi(t,s,R) = \sum_{i=1}^{3} f(R,t_i)\delta(s_i), \tag{4.3}
$$

The weight f must match the Bethe-Peierls boundary condition,

$$
\phi(t,s,R) \sim_{s\to 0} f(R,t)\left(\frac{1}{s} - \frac{1}{a}\right), \tag{4.4}
$$

and we will find the consistency condition that f must satisfy in this section. The general strategy will be analogous to previous chapters. First, we write a formal solution to the inhomogeneous Schrödinger equation as an integral involving f and the Green's function for the free Schrödinger equation. We then analyze the behavior of that solution in the region where two particles are nearly coincident, and match this behavior to the Bethe-

Peierls boundary condition. We find a match only if f satisfies a certain linear, singular integral equation, and finding a solution to this equation, and by extension the full problem, will occupy the later sections of this chapter.

As a first step, we can eliminate the dependence on the center of mass coordinate, R. If we make the ansatz that

$$\phi(t, s, R) = D(R)\Phi(t, s),$$

then this factorization must also hold when two particles coincide, and therefore

$$f(R, t_i) = D(R)G(t_i).$$

Substituting this into Eq. 4.3 we can rearrange so that

$$\frac{\nabla_R^2 D(R)}{3D(R)} = -\frac{1}{\Phi(t_1, s_1)}\left[\left(\frac{3}{2}\nabla_t^2 + 2\nabla_s^2 - 2\kappa^2\right)\Phi(t_1, s_1) + \sum_{i=1}^{3} G(t_i)\delta(s_i)\right].$$

Since the left-hand side is a function solely of R, while the right-hand side is a function solely of t and s, they are equal if and only if both sides are, in fact, constant:

$$\nabla_R^2 D(R) = 3k^2 D(R),$$

$$-\left(\frac{3}{2}\nabla_t^2 + 2\nabla_s^2 - 2\beta^2\right)\Phi(t, s) = \sum_{i=1}^{3} G(t_i)\delta(s_i), \tag{4.5}$$

with $2\beta^2 \equiv 2\kappa^2 - k^2$. The center of mass motion is unimportant for our purposes, so we will not mention $C(R)$ further. Eq. 4.5 is another example of the six dimensional Helmholtz equation, the Green's function of which is derived in Appendix A. By linearity, we can write the complete solution as a sum over three terms, each of which corresponds to one of

the inhomogeneous terms:

$$\Phi(t,s) = \eta \sum_{i=1}^{3} \int_{\mathbb{R}^6} \frac{K_2\left(\beta\sqrt{\frac{4}{3}(t_i-t')^2+(s_i-s')^2}\right)}{\frac{2}{3}(t_i-t')^2+\frac{1}{2}(s_i-s')^2} G(t')\delta(s')\, d^3t'\, d^3s'$$
$$= \eta \sum_{i=1}^{3} \int_{\mathbb{R}^6} \frac{K_2\left(\beta\sqrt{\frac{4}{3}(t_i-t')^2+s_i^2}\right)}{\frac{2}{3}(t_i-t')^2+\frac{1}{2}s_i^2} G(t')\, d^3t'. \tag{4.6}$$

We must then determine the behavior of this solution as one of the $s_i \to 0$, and we will make use of some properties of the modified Bessel functions listed in Appendix G. Due to the bosonic symmetry, which s_i we choose is irrelevant, as the behavior will be the same in all 3 cases. Suppose that we choose s_1, we can rewrite our solution so that it is expressed solely in terms of $s \equiv s_1$ and $t \equiv t_1$, and we find that

$$\Phi(t,s) = \Phi_1(t,s) + \Phi_2(t,s), \tag{4.7}$$

where

$$\Phi_1(t,s) \equiv \eta \int_{\mathbb{R}^3} \left[\frac{K_2\left(\beta\sqrt{\frac{4}{3}(t^2+t\cdot t'+t'^2)+2s\cdot t'+s^2}\right)}{\frac{2}{3}(t^2+tt'+t'^2)+s\cdot t'+\frac{1}{2}s^2} \right.$$
$$\left. + \frac{K_2\left(\beta\sqrt{\frac{4}{3}(t^2+t\cdot t'+t'^2)-2s\cdot t'+s^2}\right)}{\frac{2}{3}(t^2+t\cdot t'+t'^2)-s\cdot t'+\frac{1}{2}s^2} \right] G(t')\ d^3t', \tag{4.8}$$

$$\Phi_2(t,s) \equiv \eta \int_{\mathbb{R}^3} \frac{K_2\left(\beta\sqrt{\frac{4}{3}(t-t')^2+s^2}\right)}{\frac{2}{3}(t-t')^2+\frac{1}{2}s^2} G(t')\ d^3t'. \tag{4.9}$$

To state an important result, we first need to introduce a new notation,

$$⨍_a^c \frac{f(x)}{(x-b)^2}\, dx \equiv \lim_{\epsilon\to 0}\left[\int_a^{b-\epsilon} \frac{f(x)}{(x-b)^2}\, dx + \int_{b+\epsilon}^{c} \frac{f(x)}{(x-b)^2}\, dx - \frac{2f(b)}{\epsilon} \right].$$

The dashed integral represents a Hadamard finite part [84], which is identical to the Riemann integral for Riemann integrable functions, but assigns a finite value to integrals of

functions with quadratic singularity at $b \in (a, c)$ and f continuous. We can the state the following useful result,

Lemma 4.1.

$$\Phi(t,s) = \frac{3\sqrt{3}\eta\pi}{2\beta}\left(\frac{\Pi(t)}{s} + \Lambda(t)\right) + \mathcal{O}(s), \quad s \to 0, \tag{4.10}$$

with

$$\begin{aligned}
\Pi(t) &\equiv \frac{\pi}{\beta}G(t) \\
\Lambda(t) &\equiv \fint_0^\infty \left[\frac{K_1\left(\frac{2\beta}{\sqrt{3}}\big||t| - |t'|\big|\right)}{\big||t| - |t'|\big|} - \frac{K_1\left(\frac{2\beta}{\sqrt{3}}\big||t| + |t'|\big|\right)}{\big||t| + |t'|\big|}\right. \\
&\quad \left. - 4\frac{K_1\left(\frac{2\beta}{\sqrt{3}}\sqrt{t^2 + t'^2 + |t||t'|}\right)}{\sqrt{t^2 + t'^2 + |t||t'|}} + 4\frac{K_1\left(\frac{2\beta}{\sqrt{3}}\sqrt{t^2 + t'^2 - |t||t'|}\right)}{\sqrt{t^2 + t'^2 - |t||t'|}}\right]\frac{t'G\left(t'\right)}{t}\, d|t'|.
\end{aligned}$$

Proof. Considering the Φ_1 contribution of Eq. 2.66, at least when $t \neq 0$, the integrand is bounded for all t' and we may exchange the integral with the limit and simply set $s = 0$:

$$\begin{aligned}
\Phi_1(t,s) &= \lim_{s\to 0}\eta\int_{\mathbb{R}^3}\left[\frac{K_2\left(\beta\sqrt{\frac{4}{3}(t^2 + t\cdot t' + t'^2) + 2s\cdot t' + s^2}\right)}{\frac{2}{3}(t^2 + t\cdot t' + t'^2) + s\cdot t' + \frac{1}{2}s^2}\right. \\
&\qquad \left. + \frac{K_2\left(\beta\sqrt{\frac{4}{3}(t^2 + t\cdot t' + t'^2) - 2s\cdot t' + s^2}\right)}{\frac{2}{3}(t^2 + t\cdot t' + t'^2) - s\cdot t' + \frac{1}{2}s^2}\right]G\left(t'\right)\, d^3t' \\
&= 3\eta\int_{\mathbb{R}^3}\frac{K_2\left(\beta\sqrt{\frac{4}{3}(t^2 + |t||t'|\cos\theta + t'^2)}\right)}{t^2 + |t||t'|\cos\theta + t'^2}G\left(t'\right)\, d^3t'
\end{aligned} \tag{4.11}$$

At this point, we will specialize to s-wave states by assuming that $G(t)$ is independent of the direction of t and so we can carry out the angular integrals,

$$\begin{aligned}
\Phi_1(t,s) = \frac{6\sqrt{3}\eta\pi}{\beta}\int_0^\infty &\left[\frac{t'K_1\left(\beta\sqrt{\frac{4}{3}(t^2 - |t||t'| + t'^2)}\right)}{t\sqrt{t^2 + t'^2 - |t||t'|}}\right. \\
&\left. - \frac{t'K_1\left(\beta\sqrt{\frac{4}{3}(t^2 + |t||t'| + t'^2)}\right)}{t\sqrt{t^2 + t'^2 + |t||t'|}}\right]G\left(t'\right)\, d|t'|.
\end{aligned} \tag{4.12}$$

For the $\Phi_2(t,s)$ contribution we will make the same assumption and integrate out the angles first,

$$\Phi_2(t,s) = \lim_{s\to 0}\left[\Phi_S(t,s) + \Phi_R(t,s)\right], \tag{4.13}$$

where

$$\Phi_S(t,s) \equiv \frac{3\pi\eta}{\beta}\int_0^\infty \frac{t' K_1\left(\beta\sqrt{\frac{4}{3}(|t|-|t'|)^2+s^2}\right)}{t\sqrt{\frac{4}{3}(|t|-|t'|)^2+s^2}} G\left(t'\right)\ d|t'| \tag{4.14}$$

$$\Phi_R(t,s) \equiv -\frac{3\pi\eta}{\beta}\int_0^\infty \frac{t' K_1\left(\beta\sqrt{\frac{4}{3}(|t|+|t'|)^2+s^2}\right)}{t\sqrt{\frac{4}{3}(|t|+|t'|)^2+s^2}}\Bigg] G\left(t'\right)\ d|t'|. \tag{4.15}$$

The integrand of Φ_R again has no singularity as $s\to 0$ and so we can again pass the limit inside the integral for that term. For Φ_S, however, we will treat the singularity by dividing the region of integration into two components. Let

$$s << \epsilon << \frac{1}{\beta},$$

then divide the region of integration into $|t|-|t'|>\epsilon$ and $|t|-|t'|<\epsilon$:

$$\begin{aligned}\Phi_S(t,s) =& \frac{3\eta\pi}{\beta}\int_{|t|-|t'|<\epsilon} \frac{t' K_1\left(\beta\sqrt{\frac{4}{3}(|t|-|t'|)^2+s^2}\right)}{t\sqrt{\frac{4}{3}(|t|-|t'|)^2+s^2}} G\left(t'\right)\ d|t'| \\ &+ \frac{3\eta\pi}{\beta}\int_{|t|-|t'|>\epsilon} \frac{t' K_1\left(\beta\sqrt{\frac{4}{3}(|t|-|t'|)^2+s^2}\right)}{t\sqrt{\frac{4}{3}(|t|-|t'|)^2+s^2}} G\left(t'\right)\ d|t'|.\end{aligned}$$

When $|t|-|t'|>\epsilon$, the integrand remains bounded for all s and so we again exchange the integral and limit. However, within $|t|-|t'|<\epsilon$, we cannot neglect s compared to $|t|-|t'|$

throughout the entire region. We can, though, make two other approximations,

$$G\left(t'\right) = G\left(t\right) + \mathcal{O}(\epsilon), \quad t' \to t$$

$$\frac{t' K_1\left(\beta\sqrt{\frac{4}{3}(|t|-|t'|)^2+s^2}\right)}{t\sqrt{\frac{4}{3}(|t|-|t'|)^2+s^2}} = \frac{|t'|}{\beta|t|(\frac{4}{3}(|t|-|t'|)^2+s^2)} + \mathcal{O}(\log\beta\epsilon), \quad t' \to t, s \to 0$$

since within this region $\beta\sqrt{\frac{4}{3}(|t|-|t'|)^2+s^2} \sim \mathcal{O}(\beta\epsilon) << 1$. Applying these approximations to Φ_S,

$$\begin{aligned}
&\int_{|t|-|t'|<\epsilon} \frac{t' K_1\left(\beta\sqrt{\frac{4}{3}(|t|-|t'|)^2+s^2}\right)}{t\sqrt{\frac{4}{3}(|t|-|t'|)^2+s^2}} G\left(t'\right)\ d|t'| \\
&= G\left(t\right)\int_{|t|-|t'|<\epsilon} \frac{|t'|}{\beta|t|(\frac{4}{3}(|t|-|t'|)^2+s^2)}\ d|t'| + \mathcal{O}(\epsilon).
\end{aligned}$$

We can perform this integral and then take a series of limits, first letting $s \to 0$ and then letting $\epsilon \to 0$ in such a way that $\frac{s}{\epsilon} \to 0$, and we find that the only non-zero contributions to this integral in the limit are

$$\begin{aligned}
\lim_{s\to 0}\left[\frac{3\pi}{\beta}\int_{|t|-|t'|<\epsilon} \frac{t' K_1\left(\beta\sqrt{\frac{4}{3}(|t|-|t'|)^2+s^2}\right)}{t\sqrt{\frac{4}{3}(|t|-|t'|)^2+s^2}} G\left(|t'|\right)\ d|t'|\right] \\
\sim \frac{3\sqrt{3}\pi^2 G(|t|)}{2\beta^2 s} - \frac{9\pi G(|t|)}{2\epsilon\beta^2}. \qquad (4.16)
\end{aligned}$$

Therefore, combining the results of Eq. 4.16 with the straightforward limit of Φ_R, we find

that

$$\begin{aligned}\Phi_2(t,s) =& \frac{3\sqrt{3}\eta\pi^2 G(|t|)}{2\beta^2 s} - \frac{3\pi\eta}{\beta}\int_0^\infty \frac{t' K_1\left(\beta\sqrt{\frac{4}{3}(|t|+|t'|)^2}\right)}{t\sqrt{\frac{4}{3}(|t|+|t'|)^2}} G\left(t'\right)\ d|t'| \\ &+ \lim_{\epsilon\to 0}\left[\frac{3\eta\pi}{\beta}\int_{|t|-|t'|>\epsilon} \frac{t' K_1\left(\beta\sqrt{\frac{4}{3}(|t|-|t'|)^2}\right)}{t\sqrt{\frac{4}{3}(|t|-|t'|)^2}} G\left(t'\right)\ d|t'| - \frac{9\eta\pi G(|t|)}{2\epsilon\beta^2}\right] \\ &+ \mathcal{O}(s). \end{aligned} \tag{4.17}$$

It is easy to check that

$$\begin{aligned}&⨍_0^\infty \left[\frac{K_1\left(\frac{2\beta}{\sqrt{3}}\big||t|-|t'|\big|\right)}{\big||t|-|t'|\big|}\frac{t' G\left(t'\right)}{t}\ d|t'|\right. \\ &\left. = \lim_{\epsilon\to 0}\left[\int_{|t|-|t'|>\epsilon} \frac{t' K_1\left(\beta\sqrt{\frac{4}{3}(|t|-|t'|)^2}\right)}{t\sqrt{(|t|-|t'|)^2}} G\left(t'\right)\ d|t'| - \frac{3G(|t|)}{2\epsilon\beta}\right]\right.. \end{aligned}$$

If we then combine the Φ_1 contributions from Eq. 4.12 with those of Φ_2 from Eq. 4.17 we find that

$$\begin{aligned}\Phi(t,s) =& \frac{3\sqrt{3}\eta\pi}{2\beta}\left[\frac{\pi G(|t|)}{\beta s} - \int_0^\infty \frac{t' K_1\left(\beta\sqrt{\frac{4}{3}(|t|+|t'|)^2}\right)}{t\sqrt{(|t|+|t'|)^2}} G\left(|t'|\right)\ d|t'|\right. \\ &+ 4\int_0^\infty \left[\frac{t' K_1\left(\frac{2}{\sqrt{3}}\beta\sqrt{t^2+t'^2-|t||t'|}\right)}{t\sqrt{t^2+t'^2-|t||t'|}} - \frac{t' K_1\left(\frac{2}{\sqrt{3}}\beta\sqrt{t^2+t'^2+|t||t'|}\right)}{t\sqrt{t^2+t'^2+|t||t'|}}\right] G\left(|t'|\right)\ d|t'| \\ &\left. + ⨍_0^\infty \frac{t' K_1\left(\frac{2\beta}{\sqrt{3}}\big||t|-|t'|\big|\right)}{t\big||t|-|t'|\big|} G\left(t'\right)\ d|t'|\right] + \mathcal{O}(s), \quad s\to 0, \end{aligned} \tag{4.18}$$

so that finally, as desired,

$$\Phi(t,s) = \frac{3\sqrt{3}\eta\pi}{2\beta}\left(\frac{\Pi(t)}{s} + \Lambda(t)\right) + \mathcal{O}(s), \quad s\to 0, \tag{4.19}$$

□

The Bethe-Peierls condition for this system can be written as

$$\Phi(t,s) = B(t)\left(\frac{1}{s} - \frac{1}{a}\right), \tag{4.20}$$

and by comparing this to the result of Lemma 4.1 we find that

$$B(t) = \frac{3\sqrt{3}\eta\pi^2}{2\beta^2} G(t), \tag{4.21}$$

and further that

$$\begin{aligned}\frac{\pi G(t)}{\beta a} = \fint_0^\infty \Bigg[&\frac{t' K_1\left(\frac{2\beta}{\sqrt{3}}\big||t|+|t'|\big|\right)}{t\big||t|+|t'|\big|} - \frac{t' K_1\left(\frac{2\beta}{\sqrt{3}}\big||t|-|t'|\big|\right)}{t\big||t|-|t'|\big|} \\ &+ 4\frac{t' K_1\left(\frac{2\beta}{\sqrt{3}}\sqrt{t^2+t'^2+|t||t'|}\right)}{t\sqrt{t^2+t'^2+|t||t'|}} - 4\frac{t' K_1\left(\frac{2\beta}{\sqrt{3}}\sqrt{t^2+t'^2-|t||t'|}\right)}{t\sqrt{t^2+t'^2-|t||t'|}}\Bigg] G(t')\ d|t'|.\end{aligned}$$

Simplifying by writing in terms of $A(\frac{2}{\sqrt{3}}|t|) \equiv t\ G(t)$ and making the substitutions $u = \frac{2}{\sqrt{3}}|t|$, $u' = \frac{2}{\sqrt{3}}|t'|$, we finally arrive at the final form of the integral equation that must be satisfied for the Efimov effect,

$$\begin{aligned}\frac{\pi}{\beta a} A(u) = \fint_0^\infty \Bigg[&\frac{K_1\left(\beta\big|u+u'\big|\right)}{\big|u+u'\big|} - \frac{K_1\left(\beta\big|u-u'\big|\right)}{\big|u-u'\big|} \\ &+ 4\frac{K_1\left(\beta\sqrt{u^2+u'^2+uu'}\right)}{\sqrt{u^2+u'^2+uu'}} - 4\frac{K_1\left(\beta\sqrt{u^2+u'^2-uu'}\right)}{\sqrt{u^2+u'^2-uu'}}\Bigg] A(u')\ du'. \end{aligned} \tag{4.22}$$

This integral equation allows for very accurate calculations of the binding energy of Efimov trimers at arbitrary scattering length via methods similar to those in Section 2.4. Since it is a single relationship for a function of just one variable, it can be solved much more efficiently than numerical calculations of the full wavefunction or hyperspherical approaches that must use several coupled equations. It can also be used to find the source distribution and reconstruct the spatial profile of an Efimov trimer. In this work, however, we will focus on the zero binding energy limit of this relation and its solution.

4.2 Solution for Zero Energy Trimers

In the limit that the binding energy of the trimer approaches zero while the scattering length remains finite (as opposed to the case of weakly bound trimers at unitarity where $\beta \to 0$, but $\beta a \to \infty$), our integral equation reduces to the simplified form:

$$\frac{\pi}{a} A(u) = \int_0^\infty \left[\frac{1}{\left(u+u'\right)^2} - \frac{1}{\left(u-u'\right)^2} + \frac{4}{u^2+u'^2+uu'} - \frac{4}{u^2+u'^2-uu'} \right] A(u') \; du'. \tag{4.23}$$

If we rewrite this relation in terms of the Mellin transform,

$$A(u) = \frac{1}{2\pi i} \int_{c-i\infty}^{c+i\infty} X(\nu) \left(\frac{u}{|a|} \right)^{-\nu} \; d\nu, \tag{4.24}$$

which we will later abbreviate by

$$X(\nu) = \mathcal{M}(A, \nu).$$

Substituting into 4.23, we find that

$$\begin{aligned} &\int_{c-i\infty}^{c+i\infty} X(\nu) \left(\frac{u}{|a|} \right)^{-\nu} \; d\nu \\ &= \text{sign}(a) \int_{c-i\infty}^{c+i\infty} \nu \cot\left(\frac{\pi\nu}{2}\right) \left(1 - \frac{8 \sin\left(\frac{\pi\nu}{6}\right)}{\sqrt{3}\nu \cos\left(\frac{\pi\nu}{2}\right)} \right) X(\nu) \left(\frac{u}{|a|} \right)^{-\nu-1} \; d\nu, \end{aligned}$$

provided at least that $c \in (-2, 2)$ so that the contour in the complex plane lies entirely within the strip of analyticity $-2 < \text{Re}(\nu) < 2$. So long as we can choose c so that the Mellin transform $X(\nu)$ has no poles in the region $c-1 < \text{Re}(\nu) < c$, then we can displace

the contour of the integral on the left hand side so that

$$\int_{c-i\infty}^{c+i\infty} X(\nu)\left(\frac{u}{|a|}\right)^{-\nu} d\nu$$
$$= \text{sign}(a)\int_{c-1-i\infty}^{c-1+i\infty} \nu\cot\left(\frac{\pi\nu}{2}\right)\left(1-\frac{8\sin\left(\frac{\pi\nu}{6}\right)}{\sqrt{3}\nu\cos\left(\frac{\pi\nu}{2}\right)}\right) X(\nu)\left(\frac{u}{|a|}\right)^{-\nu-1} d\nu.$$

Then we relabel $\nu \to \nu - 1$ on the right-had side

$$\int_{c-i\infty}^{c+i\infty} X(\nu)\left(\frac{u}{|a|}\right)^{-\nu} d\nu$$
$$= \text{sign}(a)\int_{c-i\infty}^{c+i\infty} (\nu-1)\cot\left(\frac{\pi(\nu-1)}{2}\right)$$
$$\times\left(1-\frac{8\sin\left(\frac{\pi(\nu-1)}{6}\right)}{\sqrt{3}(\nu-1)\cos\left(\frac{\pi(\nu-1)}{2}\right)}\right) X(\nu-1)\left(\frac{u}{|a|}\right)^{-\nu} d\nu.$$

Since the Mellin transform is invertible within the fundamental strip, we have that

$$X(\nu) = \text{sign}(a)(\nu-1)\cot\left(\frac{\pi(\nu-1)}{2}\right)\left(1-\frac{8\sin\left(\frac{\pi(\nu-1)}{6}\right)}{\sqrt{3}(\nu-1)\cos\left(\frac{\pi(\nu-1)}{2}\right)}\right) X(\nu-1),$$

provided that we take ν to be within $-1 < \text{Re}(\nu) < 1$ so that the integrals converge in the usual sense. For negative scattering lengths,

$$X(\nu+1) = -\nu\cot\left(\frac{\pi\nu}{2}\right)\left(1-\frac{8\sin\left(\frac{\pi\nu}{6}\right)}{\sqrt{3}\nu\cos\left(\frac{\pi\nu}{2}\right)}\right) X(\nu). \tag{4.25}$$

A solution to this functional relation can be constructed by considering the various

factors:

$$
\begin{aligned}
X_1(\nu+1) &= \nu\, X_1(\nu), \\
X_2(\nu+1) &= \cot\left(\frac{\pi\nu}{2}\right) X_2(\nu), \\
X_3(\nu+1) &= \left(\frac{8\sin\left(\frac{\pi\nu}{6}\right)}{\sqrt{3}\nu\cos\left(\frac{\pi\nu}{2}\right)} - 1\right) X_3(\nu).
\end{aligned}
$$

The first two relations are well known and can be solved immediately,

$$
\begin{aligned}
X_1(\nu) &= \Gamma(\nu), \\
X_2(\nu) &= \sin\left(\frac{\pi\nu}{2}\right).
\end{aligned}
$$

For the third, we use the Weierstrass-Hadamard Factorization Theorem discussed in Appendix F. This allows us to rewrite

$$
\left(\frac{8\sin\left(\frac{\pi\nu}{6}\right)}{\sqrt{3}\nu\cos\left(\frac{\pi\nu}{2}\right)} - 1\right) = -\prod_{p=0}^{\infty}\frac{\nu^2-u_p^2}{\nu^2-b_p^2},
$$

where the b_p are the poles of the function being represented, $b_p = 2p+1,\ p \in \mathbb{N}$, the u_p are the set of zeroes, and $u_0 = is_0$ is the only complex zero with positive imaginary part. All the remaining u_p are the positive zeroes arranged in increasing order.

We will solve this third relation factor by factor as we first demonstrated in Section 2.3.3. The same discussion of how to accommodate the negative sign applies to this case as it did the case of how to solve Equation 2.41. Associating this sign with any factor except that corresponding to u_0 will cause the solution to have a sequence of poles within the necessary critical strip, $-2 < \mathrm{Re}(\nu) < 2$. Whereas, associating it with the u_0 factor leaves the strip $0 < \mathrm{Re}(\nu) < 2$ free of poles and thus wide enough to be consistent with displacing the contour as we have done above. Combining these elements, we then have

the full solution, which is equivalent to that of [23],

$$X(\nu) = F(\nu) \prod_{p=1}^{\infty} \frac{\Gamma(u_p + \nu)\Gamma(1 + b_p - \nu)}{\Gamma(1 + u_p - \nu)\Gamma(b_p + \nu)}, \tag{4.26}$$

$$F(\nu) \equiv \Gamma(\nu) \sin\left(\frac{\pi\nu}{2}\right) \frac{\Gamma(-is_0 + \nu)\Gamma(is_0 + \nu)\Gamma(2 - \nu)}{\Gamma(1 + \nu)}. \tag{4.27}$$

From this representation of the solution, we can identify a useful reflection identity, similar to that observed in the Riemann zeta function. Replacing $\nu \to 1 - \nu$ interchanges the numerator and denominator of the infinite product and therefore

$$\begin{aligned} X(\nu)X(1-\nu) &= F(\nu)F(1-\nu) \\ &= \frac{\pi^3}{\cosh(2\pi s_0) - \cos(2\pi\nu)}. \end{aligned} \tag{4.28}$$

This solution and the reflection relation that follows from it will be integral to our calculation of the contacts in the following sections.

4.3 The Two-body Contact at Threshold

The function $X(\nu)$ completely determines the wavefunction of the Efimov trimer at threshold and so in principle all of the properties of the state are known. However, calculating such properties with the infinite product representation is difficult since there is no closed-form representation of the zeroes, u_p. However, some properties depend on the solution in a combination that removes any need to consider the infinite product by using the reflection formula Eq. 4.28 and the recurrence relation Eq. 4.25. We are then left to compute the values of a set of integrals in the complex ν plane involving only elementary meromorphic functions, all of which can be evaluated by the residue theorem. One such property is the two-body contact, which characterizes the probability that two atoms closely approach each other.

Letting $\hat{n}(\vec{r}) \equiv \psi^\dagger(\vec{r})\psi(\vec{r})$ be the number density operator, then the contact can be

found from the pair correlation function [25, 28]

$$\begin{aligned}\langle \hat{n}(x)\hat{n}(y)\rangle &= 6\int_{\mathbb{R}^3} |\psi(x,y,z)|^2 \; d^3z \\ &= \frac{C_2}{16\pi^2|x-y|^2}, \quad x \to y,\end{aligned} \tag{4.29}$$

where

$$C_2 \equiv \lim_{k\to\infty} k^4 n(k)$$

$$n(k) = 3\int_{\mathbb{R}^3}\int_{\mathbb{R}^3} \left|\widetilde{\psi}(k,k',k'')\right|^2 \; \frac{d^3k'}{(2\pi)^3}\,\frac{d^3k''}{(2\pi)^3}$$

is the single-particle momentum distribution normalized such that

$$\int_{\mathbb{R}^3} n(k)\,\frac{d^3k}{(2\pi)^3} = 3.$$

By applying the Bethe-Peierls boundary condition to Eq. 4.30 we can calculate

$$\langle \hat{n}(x)\hat{n}(y)\rangle = \frac{81|\eta|^2\pi^4}{2\beta^4|x-y|^2}\int_{\mathbb{R}^3} |G\left(|t|\right)|^2 \; d^3t, \tag{4.30}$$

which then leads to

$$\begin{aligned}C_2 &= \frac{648|\eta|^2\pi^6}{\beta^4}\int_{\mathbb{R}^3} |G\left(|t|\right)|^2 \; d^3t \\ &= \frac{2592|\eta|^2\pi^7}{\beta^4}\int_{\mathbb{R}^+} \left|A\left(\frac{2}{\sqrt{3}}|t|\right)\right|^2 \; d|t| \\ &= \frac{1296\sqrt{3}|\eta|^2\pi^7}{\beta^4}\int_0^\infty |A\left(y\right)|^2 \; dy.\end{aligned} \tag{4.31}$$

We are then left to calculate both the L^2 norm of the function $A(y)$ and the normalization constant $|\eta|^2$. We will tackle these in turn.

4.3.1 The L^2 norm of $A(y)$

By the Parseval theorem for the Mellin transform [85], we have that

$$\int_0^\infty |A(y)|^2 \, dy = \frac{1}{2\pi i|a|} \int_{c-i\infty}^{c+i\infty} X(\nu)X(1-\nu) \, d\nu, \tag{4.32}$$

with $0 < c < 1$. By Eq. 4.28, this combination is known in closed form and we find

$$\begin{aligned} \frac{1}{2\pi i|a|} \int_{c-i\infty}^{c+i\infty} X(\nu)X(1-\nu) \, d\nu &= \frac{1}{2\pi i|a|} \int_{c-i\infty}^{c+i\infty} \frac{\pi^3}{\cosh(2\pi s_0) - \cos(2\pi\nu)} \, d\nu \\ &= \frac{\pi^2 s_0}{|a| \sinh 2\pi s_0} \end{aligned} \tag{4.33}$$

For now, we will merely store this calculation so that later, after we have found the normalization constant, it can be used in Eq. 4.31 to find the two-body contact.

4.3.2 The normalization constant at threshold

Taking the Fourier transform of our formal solution for the wavefunction, Eq. 4.6, we find that

$$\widetilde{\Phi}(k_s, k_t) = \frac{12\sqrt{3}\eta\pi^3}{\beta^2(\frac{3}{2}k_t^2 + 2k_s^2)} \left(\widetilde{G}(k_t) + \widetilde{G}\left(k_s - \frac{k_t}{2}\right) + \widetilde{G}\left(k_s + \frac{k_t}{2}\right) \right) \tag{4.34}$$

We can find the normalization constant by invoking the Plancherel Theorem,

$$\int_{\mathbb{R}^3} \int_{\mathbb{R}^3} |\Phi(t,s)|^2 \, d^3t_i \, d^3s_i = \int_{\mathbb{R}^3} \int_{\mathbb{R}^3} \left|\widetilde{\Phi}(k_t, k_s)\right|^2 \frac{d^3k_t}{(2\pi)^3} \frac{d^3k_s}{(2\pi)^3}.$$

Substituting the expression in Eq. 4.34 into the Plancheral Theorem, we can rewrite $\widetilde{G}$ in terms of its Fourier transform and integrate each of the resulting 9 terms using spherical

coordinates to find that

$$\begin{aligned}
&\int_{\mathbb{R}^3}\int_{\mathbb{R}^3}\left|\widetilde{\Phi}(k_t,k_s)\right|^2\frac{d^3k_t}{(2\pi)^3}\,\frac{d^3k_s}{(2\pi)^3}\\
&=\frac{9\sqrt{3}|\eta|^2\pi^3}{2\beta^4}\int_{\mathbb{R}^6}\left(\frac{3G(t)G(t')}{t^2+t'^2-2t\cdot t'}+\frac{4G(t)G(t')}{t^2+t'^2-t\cdot t'}+\frac{2G(t)G(t')}{t^2+t'^2+t\cdot t'}\right)\,d^3t\,d^3t'\\
&=\frac{81\sqrt{3}|\eta|^2\pi^5}{\beta^4}\int_0^\infty\int_0^\infty\left(\log\left(\frac{y+y'}{y-y'}\right)+4\text{ArcTanh}\left(\frac{y\,y'}{y^2+y'^2}\right)\right)A^*(y)\,A(y')\;dy\,dy'.
\end{aligned}\tag{4.35}$$

Therefore, normalizing the wavefunction to unity we find that

$$|\eta|^2=\left(\frac{81\sqrt{3}\pi^5}{\beta^4}\int_0^\infty\int_0^\infty h(y,y')A^*(y)\,A(y')\;dy\,dy'\right)^{-1},\tag{4.36}$$

where

$$h(y,y')\equiv\left(\log\left(\frac{y+y'}{y-y'}\right)+4\text{ArcTanh}\left(\frac{y\,y'}{y^2+y'^2}\right)\right)$$

In order to evaluate this expression, we need to recast it in terms of the Mellin transform, $X(\nu)$, for which we have an explicit solution. Given that the functions above are not particularly simple, it may seem far-fetched that rewriting using the Mellin transform creates any great simplification. However, the clever observer may discover that this integral is in convolution form for the Mellin transform. We can therefore reorganize by defining

$$H(y')\equiv\int_0^\infty\left(\log\left(\frac{1+\frac{y'}{y}}{1-\frac{y'}{y}}\right)+4\text{ArcTanh}\left(\frac{\frac{y'}{y}}{1+\frac{y'^2}{y^2}}\right)\right)(yA^*(y))\,\frac{dy}{y}$$

and replace $A(y')$ with its Mellin transform so that the normalization constant is given by

$$\begin{aligned}
|\eta|^{-2}&=\frac{81\sqrt{3}\pi^5}{\beta^4}\frac{1}{2\pi i}\int_{c-i\infty}^{c+i\infty}X(\nu)\int_0^\infty H(y')\left(\frac{y'}{|a|}\right)^{-\nu}\,dy'\,d\nu\\
&=\frac{81\sqrt{3}\pi^5}{\beta^4}\frac{1}{2\pi i}\int_{c-i\infty}^{c+i\infty}X(\nu)\mathcal{M}(H,1-\nu)\,d\nu.
\end{aligned}$$

Recall that we have determined earlier that we must choose $0<c<1$. Because H is a

Mellin convolution, its transform is a product in the Mellin space,

$$\begin{aligned}\mathcal{M}(H,1-\nu) &= \mathcal{M}\left(\log\left(\frac{1+y}{1-y}\right)+4\text{ArcTanh}\left(\frac{y}{1+y^2}\right),1-\nu\right)\mathcal{M}(yA(y),1-\nu)\\ &= \left(\frac{2\pi\left(\sqrt{3}\sin\left(\frac{\pi\nu}{6}\right)-\cos\left(\frac{\pi\nu}{6}\right)\right)}{(\nu-1)\sin\left(\frac{\pi\nu}{2}\right)}-\frac{\pi\cot\left(\frac{\pi\nu}{2}\right)}{\nu-1}\right)X(2-\nu).\end{aligned}$$

Further, note that we can use the recurrence relation Eq. 4.25 to write

$$X(2-\nu)=\left((\nu-1)\tan\left(\frac{\pi\nu}{2}\right)+\frac{8\cos\left(\frac{\pi\nu}{6}+\frac{\pi}{3}\right)}{\sqrt{3}\cos\left(\frac{\pi\nu}{2}\right)}\right)X(1-\nu).$$

and therefore the normalization constant is given by the integral

$$\begin{aligned}|\eta|^{-2} &= \frac{81\sqrt{3}\pi^5}{\beta^4}\frac{1}{2\pi i}\int_{c-i\infty}^{c+i\infty}\left(h_1(\nu)+h_2(\nu)+h_3(\nu)-\pi\right)X(\nu)X(1-\nu)\,d\nu\\ &= \frac{81\sqrt{3}\pi^5}{\beta^4}\frac{1}{2\pi i}\int_{c-i\infty}^{c+i\infty}\frac{\pi^3\left(h_1(\nu)+h_2(\nu)+h_3(\nu)-\pi\right)}{\cosh 2\pi s_0-\cos 2\pi\nu}\,d\nu\\ &= \frac{81\sqrt{3}\pi^5}{\beta^4}J\end{aligned}$$

where

$$\begin{aligned}J &\equiv \frac{1}{2\pi i}\int_{c-i\infty}^{c+i\infty}\frac{\pi^3\left(h_1(\nu)+h_2(\nu)+h_3(\nu)-\pi\right)}{\cosh 2\pi s_0-\cos 2\pi\nu}\,d\nu,\\ h_1(\nu) &\equiv \frac{2\pi\left(\sqrt{3}\sin\left(\frac{\pi\nu}{6}\right)-\cos\left(\frac{\pi\nu}{6}\right)\right)}{\cos\left(\frac{\pi\nu}{2}\right)},\\ h_2(\nu) &\equiv -\frac{8\pi\cos\left(\frac{\pi\nu}{6}+\frac{\pi}{3}\right)}{\sqrt{3}(\nu-1)\sin\left(\frac{\pi\nu}{2}\right)},\\ h_3(\nu) &\equiv \frac{16\pi\left(\sqrt{3}\sin\left(\frac{\pi\nu}{3}\right)+\cos\left(\frac{\pi\nu}{3}\right)-2\right)}{\sqrt{3}(\nu-1)\sin\left(\pi\nu\right)}.\end{aligned}$$

We are then left with four integrals to perform to compute J. The simplest, is propor-

tional to a result that we have already established,

$$\int_{c-i\infty}^{c+i\infty} \frac{-\pi^4}{\cosh 2\pi s_0 - \cos 2\pi\nu}\, d\nu = -\frac{2\pi^4 i s_0}{\sinh(2\pi s_0)}. \tag{4.37}$$

The second,

$$\int_{c-i\infty}^{c+i\infty} \frac{h_1(\nu)\pi^3}{\cosh 2\pi s_0 - \cos 2\pi\nu}\, d\nu = \int_{c-i\infty}^{c+i\infty} \frac{2\pi^4\left(\sqrt{3}\sin\left(\frac{\pi\nu}{6}\right) - \cos\left(\frac{\pi\nu}{6}\right)\right)}{\cos\left(\frac{\pi\nu}{2}\right)(\cosh 2\pi s_0 - \cos 2\pi\nu)}\, d\nu,$$

can be established by dividing the integrand into even and odd parts, $h_1^+(\nu)$ and $h_1^-(\nu)$, respectively:

$$h_1^+(\nu) \equiv \frac{-2\pi^4 \cos\left(\frac{\pi\nu}{6}\right)}{\cos\left(\frac{\pi\nu}{2}\right)(\cosh 2\pi s_0 - \cos 2\pi\nu)},$$
$$h_1^-(\nu) \equiv \frac{2\sqrt{3}\pi^4 \sin\left(\frac{\pi\nu}{6}\right)}{\cos\left(\frac{\pi\nu}{2}\right)(\cosh 2\pi s_0 - \cos 2\pi\nu)}.$$

Note for both parts that the integrand is meromorphic with poles due to the factor $\sec\left(\frac{\pi\nu}{2}\right)$ at $\nu = 2j+1,\ j \in \mathbb{Z}$ and also due to the factor $(\cosh 2\pi s_0 - \cos 2\pi\nu)^{-1}$ at $\nu = \pm i s_0 + j,\ j \in \mathbb{Z}$. For the odd part, consider a rectangular rectangular contour in the complex ν plane centered at the origin,

$$\begin{aligned}\lim_{R\to\infty}\Bigg[&\int_{c-iR}^{c+iR} h_1^-(\nu)X(\nu)X(1-\nu)\, d\nu + \int_{c+iR}^{-c+iR} h_1^-(\nu)X(\nu)X(1-\nu)\, d\nu \\ &+ \int_{-c+iR}^{-c-iR} h_1^-(\nu)X(\nu)X(1-\nu)\, d\nu + \int_{-c-iR}^{c-iR} h_1^-(\nu)X(\nu)X(1-\nu)\, d\nu\Bigg] \\ &= 2\pi i \sum_{\nu=\pm i s_0} \text{Res}(h_1^-(\nu)X(\nu)X(1-\nu)).\end{aligned}$$

The integrand is exponentially decreasing for large imaginary part, and therefore the contributions from the sides with fixed imaginary part vanish in the limit. Further, the integrand is odd and so the contributions from sides with fixed but opposite real part are identical.

Therefore,

$$\int_{c-i\infty}^{c+i\infty} h_1^-(\nu)X(\nu)X(1-\nu)\,d\nu = \pi i \sum_{\nu=\pm is_0} \text{Res}(h_1^-(\nu)X(\nu)X(1-\nu)) = \frac{3i\pi^4 s_0}{4\sinh(2\pi s_0)}.$$

The even portion of the integrand is more difficult because there is no clear way to exploit the periodicity to relate a single integral to a finite sum of poles. However, if we could close our vertical line with a semi-circle in the right half-plane then the sum of these two contributions would be given by an infinite sum over all poles to the right of our line. Unfortunately, the integrand does not necessarily decrease for large real ν and so the contribution from the infinite arc cannot immediately be neglected. We can remedy this defect by considering the more general integral,

$$I(\alpha) = \int_{c-i\infty}^{c+i\infty} h_1^+(\nu)X(\nu)X(1-\nu)e^{-\alpha\nu}\,d\nu.$$

Let $c = \frac{1}{2}$ and note that for $\alpha \geq 0$

$$\int_{\frac{1}{2}-i\infty}^{\frac{1}{2}+i\infty} \left|h_1^+(\nu)X(\nu)X(1-\nu)e^{-\alpha\nu}\right|\,d\nu \leq \int_{-\infty}^{\infty} \frac{1}{\sqrt{3}\cosh\left(\frac{\pi y}{3}\right)-1}\,dy = \frac{6\sqrt{2}}{\pi}\arctan\left(\frac{1+\sqrt{3}}{\sqrt{2}}\right),$$

and therefore by dominated convergence we have that

$$\int_{c-i\infty}^{c+i\infty} h_1^+(\nu)X(\nu)X(1-\nu)\,d\nu = \lim_{\alpha\to 0} I(\alpha)$$

To compute $I(\alpha)$, then, we can close the contour with a semi-circle in the right half-plane and the circular arc will now give 0 contribution due to the exponential decrease in the real

and imaginary directions. Therefore,

$$I(\alpha) = -2\pi i\Bigg(\sum_{j=1}^{\infty} \text{Res}\left(h_2^+(j \pm is_0)X(j \pm is_0)X(1-j \pm is_0)e^{-\alpha(j \pm is_0)}\right) + \sum_{j=0}^{\infty} \text{Res}\left(h_2^+(2j+1)X(2j+1)X(1-2j+1)e^{-\alpha(2j+1)}\right)\Bigg).$$

These sums appear daunting, but can be computed thanks to the periodicity of the integrand. Evaluating and taking the limit, we find that

$$I(0) = \frac{i\pi^3\left(\cosh\left(\frac{\pi s_0}{3}\right) + 3\cosh\left(\frac{2\pi s_0}{3}\right)\right)}{\sqrt{3}\cosh(\pi s_0)\sinh^2(\pi s_0)} - \frac{4i\pi^3}{\sqrt{3}\sinh^2(\pi s_0)}, \tag{4.38}$$

and therefore the full calculation involving $h_1(\nu)$ gives

$$\begin{aligned}\int_{c-i\infty}^{c+i\infty} h_1(\nu)X(\nu)X(1-\nu)\,d\nu = &\ \frac{3i\pi^4 s_0}{4\sinh(2\pi s_0)} - \frac{4i\pi^3}{\sqrt{3}\sinh^2(\pi s_0)} \\ &+ \frac{i\pi^3\left(\cosh\left(\frac{\pi s_0}{3}\right) + 3\cosh\left(\frac{2\pi s_0}{3}\right)\right)}{\sqrt{3}\cosh(\pi s_0)\sinh^2(\pi s_0)}\end{aligned} \tag{4.39}$$

Precisely the same procedure can be applied to the integrals involving h_2 and h_3: multiply by a convergence factor so that the contour can be closed in the right half-plane, find the sum over all the residues, then take the limit that the convergence factor goes to 1

everywhere. Applying this procedure for h_2 we have

$$\begin{aligned}
&\int_{c-i\infty}^{c+i\infty} \frac{\pi^3 h_2(\nu)}{\cosh 2\pi s_0 - \cos 2\pi\nu}\, d\nu = \frac{8\pi^4 i \operatorname{arccoth}(2)}{\sqrt{3}\sinh^2(\pi s_0)} \\
&- \frac{8\pi^4 i \cosh\left(\frac{\pi s_0}{3}\right)}{3\sqrt{3}\sinh(\pi s_0)\sinh(2\pi s_0)} \left(\Psi\left(\frac{is_0}{3}\right) + \Psi\left(\frac{-is_0}{3}\right) - \log 4\right) \\
&- \left(3i\sinh\left(\frac{\pi s_0}{6}\right) + \sqrt{3}\cosh\left(\frac{\pi s_0}{6}\right)\right)\left(\Psi\left(\frac{1}{6} + \frac{is_0}{6}\right) + \Psi\left(\frac{1}{6} - \frac{5is_0}{6}\right)\right)\Bigg) \\
&+ \left(3i\cosh\left(\frac{\pi s_0}{6}\right) + \sqrt{3}\sinh\left(\frac{\pi s_0}{6}\right)\right)\left(\Psi\left(\frac{1}{3} - \frac{is_0}{6}\right) + \Psi\left(\frac{2}{3} + \frac{is_0}{6}\right)\right) \\
&- \frac{4\pi^4 i \cosh\left(\frac{2\pi s_0}{3}\right)}{3\sqrt{3}\sinh(\pi s_0)\sinh(2\pi s_0)} \left(\Psi\left(\frac{1}{2} + \frac{is_0}{6}\right) + \Psi\left(\frac{1}{2} - \frac{is_0}{6}\right) - \Psi\left(\frac{is_0}{6}\right) - \Psi\left(-\frac{is_0}{6}\right)\right) \\
&- \frac{2\pi^4 i}{9\sinh\left(\frac{\pi s_0}{2}\right)\sinh(2\pi s_0)} \\
&\times \Bigg[\left(3i\sinh\left(\frac{\pi s_0}{6}\right) - \sqrt{3}\cosh\left(\frac{\pi s_0}{6}\right)\right)\left(\Psi\left(\frac{1}{6} - \frac{is_0}{6}\right) + \Psi\left(\frac{1}{6} + \frac{5is_0}{6}\right)\right) \\
&\quad - \left(3i\cosh\left(\frac{\pi s_0}{6}\right) - \sqrt{3}\sinh\left(\frac{\pi s_0}{6}\right)\right)\left(\Psi\left(\frac{2}{3} - \frac{is_0}{6}\right) + \Psi\left(\frac{1}{3} + \frac{is_0}{6}\right)\right)\Bigg],
\end{aligned} \tag{4.40}$$

and then for that involving h_3,

$$\begin{aligned}
&\int_{c-i\infty}^{c+i\infty} \frac{\pi^3 h_3(\nu)}{\cosh 2\pi s_0 - \cos 2\pi\nu}\, d\nu = -\frac{16i\pi^4 \log\left(\frac{4}{3}\right)}{\sqrt{3}\sinh^2(\pi s_0)} \\
&+ \frac{16i\pi^4 e^{\pi s_0}}{\sqrt{3}\sinh(\pi s_0)} \left(\Psi\left(\frac{1}{2} - \frac{is_0}{2}\right) + \Psi\left(\frac{1}{2} + \frac{is_0}{2}\right) - \Psi\left(1 - \frac{is_0}{2}\right) - \Psi\left(1 + \frac{is_0}{2}\right)\right) \\
&- \frac{16i\pi^4 \log\left(\frac{4}{3}\right) e^{-\pi s_0}}{\sqrt{3}\sinh(\pi s_0)\sinh(2\pi s_0)} \Big[B_{-\frac{1}{2}(1+i\sqrt{3})}(is_0, 0) + B_{\frac{1}{2}(-1+i\sqrt{3})}(-is_0, 0) + \\
&\qquad\qquad e^{2\pi s_0}\left(B_{-\frac{1}{2}(1+i\sqrt{3})}(-is_0, 0) + B_{\frac{1}{2}(-1+i\sqrt{3})}(is_0, 0)\right)\Big],
\end{aligned} \tag{4.41}$$

where $\Psi(x)$ is the digamma function and $B_z(a, b)$ is the incomplete beta function.

Combining the contributions from Eqs. 4.37, 4.39, 4.40, and 4.41 while simplifying

leads to the expression

$$\begin{aligned} J =&\delta_0 \Bigg[6 \left(\log \frac{256}{27} - 1 \right) \cosh\left(\pi s_0\right) + 9 \cosh\left(\frac{\pi s_0}{3} \right) - 3 \cosh\left(\frac{2\pi s_0}{3} \right) \\ &+ 2 \,\mathrm{Re} \left(\sum_{k=0}^{5} c(k) \Psi \left(\frac{k + i s_0}{6} \right) \right) \Bigg], \end{aligned} \tag{4.42}$$

with

$$\begin{aligned} \delta_0 &\equiv \frac{2\sqrt{3}\pi^3}{9 \sinh\left(\pi s_0\right) \sinh\left(2\pi s_0\right)}, \\ c(k) &\equiv 4(-1)^{k+1} + 3\cos\left(\frac{\pi(2k - i s_0)}{3} \right) + \cos\left(\frac{\pi(k - 2i s_0)}{3} \right). \end{aligned}$$

Finally for the two-body contact we can calculate,

$$\begin{aligned} C_2 &= \frac{(2\pi)^4 s_0}{J \sinh\left(2\pi s_0\right)} \frac{1}{|a|} \\ &\approx 24.72 \, |a_-|^{-1} \\ &\approx 16.40 \kappa_0, \end{aligned} \tag{4.43}$$

where we have used the value of the scattering length at the three atom threshold of Ref. [23] and κ_0 is the binding wavenumber of the trimer at unitarity. Note that we have given an exact formula for the two-body contact, so further digits of precision can be calculated if required. We give the first few digits here just for easy comparison.

The numerical value we have computed can be compared to the value of the trimer contact at unitarity, $C_2^{\infty} \approx 53.1 \kappa_0$ [75] and thus the threshold value is over 3 times smaller. It also contrasts with the threshold value for two particles interacting with a surface, which we found to be zero by combining the results of Chapters 2 and 3. We also point out that the methodology demonstrated here is not limited to this particular system. Zero-range models with discrete scaling symmetry show remarkably similar mathematical structure across different physical systems, and so we anticipate that the contact at threshold may be

calculated in a substantially similar way as that shown here.

4.4 Three-body Contact and the Relation between the Contacts and the Binding Energy

The Efimov problem can be completely specified using just two length scales: the scattering length, a which sets the two-body physics, and the three-body parameter, β_0, which specifies the result of three-particle scattering. There are several equivalent ways to choose a three-body parameter, including by specifying the scattering phase of the wavefunction in the region where three particles are nearly coincident. Here, we choose to set it by defining the binding wavenumber of a particular Efimov trimer at unitarity to be β_0, and therefore the energy will be

$$\lim_{a\to\pm\infty} E\left(\frac{1}{\beta_0 a}\right) = -\frac{\hbar^2\beta_0^2}{m}$$

at unitarity. As we tune away from unitarity, there is only one dimensionless combination of these two numbers, $\beta_0 a$, and therefore the binding energy must evolve according to a dimensionless function (Δ) of this parameter,

$$E\left(\frac{1}{a}\right) = -\frac{\hbar^2\beta_0^2}{m}\,\Delta\left(\frac{1}{\beta_0 a}\right).$$

In terms of this function, the derivatives of the binding energy can then be given by

$$\begin{aligned}
\frac{\partial E}{\partial\left(-\frac{1}{a}\right)} &= \frac{\hbar^2\beta_0}{m}\Delta'\left(\frac{1}{\beta_0 a}\right) \\
\frac{\partial E}{\partial\left(\log\beta_0\right)} &= \beta_0\frac{\partial E}{\partial\beta_0} \\
&= -\frac{2\hbar^2\beta_0^2}{m}\Delta\left(\frac{1}{\beta_0 a}\right) + \frac{\hbar^2\beta_0}{ma}\Delta'\left(\frac{1}{\beta_0 a}\right).
\end{aligned}$$

Combining these expressions to eliminate the derivative of Δ we find the relation

$$\frac{a}{2}\frac{\partial E}{\partial\left(\log\beta_0\right)} - 2\frac{\partial E}{\partial\left(-\frac{1}{a}\right)} = aE. \tag{4.44}$$

We can also replace each derivative term with its equivalent in terms of the contact,

$$\begin{aligned}\frac{\partial E}{\partial\left(-\frac{1}{a}\right)} &= \frac{\hbar^2 C_2}{8\pi m},\\ \frac{\partial E}{\partial\left(\log\beta_0\right)} &= -\frac{2\hbar^2 C_3}{m},\\ E &= -\frac{\hbar^2\beta^2}{m},\end{aligned}$$

therefore

$$C_3 + \frac{C_2}{4\pi a} = \beta^2. \tag{4.45}$$

At the trimer threshold, $\beta = 0$ and therefore the three-body contact is given by

$$\begin{aligned}C_3 &= -\frac{C_2}{4\pi a}\\ &\approx 0.866\kappa_0.\end{aligned} \tag{4.46}$$

At unitarity, the three-body contact is by definition equal to the binding wavenumber. At threshold, then, the value is quite similar: it has changed by only about 14%. Again this contrasts strongly with the case of two particles interacting with a surface, where the three-body contact will be zero at threshold.

4.5 Conclusion

Within this chapter, we have showed how the methods developed in Chapter 2 can similarly be applied to the Efimov effect. We derived a singular integral equation, constructed a solution at zero binding energy, and then used that solution to find the two- and three-body contacts at this threshold.

As presented, these results deepen the understanding of the Efimov effect and its parameters. They allow for very precise calculations of the sequence of trimer binding energies at arbitrary scattering length and also for mapping the spatial structure of Efimov trimers. When considering our calculations of the contact, a precise connection between the contact of Efimov trimers, and those of an interacting bose gas has not yet been shown. Still, we know both that the contacts describe the short-distance correlations in the trimer and that at the three-atom threshold the loss rate of atoms in a gas is significantly enhanced because the three free atom state can form a meta-stable trimer before recombining. We hope, therefore, that the calculation of these contacts will be relevant to further investigations and measurements at such resonances and similar resonances in other systems.

Appendices

APPENDIX A

GREEN'S FUNCTION OF THE 6D HELMHOLTZ EQUATION WITH HOMOGENEOUS NEUMANN BOUNDARY CONDITIONS

The 6D free time-independent Schrödinger Equation is just a 6D Helmholtz equation, whose Green's function satisfies

$$\nabla^2 G\left(\vec{r}, \vec{r_0}\right) - \kappa^2 G\left(\vec{r}, \vec{r_0}\right) = \delta^{(6)}(\vec{r} - \vec{r_0}) \tag{A.1}$$

with the (negative) energy, $E = -\frac{\hbar^2\kappa^2}{2m}$ and $\vec{r}, \vec{r}_0 \in \mathbb{R}^6$. If we make the change of origin $\vec{r} \to \vec{r} + \vec{r_0}$ then we are left with a spherically symmetric equation. Taking the Fourier transform of this relation,

$$\widetilde{G}(\vec{k}) = \int_{\mathbb{R}^6} G\left(\vec{r}, 0\right) e^{-i\vec{k}\cdot\vec{r}}\, d^6 r,$$

where the dot product is the Euclidian one. We then have that

$$\left(-k^2 - \kappa^2\right) \widetilde{G}(\vec{k}) = 1, \tag{A.2}$$

and then via the inverse Fourier transform,

$$G\left(\vec{r}, 0\right) = \frac{1}{(2\pi)^6} \int_{\mathbb{R}^6} \frac{-1}{k^2 + \kappa^2} e^{i\vec{k}\cdot\vec{r}}\, d^6 k.$$

This expression can be evaluated using hyperspherical coordinates,

$$G\left(\vec{r}, 0\right) = \frac{1}{(2\pi)^6} \int_0^\infty \int_{\mathbb{S}^5} \frac{-e^{ikr\cos\theta_1}}{k^2 + \kappa^2} k^5\, d\Omega_5\, dk,$$

where $d\Omega_5 \equiv \sin^4\theta_1 \sin^3\theta_2 \sin^2\theta_3 \sin\theta_4 \; d\theta_1 \; d\theta_2 \; d\theta_3 \; d\theta_4 \; d\phi$ is the differential element of the 5-sphere, and after completing the angular integrals,

$$G\left(\vec{r},0\right) = -\frac{1}{(2\pi)^3}\int_0^\infty \frac{k^3 J_2(kr)}{r^2(k^2+\kappa^2)}\, dk,$$

where J_ν is the Bessel Function of the first kind of order ν. Note that

$$\frac{k^2}{r}J_2(kr) = \frac{\partial}{\partial r}\left(\frac{1}{r}\frac{\partial J_0(kr)}{\partial r}\right),$$

so that we can differentiate under the integral sign and rewrite this as

$$\begin{aligned} G\left(\vec{r},0\right) &= \frac{-1}{(2\pi)^3 r}\frac{\partial}{\partial r}\left(\frac{1}{r}\frac{\partial}{\partial r}\int_0^\infty \frac{kJ_0(kr)}{(k^2+\kappa^2)}\, dk\right), \\ &= \frac{-1}{(2\pi)^3 r}\frac{\partial}{\partial r}\left(\frac{1}{r}\frac{\partial K_0(kr)}{\partial r}\right), \end{aligned}$$

where K_ν is the modified Bessel function of the second kind of order ν. Finally, evaluating the derivatives and restoring the original origin we have

$$G\left(\vec{r},\vec{r}_0\right) = -\frac{k^2 K_2(k|\vec{r}-\vec{r}_0|)}{8\pi^3|\vec{r}-\vec{r}_0|^2}. \tag{A.3}$$

This result is not a unique solution to (A.1), but can be modified by including any linear combination of solutions to the homogeneous version of the Schrödinger equation. And for the particular case of homogeneous boundary conditions, whether Dirichlet or Neumann, this is particularly useful since any linear combination of functions satisfying such homogeneous boundary conditions will itself satisfy the same homogeneous boundary conditions. We will make use of this fact to modify our Green's function in the next subsection.

If we return to the inhomogeneous Schrödinger equation of Section 2.2 with $x, y \in \mathbb{R}^3$,

$$\nabla^2\psi(x,y) - \kappa^2\,\psi(x,y) = -8\pi\mathcal{A}\Big(\frac{x_1+x_2}{2}\Big)\delta^{(3)}(x-y), \tag{A.4}$$

a formal solution can be written down using the just derived Green's function. We write the the fundamental solution as

$$G_6\left(x,y,x',y'\right) \equiv -\frac{\kappa^2 K_2(\kappa\sqrt{|x-x'|^2+|y-y'|^2})}{\pi^2\left(|x-x'|^2+|y-y'|^2\right)} + G_{hom}\left(x,y,x',y'\right),$$

where G_{hom} is a homogeneous solution to the defining equation that will be specified later to ensure that the boundary conditions are satisfied. By the linearity of the Schrödinger equation, a solution to Eq. A.4 is then

$$\psi(x,y) = -\int_{\mathbb{R}^6} G_6\left(x,y,x',y'\right)\mathcal{A}\Big(\frac{x_1'+x_2'}{2}\Big)\delta^{(3)}(x'-y')\;d^3x'\;d^3y', \tag{A.5}$$

$$= -\int_{\mathbb{R}^3} G_6\left(x,y,x',x'\right)\mathcal{A}(x_1')\;\;d^3x', \tag{A.6}$$

$$= -\int_{\mathbb{R}^2}\int_0^\infty G_6\left(x,y,x',x'\right)\mathcal{A}(x_1')\;d^3x'. \tag{A.7}$$

The final step is justified since $A(x) \equiv 0$ when $x < 0$ because the particles are each confined to the positive half-space.

We will return to the terms involving G_{hom} to ensure we satisfy the proper boundary conditions in a moment, but first focus on the already computed contribution to the Green's function:

$$\psi_0(x,y) \equiv \frac{\kappa^2}{\pi^2}\int_{\mathbb{R}^+\times\mathbb{R}^2}\frac{K_2(\kappa\sqrt{|x-x'|^2+|y-x'|^2})}{(|x-x'|^2+|y-x'|^2)}\mathcal{A}(x_1')\;\;dx_1'\,dx_2'\,dx_3'.$$

Since only the Green's function depends on x_2' and x_3', we can explicitly compute these integrals, first by shifting the origin parallel to the surface using

$$x_2' = \frac{x_2+y_2}{2}+\rho_2,\; x_3' = \frac{x_3+y_3}{2}+\rho_3,$$

which will transform the argument of the Green's function to a more amenable form,

$$|x - x'|^2 + |y - x'|^2 = \Xi^2 + 2\left(\rho_2^2 + \rho_3^2\right),$$

where because it is a collection of constants for the purposes of this integral, we define for convenience

$$\Xi^2 \equiv (x_1 - x_1')^2 + (y_1 - x_1')^2 + \frac{1}{2}\left((x_2 - y_2)^2 + (x_3 - y_3)^2\right).$$

Our integral to compute is then

$$\int_{\mathbb{R}^2} \frac{K_2(\kappa\sqrt{\Xi^2 + 2\left(\rho_2^2 + \rho_3^2\right)})}{(\Xi^2 + 2\left(\rho_2^2 + \rho_3^2\right))}\ d\rho_2\, d\rho_3,$$

which we will do by a change to polar coordinates $\zeta^2 = 2k^2(\rho_2^2 + \rho_3^2)$, $d\rho_2\, d\rho_3 = \frac{\zeta}{2k^2} d\zeta d\theta$

$$\int_0^\infty \frac{\pi K_2(\sqrt{\kappa^2\Xi^2 + \zeta^2})}{(\kappa^2\Xi^2 + \zeta^2)} \zeta\, d\zeta = \frac{\pi K_1(\kappa\Xi)}{\kappa\Xi}.$$

Substituting this into our expression for ψ_0, we have a reduced expression for this contribution to the wavefunction;

$$\psi_0(x,y) = \frac{\kappa}{\pi}\int_0^\infty \frac{K_1(\kappa\sqrt{(x_1 - x_1')^2 + (x_2 - x_1')^2 + \frac{1}{2}\left((y_1 - y_2)^2 + (z_1 - z_2)^2\right)})}{\sqrt{(x_1 - x_1')^2 + (x_2 - x_1')^2 + \frac{1}{2}\left((y_1 - y_2)^2 + (z_1 - z_2)^2\right)}} A(x_1')\ dx_1'.$$

Or rewriting in terms of center of mass and relative coordinates,

$$R \equiv \frac{x + y}{2} = \{R_1, R_2, R_3\}, \qquad r \equiv x - y = \{r_1, r_2, r_3\},$$

$$\psi_0\left(R + \frac{r}{2}, R - \frac{r}{2}\right) = \frac{\kappa}{\pi}\int_0^\infty \frac{K_1\left(k\sqrt{2(R_1 - x')^2 + \frac{1}{2}(r_1^2 + r_2^2 + r_3^2)}\right)}{\sqrt{2(R_1 - x')^2 + \frac{1}{2}(r_1 + r_2^2 + r_3^2)}} A(x')\ dx'.$$

Enforcing the Neumann boundary conditions

Now, we can return to the question of how to choose $G_{hom}(\cdot)$ to satisfy our Neumann boundary conditions. There are two elementary facts that allow us to determine this function. The first is that if the Green's function were even in x_1 and x_2, then it would satisfy the homogeneous Neumann boundary condition. And the second is that since the homogeneous Schrödinger equation for this system has no potential and does not depend on any odd number of spatial derivatives of the wavefunction in Cartesian coordinates, from any solution, another can be found by negating any of the coordinates.

With these facts in mind, let $\hat{\sigma}_{x_i} f(x_i) \equiv f(-x_i)$ then a formal solution to our Schrödinger equation satisfying all the boundary conditions is

$$\begin{aligned}
\psi\left(R+\frac{r}{2}, R-\frac{r}{2}\right) &= \psi_0\left(R+\frac{r}{2}, R-\frac{r}{2}\right) + \hat{\sigma}_{x_1}\psi_0\left(R+\frac{r}{2}, R-\frac{r}{2}\right) \\
&\quad + \hat{\sigma}_{x_2}\psi_0\left(R+\frac{r}{2}, R-\frac{r}{2}\right) + \hat{\sigma}_{x_1}\hat{\sigma}_{x_2}\psi_0\left(R+\frac{r}{2}, R-\frac{r}{2}\right) \\
&= \frac{\kappa}{\pi}\int_0^\infty \left[\frac{K_1(\kappa\sqrt{2(R_1-x')^2+\frac{1}{2}(r_1^2+r_2^2+r_3^2)})}{\sqrt{2(R_1-x')^2+\frac{1}{2}(r_1^2+r_2^2+r_3^2)}}\right. \\
&\qquad + \frac{K_1(\kappa\sqrt{2R_1^2+\frac{1}{2}((r_1+2x')^2+r_2^2+r_3^2)})}{\sqrt{2R_1^2+\frac{1}{2}((r_1+2x')^2+r_2^2+r_3^2)}} \\
&\qquad + \frac{K_1(\kappa\sqrt{2R_1^2+\frac{1}{2}((r_1-2x')^2+r_2^2+r_3^2)})}{\sqrt{2R_1^2+\frac{1}{2}((r_1-2x')^2+r_2^2+r_3^2)}} \\
&\qquad \left. + \frac{K_1(\kappa\sqrt{2(R_1+x')^2+\frac{1}{2}(r_1^2+r_2^2+r_3^2)})}{\sqrt{2(R_1+x')^2+\frac{1}{2}(r_1^2+r_2^2+r_3^2)}}\right] A(x')\ dx'.
\end{aligned}$$

APPENDIX B

BEHAVIOR OF THE WAVEFUNCTION DURING A TRIPLE COLLISION

One special region of the configuration space is the region where the two particles are close together (and so the wavefunction approximately factorizes according to the Bethe-Peierls boundary condition) and the center of mass of the two particles is also close to the confining surface. We refer to this region where the two particles and the surface are all roughly coincident as a triple collision. Given the approximate factorization, the probability density of finding the two particles close to the surface scales as

$$|\psi(R-r, R+r)|^2 \propto |\mathcal{A}(R)|^2, \quad r \to 0.$$

And therefore the behavior of $\mathcal{A}$ at small distances corresponds to the behavior of the wavefunction during a triple collision.

To investigate this behavior more precisely, suppose as an ansatz that $\mathcal{A}$ has an asymptotic expansion

$$\mathcal{A}(x) \sim \sum_{j=0}^{\infty} \alpha_{z_j} x^{z_j}, \quad x \to 0^+,$$

where $\{z_j\}$ is a sequence of complex numbers with $\mathrm{Re}(z_j)$ strictly increasing with j. Then, z_0 has the least positive real part and is thus the most dominant term in the expansion for small x. In Eq. 2.19, we see that the kernel of our integral equation is dominated by values of x' for which the arguments of the bessel functions are small. When $\beta x << 1$, this corresponds to values such that $\beta x' << 1$. Contributions from the region of larger x' are exponentially suppressed by the decay of the kernel. Therefore, we can replace $\mathcal{A}$ by the preceding asymptotic expansion ansatz both inside and outside of the integral, and attempt a term-by-term comparison.

We divide the integral

$$I(x) \equiv \int\!\!\!\!\!\!=_0^\infty \left(\frac{K_1(\beta\sqrt{x^2+x'^2})}{\sqrt{x^2+x'^2}} + \frac{K_1(\beta(x+x'))}{x+x'} + \frac{K_1(\beta|x-x'|)}{|x-x'|} \right) x'^{z_j}\, dx' \qquad \text{(B.1)}$$
$$= I_1(x) + I_2(x) + I_3(x)$$

into three terms, two of which exist when interpreted in the ordinary sense:

$$I_1(x) \equiv \int_0^\infty \frac{K_1(\beta\sqrt{x^2+x'^2})}{\sqrt{x^2+x'^2}} x'^{z_j}\, dx' = \sqrt{\frac{(2x)^{z_j-1}}{\beta^{z_j+1}}}\Gamma\left(\frac{z_j+1}{2}\right) K_{\frac{1}{2}(z_j-1)}(\beta x)$$
$$\to \frac{\pi x^{z_j-1}}{2\beta}\sec\frac{\pi z_j}{2}, \qquad x \to 0,$$

and the more complicated expression

$$I_2(x) \equiv \int_0^\infty \frac{K_1(\beta(x+x'))}{x+x'} x'^{z_j}\, dx'$$
$$= \frac{\pi x^{z_j-1} z_j \csc \pi z_j}{\beta} {}_1F_2\left(-\frac{1}{2}; \frac{z_j+1}{2}, \frac{z_j}{2}; \frac{\beta^2 x^2}{4}\right)$$
$$- 2^{z_j-2} x \beta^{1-z_j}\Gamma\left(\frac{z_j}{2}-1\right)\Gamma\left(\frac{z_j}{2}+1\right) {}_1F_2\left(\frac{1-z_j}{2}; \frac{3}{2}, 2-\frac{z_j}{2}; \frac{\beta^2 x^2}{4}\right)$$
$$+ \frac{2^{z_j-2}}{\beta^{z_j}}\Gamma\left(\frac{z_j-1}{2}\right)\Gamma\left(\frac{z_j+1}{2}\right) {}_1F_2\left(-\frac{z_j}{2}; \frac{1}{2}, \frac{3-z_j}{2}; \frac{\beta^2 x^2}{4}\right)$$
$$\to \frac{\pi x^{z_j-1} z_j \csc \pi z_j}{\beta}, \qquad x \to 0.$$

The third, however, exists only as a Hadamard regularized integral

$$\begin{aligned} I_3(x) \equiv \fint_0^\infty & \frac{K_1(\beta|x-x'|)}{|x-x'|} x'^{z_j}\, dx' \\ &= -\frac{\pi x^{z_j-1} z_j \cot \pi z_j}{\beta} {}_1F_2\left(-\frac{1}{2}; \frac{z_j+1}{2}, \frac{z_j}{2}; \frac{\beta^2 x^2}{4}\right) \\ &\quad - 2^{z_j-3}\pi^{\frac{3}{2}} x \beta^{1-z_j} \csc\frac{\pi z_j}{2} \Gamma\left(1+\frac{z_j}{2}\right) {}_1F_2\left(\frac{1-z_j}{2}; \frac{3}{2}, 2-\frac{z_j}{2}; \frac{\beta^2 x^2}{4}\right) \\ &\quad - \frac{2^{z_j-2}\pi^{\frac{3}{2}}}{\beta^{z_j}} \Gamma\left(\frac{z_j+1}{2}\right) \sec\frac{\pi z_j}{2} {}_1F_2\left(-\frac{z_j}{2}; \frac{1}{2}, \frac{3-z_j}{2}; \frac{\beta^2 x^2}{4}\right) \\ &\to -\frac{\pi x^{z_j-1} z_j \cot \pi z_j}{\beta}, \qquad x \to 0. \end{aligned}$$

Combining all three terms when $\beta x << 1$ we have

$$\begin{aligned} I(x) &\to \frac{\pi x^{z_j-1}}{\beta} \sec\frac{\pi z_j}{2} + \frac{\pi x^{z_j-1} z_j \csc \pi z_j}{\beta} - \frac{\pi x^{z_j-1} z_j \cot \pi z_j}{\beta} \\ &= \frac{\pi x^{z_j-1}}{\beta}\left(\sec\frac{\pi z_j}{2} + z_j \tan\frac{\pi z_j}{2}\right), \quad x \to 0, \end{aligned}$$

which must be balanced against terms of the same order in x from the right hand side of the integral equation,

$$\alpha_{j-1} = \alpha_j \frac{\pi}{\beta}\left(\sec\frac{\pi z_j}{2} + z_j \tan\frac{\pi z_j}{2}\right)$$

except that by hypothesis for $j = 0$, there are no terms on the right hand side proportional to x^{z_0-1}. Therefore, the coefficient of this term must be zero, which restricts the possibilities for z_0 to solutions of the transcendental equation

$$\sec\frac{\pi z_j}{2} + z_j \tan\frac{\pi z_j}{2} = 0,$$

of which there are many solutions. We can exclude any solutions with $\mathrm{Re}(z_0) < -1$ because they would lead to a wavefunction that is too singular to be normalizable as $x \to 0$. Let $z_0 \equiv r_0 + is_0$; the remaining solutions with the smallest real part are the purely

imaginary conjugate solutions

$$z_0 = \pm i s_0,$$

where $s_0 \approx 0.72011977502$.

APPENDIX C

REVISED RESULT IN GRADSHETYN AND RHYZIK

Gradshetyn and Rhyzik Equation 6.582 claims that [67]

$$\int_0^\infty x^{\mu-1}|x-b|^{-\mu}K_\mu(|x-b|)K_\nu(x)\,dx \stackrel{?}{=} \frac{\Gamma(\frac{1}{2}-\mu)\Gamma(\mu+\nu)\Gamma(\mu-\nu)}{\sqrt{\pi}(2b)^\mu}K_\nu(b).$$

We can show that this is incorrect by considering the analytic continuation of this result to the case $\mu = 1$, which appears in our problem. Start with an integral that has the same $\mu \to 1$ limit as that above,

$$\int_0^\infty |x-b|^{-\mu}K_\mu(|x-b|)K_\nu(x)\,dx,$$

and take the Fourier transform from b to k. After then integrating over x, the result is

$$\frac{\pi^{\frac{3}{2}}\csc\pi\nu\,\Gamma(\frac{1}{2}-\mu)}{(k^2+1)^{\mu-1}2^\mu}\sin\Big(\frac{\nu}{2}\left(\pi - 2i\ \text{ArcSinh}(k)\right)\Big).$$

Luckily, when $\mu = 1$ this expression has a simple inverse Fourier transform,

$$\frac{-\pi\nu\cot\pi\nu}{x}K_\nu(x), \qquad x > 0.$$

Whereas, the result from Gradshetyn and Rhyzik reduces to

$$\frac{-\pi\nu\csc\pi\nu}{x}K_\nu(x),$$

differing by a factor $\cos \pi\nu$. And, in fact, replacing this missing factor gives an expression that is correct for all μ, ν:

$$\int_0^\infty x^{\mu-1}|x-b|^{-\mu}K_\mu(|x-b|)K_\nu(x)\,dx = \frac{\Gamma(\frac{1}{2}-\mu)\Gamma(\mu+\nu)\Gamma(\mu-\nu)\cos\pi\nu}{\sqrt{\pi}(2b)^\mu}K_\nu(b).$$

And, thus, the $\mu = 1$ case relevant to our system gives

$$⨍_0^\infty \frac{K_1(\beta|x_c-x'|)}{|x_c-x'|}K_{is}(\beta x')\,dx' = \frac{-\pi s\coth(\pi s)}{\beta x_c}K_{is}(\beta x_c).$$

APPENDIX D

WAVEFUNCTION NORMALIZATION

In this appendix we will calculate the normalization coefficient of the wavefunction for our system of two atoms resonantly interacting with a planar surface, starting from the expression for the wavefunction as an integral of the source distribution times the Green's function.

We will represent the positions of the first and second atoms by $x \equiv (x_1, x_2, x_3)$ and $y \equiv (y_1, y_2, y_3)$ respectively, and recall our choice of preferred variables,

$$R = \frac{x+y}{2} \equiv (R_1, R_2, R_3), \quad r = \frac{x-y}{2} \equiv (r_1, r_2, r_3).$$

Because the atoms are confined such that $x_1 > 0$ and $y_1 > 0$, our choice for the normalization coefficient, η, will satisfy

$$N \equiv |\eta|^2 \int_{x_1>0, y_1>0} |\psi(x,y)|^2 \, d^3x \, d^3y = 1.$$

However, since our expression for the wavefunction, Eq. 2.13, is even in both x_1 and y_1, we can rewrite this expression in terms of an integral over the whole space,

$$\frac{|\eta|^2}{4} \int_{\mathbb{R}^6} |\psi(x,y)|^2 \, d^3x \, d^3y = 1. \tag{D.1}$$

Converting to our peculiar center of mass and relative coordinates, we have

$$2|\eta|^2 \int_{\mathbb{R}^6} |\psi(R+r, R-r)|^2 \, d^3R \, d^3r = 1,$$

where the factor of 8 arises because unlike the usual Jacobi coordinates, the Jacobian matrix

of our transformation is not unitary. At this point, we can substitute in our expression for the wavefunction:

$$\psi(R+r,R-r) = \eta \int_{-\infty}^{\infty} \left[\frac{K_1(\beta\sqrt{(R_1-u')^2+r_1^2+r_2^2+r_3^2})}{\sqrt{(R_1-u')^2+r_1^2+r_2^2+r_3^2}} + \frac{K_1(\beta\sqrt{R_1^2+(r_1-u')^2+r_2^2+r_3^2})}{\sqrt{R_1^2+(r_1-u')^2+r_2^2+r_3^2}} \right] A(u')\, du', \quad \text{(D.2)}$$

$$\equiv \eta \int_{-\infty}^{\infty} \Big[G(R_1-u',r_1,r_2,r_3) + G(R_1,r_1-u',r_2,r_3) \Big] A(u')\, du',$$

and the function A is the symmetrized source distribution which appears in the Bethe-Peierls boundary condition Eq. 2.6. After substituting, there will be 4 terms:

$$\begin{aligned} N = 2|\eta|^2 \int_{\mathbb{R}^6} \int_{-\infty}^{\infty} \int_{-\infty}^{\infty} & A(u')A(u) \\ & \times \Big[G(R_1-u',r_1,r_2,r_3)\, G(R_1-u,r_1,r_2,r_3) \\ & + G(R_1-u',r_1,r_2,r_3)\, G(R_1,r_1-u,r_2,r_3) \\ & + G(R_1-u,r_1,r_2,r_3)\, G(R_1,r_1-u',r_2,r_3) \\ & + G(R_1,r_1-u',r_2,r_3)\, G(R_1,r_1-u,r_2,r_3) \Big]\, du'\, du\, d^3R\, d^3r. \end{aligned}$$

The first and fourth terms differ only by by exchanging R_1 and r_1, but since each term is symmetric under the exchange of any two arguments, and the region of integration is symmetric under such exchange, both terms have the same value. Similarly, the second and third terms differ only by exchange of u and u', but again these dummy variables are treated symmetrically and so their exchange does not alter the value. This reduces our

expression to just two terms.

$$N = 4\eta \int_{\mathbb{R}^6} \int_{-\infty}^{\infty} \int_{-\infty}^{\infty} A(u')A(u) \times \Big[G(R_1 - u', r_1, r_2, r_3)\, G(R_1 - u, r_1, r_2, r_3) + G(R_1 - u', r_1, r_2, r_3)\, G(R_1, r_1 - u, r_2, r_3) \Big]\, du'\, du\, d^3R\, d^3r.$$

Note that the integrand does not depend on R_2 or R_3 and so to regularize, we place the center-of-mass coordinates parallel to the plane in a periodic box of side length L:

$$N = 4L^2|\eta|^2 \int_{\mathbb{R}^4} \int_{-\infty}^{\infty} \int_{-\infty}^{\infty} A(u')A(u) \times \Big[G(R_1 - u', r_1, r_2, r_3)\, G(R_1 - u, r_1, r_2, r_3) + G(R_1 - u', r_1, r_2, r_3)\, G(R_1, r_1 - u, r_2, r_3) \Big]\, du'\, du\, dR_1\, d^3r.$$

Our strategy for both terms is the same; replace the function G by its Fourier transform over all 4 coordinates, integrate out the position variables and then carry out a much simpler set of integrals over the wave-numbers. To that end, we note that

$$G(\vec{q}) = \frac{1}{(2\pi)^4} \int_{\mathbb{R}^4} \frac{4\pi^2}{\beta(k^2 + \beta^2)} e^{i\vec{k}\cdot\vec{q}}\, d^4k,$$

where $q, k \in \mathbb{R}^4$ and the dot product in 4 dimensions, $\vec{k} \cdot \vec{q}$, is the Euclidian one. Inserting this identity we have

$$N = 4L^2|\eta|^2 \int_{\mathbb{R}^4} \int_{-\infty}^{\infty} \int_{-\infty}^{\infty} A(u')A(u) \times \Bigg[\frac{1}{(2\pi)^4} \int_{\mathbb{R}^4} \frac{4\pi^2 e^{-ik_1u'}}{\beta(k^2 + \beta^2)} e^{i\vec{k}\cdot\vec{s}}\, d^4k\, \frac{1}{(2\pi)^4} \int_{\mathbb{R}^4} \frac{4\pi^2 e^{-il_1u}}{\beta(l^2 + \beta^2)} e^{i\vec{l}\cdot\vec{s}}\, d^4l + \frac{1}{(2\pi)^4} \int_{\mathbb{R}^4} \frac{4\pi^2 e^{-ik_1u'}}{\beta(k^2 + \beta^2)} e^{i\vec{k}\cdot\vec{s}}\, d^4k\, \frac{1}{(2\pi)^4} \int_{\mathbb{R}^4} \frac{4\pi^2 e^{-il_2u}}{\beta(l^2 + \beta^2)} e^{i\vec{l}\cdot\vec{s}}\, d^4l \Bigg]\, du'\, du\, dR_1\, d^3r,$$

where $s \equiv (R_1, r_1, r_2, r_3)$.

$$
\begin{aligned}
&= \frac{4L^2|\eta|^2}{\beta^2} \int_{-\infty}^{\infty}\int_{-\infty}^{\infty}\int_{\mathbb{R}^4}\int_{\mathbb{R}^4} A(u')A(u) \\
&\qquad\qquad \times\left[\frac{e^{-ik_1u'}}{(k^2+\beta^2)}\frac{e^{-il_1u}}{(l^2+\beta^2)}\delta^4(\vec{k}+\vec{l})\right. \\
&\qquad\qquad \left. +\ \frac{e^{-ik_1u'}}{(k^2+\beta^2)}\frac{e^{-il_2u}}{(l^2+\beta^2)}\delta^4(\vec{k}+\vec{l})\right] d^4k\, d^4l\, du'\, du \\
&= \frac{4L^2|\eta|^2}{\beta^2} \int_{-\infty}^{\infty}\int_{-\infty}^{\infty}\int_{\mathbb{R}^4} A(u')A(u)\left[\frac{e^{ik_1(u-u')}}{(k^2+\beta^2)^2}+\frac{e^{-ik_1u'+ik_2u}}{(k^2+\beta^2)^2}\right] d^4k\, du'\, du,
\end{aligned}
$$

which can be evaluated relatively straight-forwardly by using spherical coordinates in the k-space to find that

$$
N = \frac{8\pi^2L^2|\eta|^2}{\beta^2} \int_{-\infty}^{\infty}\int_{-\infty}^{\infty} A(u')A(u)\left[K_0\left(\beta|u-u'|\right)+K_0\left(\beta\sqrt{u^2+u'^2}\right)\right] du'\, du.
$$

Imposing our normalization condition that $N = 1$, we have that

$$
|\eta|^2 = \left(\frac{8\pi^2L^2}{\beta^2} \int_{-\infty}^{\infty}\int_{-\infty}^{\infty} A(u')A(u)\left[K_0\left(\beta|u-u'|\right)+K_0\left(\beta\sqrt{u^2+u'^2}\right)\right] du'\, du\right)^{-1}.
$$

Throughout this work, we have adopted the condition that the wavefunction is normalized to unity3 . However, when comparing to other published results, it is important to remember that a different convention is often used. In particular, it is also common to find the wavefunction normalized such that for a system of N identical bosons with $\vec{r}_i$ the position of the ith particle and $\vec{k}_i$ its wavenumber,

$$
\int_{\mathbb{R}^{3N}} |\Psi\left(\vec{r}_1, ..., \vec{r}_N\right)|^2 d^{3N}r = \int_{\mathbb{R}^{3N}} |\widetilde{\Psi}\left(\vec{k}_1, ..., \vec{k}_N\right)|^2 \frac{d^{3N}k}{(2\pi)^{3N}} = N. \tag{D.3}
$$

Within this convention, we will have a new normalization constant ζ $\left(|\zeta| = \sqrt{2}|\eta|\right)$.

Our asymptotic results of Chapter 3 are unaffected modulo the replacement of $|\eta|$ with

$|\zeta|$. For instance, we will have that

$$\frac{1}{(2\pi)^4}\int_{-\infty}^{\infty}\int_{\mathbb{R}^3}|\widetilde{\Psi}(q,k)|^2\,d^3q\,dk_1 \sim \frac{(2\pi)^4L^2\zeta^2}{\beta^2k_\parallel^3}\int_0^\infty |A(x)|^2\,dx + \mathcal{O}(k_\parallel^{-4}); \tag{D.4}$$

however, our other results will take a different form because at some point in the calculation we have divided by the L^2 norm of the wavefunction.

In particular we have that

$$N_{pairs}(\epsilon) = \frac{\int_{r<\epsilon}\int_{\mathbb{R}^3}\left|\Psi\left(R+\frac{r}{2},R-\frac{r}{2}\right)\right|^2\,d^3R\,d^3r}{\int_{\mathbb{R}^3}\int_{\mathbb{R}^3}\left|\Psi\left(R+\frac{r}{2},R-\frac{r}{2}\right)\right|^2\,d^3R\,d^3r}$$

$$= \frac{1}{2}\int_{r<\epsilon}\int_{\mathbb{R}^3}\left|\Psi\left(R+\frac{r}{2},R-\frac{r}{2}\right)\right|^2\,d^3R\,d^3r$$

$$\sim \frac{4\pi^3L^2|\zeta|^2\epsilon}{\beta^2}\int_0^\infty |A(x)|^2\,dx + \mathcal{O}(\epsilon^2). \tag{D.5}$$

And similarly that the adiabatic derivative of the energy with respect to the scattering length is given by

$$\frac{dE}{d\left(-\frac{1}{a}\right)} = \frac{4\pi^3L^2\zeta^2\hbar^2}{\beta^2 m}\int_0^\infty A(x)^2\,dx. \tag{D.6}$$

As expected, this does not alter the relationship between $N_{pairs}(\epsilon)$ and $\frac{dE}{d\left(-\frac{1}{a}\right)}$,

$$\frac{dE}{d\left(-\frac{1}{a}\right)} = \frac{\hbar^2}{m}\lim_{\epsilon\to 0}\frac{N_{pairs}(\epsilon)}{\epsilon}, \tag{D.7}$$

however if the contact, C_2 is still defined as the coefficient of the leading order term in our asymptotic expansion, then the relations between both quantities above and C_2 are altered such that

$$\frac{dE}{d\left(-\frac{1}{a}\right)} = \frac{\hbar^2}{4\pi m}C_2, \quad N_{pairs}(\epsilon) = \frac{C_2}{4\pi}\epsilon + \mathcal{O}(\epsilon^2) \tag{D.8}$$

APPENDIX E

PROOF OF CONVERGENCE TO THE NEAREST ROOT USING NEWTON-RAPHSON METHOD

Although the Newton-Raphson method applied to a smooth function often converges to *some* root, conditions which guarantee convergence, and particularly guarantee convergence to a nearby root, are somewhat involved. For example, even for some cubic polynomials, the basins of attraction to each root exhibit a fractal structure [86].

In this appendix, however, we prove that the initial guesses $u_{p,0} = 2p$ are "sufficiently close" to the true solutions of

$$z(u) \equiv 1 + u \sin\left(\tfrac{\pi u}{2}\right) = 0 \tag{E.1}$$

such that each guess converges to the closest root of $z(u)$, and for each positive root, one of the $u_{0,p}$ converges to it. The main element in the proof is a theorem by Kantorovich which gives sufficient conditions for such convergence to a unique nearby root [87, 88]:

Theorem E.1 (The Newton-Kantorovich Theorem)**.** *Let $F : \Omega \subseteq X \to Y$ be a twice continuously differentiable operator defined on a non-empty open convex domain Ω of a Banach space X with values in a Banach space Y. Suppose that*

- *There exists the non-singular operator $\Gamma_0 = [F'(x_0)]^{-1}$ for some $x_0 \in \Omega$ with $\| \Gamma_0 \| \leq \beta$ and $\| \Gamma_0 F(x_0) \| \leq \eta$*
- *$\| F''(x_0) \| \leq M$, for $x \in \Omega$.*

Let $s^* = \frac{1-\sqrt{1-2M\beta\eta}}{M\beta}$ and $s^{**} = \frac{1+\sqrt{1-2M\beta\eta}}{M\beta}$. If $M\beta\eta < \frac{1}{2}$, and the closed ball $\overline{B(x_0, s^*)} \subseteq$

Ω, then the Newton's sequence given by

$$\begin{aligned} &x_0 \in \Omega \\ &x_n = x_{n-1} - [F'(x_{n-1})]^{-1} F(x_{n-1}),\ n \in \mathbb{N} \end{aligned} \tag{E.2}$$

converges to the unique solution x^* of $F(x) = 0$ in $B(x_0, s^{**}) \cap \Omega$, with every $x_n \in \overline{B(x_0, s^*)}$ and hence $x^* \in \overline{B(x_0, s^*)}$.

In our case, then, $z : \mathbb{R} \to \mathbb{R}$ is a smooth function and it is simple to check that

$$\beta_p = \left| \frac{1}{z'(2p)} \right| = \frac{1}{\pi p} \neq 0, \tag{E.3}$$

$$\eta_p = \left| \frac{z(2p)}{z'(2p)} \right| = \frac{1}{\pi p}. \tag{E.4}$$

It remains then to find intervals Ω_p over which $z''(u)$ is bounded such that $2M_p\beta_p\eta_p < 1$ for each p. Note that the first Newton step

$$d_0(p) = -\frac{z(2p)}{z'(2p)} = \frac{(-1)^p}{\pi p}, \tag{E.5}$$

and so we will seek to bound the second derivative on $u \in (2p - \frac{1}{\pi p}, 2p + \frac{1}{\pi p})$.

Lemma E.2. *For $u \in \Omega_p = (2p - \frac{1}{\pi p}, 2p + \frac{1}{\pi p})$, $z''(u)$ is monotonic.*

Proof. Consider the third derivative

$$z'''(2p + \epsilon) = \frac{(-1)^{p+1}\pi^2}{8} \left(\pi(2p + \epsilon) \cos\left(\tfrac{\pi\epsilon}{2}\right) + 6 \sin\left(\tfrac{\pi\epsilon}{2}\right) \right). \tag{E.6}$$

The second derivative fails to be monotonic only if $z'''(u) = 0$ for some $u \in \Omega_p$, which requires that

$$\pi(2p + \epsilon) \cos\left(\tfrac{\pi\epsilon}{2}\right) + 6 \sin\left(\tfrac{\pi\epsilon}{2}\right) = 0. \tag{E.7}$$

At least for $\epsilon \in [0, 1]$, the left-hand side is strictly positive for positive p, and therefore there

can be no zero. For $\epsilon \in (-\frac{1}{3}, 0)$, both terms in Eq. E.7 are increasing, therefore the sum is increasing. Note that for $\epsilon = -\frac{1}{3}$,

$$\begin{aligned}\pi(2p - \tfrac{1}{3})\cos\left(-\tfrac{\pi}{6}\right) + 6\sin\left(-\tfrac{\pi}{6}\right) &= \pi\frac{6p-1}{2\sqrt{3}} - 3 \\ &\geq \frac{5\pi}{2\sqrt{3}} - 3 > 0, \quad p \in \mathbb{N}^+.\end{aligned}$$

Therefore the left-hand side of Eq. E.7 is positive and increasing throught $\epsilon \in (-\frac{1}{3}, 1)$ for all $p \in \mathbb{N}^+$, and so the third derivative has no zeroes in this interval. Since for any $p > 1,\ \Omega_p \subset (2p - \frac{1}{3}, 2p + 1)$, the second derivative is therefore monotonic throughout each Ω_p. □

Lemma E.3. *For all $p \in \mathbb{N}^+$, let $M_p = \sup_{u\in\Omega_p} z''(u)$, then $M_p\beta_p\eta_p < \frac{1}{2}$*

Proof. Since the second derivative is monotonic throughout each Ω_p, it suffices to check the boundary to bound the magnitude.

We have that

$$\left|z''\left(2p - \frac{1}{\pi p}\right)\right| = \left|\frac{\pi}{4p}\left(4p\cos\left(\tfrac{1}{2p}\right) + (2\pi p^2 - 1)\sin\left(\tfrac{1}{2p}\right)\right)\right|, \tag{E.8}$$

$$\left|z''\left(2p + \frac{1}{\pi p}\right)\right| = \left|\frac{\pi}{4p}\left(4p\cos\left(\tfrac{1}{2p}\right) - (2\pi p^2 + 1)\sin\left(\tfrac{1}{2p}\right)\right)\right|. \tag{E.9}$$

For $p = 1$ we can check directly that

$$\begin{aligned}M_1\beta_1\eta_1 &= \left|z''\left(2 - \tfrac{1}{\pi}\right)\right| \frac{|z(2)|}{|z'(2)|} \\ &\approx 0.48 < \tfrac{1}{2}\end{aligned} \tag{E.10}$$

While for $p \geq 2$ we use that $\cos x \leq 1$, $\sin x \leq x$, and for $A, B > 0$, $|A - B| \leq$

Max$(|A|, |B|)$ to find

$$\left|z''\left(2p - \frac{1}{\pi p}\right)\right| \leq \pi\left(1 + \frac{\pi}{4}\right), \qquad \left|z''\left(2p + \frac{1}{\pi p}\right)\right| \leq \pi\left(\frac{1}{8p^2} + \frac{\pi}{4}\right). \tag{E.11}$$

Our bound on the second derivative will then be

$$|z''(u)| \leq M_p \leq \pi\left(1 + \frac{\pi}{4}\right), \quad u \in \Omega_p, \tag{E.12}$$

and so

$$\begin{aligned} M_p\beta_p\eta_p &\leq \frac{1}{p^2}\left(1 + \frac{\pi}{4}\right) \\ &\leq \frac{1}{2}, \qquad\qquad p \geq 2 \end{aligned} \tag{E.13}$$

□

These results allow us to prove the following theorem

Theorem E.4. *Let* $\{u_i\}$, $i \in \mathbb{N}^+$ *be the set of all real, positive zeroes of* $z(u) = 1 + u\sin\left(\frac{\pi u}{2}\right)$ *ordered by increasing magnitude, then for every interval* $[2p-1, 2p+1]$, $p \in \mathbb{N}^+$, *there exists a unique zero,* u_p *within that interval and the Newton-Raphson method applied with the initial guess* $u_{p,0} = 2p$ *converges to it.*

Proof. We begin by partitioning $\mathbb{R}^+$ as the collection of intervals $\mathbb{R}^+ = \bigcup_{p\in\mathbb{N}^+}[2p-1, 2p+1] \cup [0, 1]$ and consider the presence of zeroes in each interval.

In $[0, 1]$, $z(u)$ is strictly positive and therefore there is no zero.

Within $[2p - 1, 2p + 1]$, the sine function is the only component of $z(u)$ that changes sign, doing so exactly one time; therefore, there is at most one zero within this interval. To show that there is exactly one, note that for $p > 1$, $\sup_{u\in[2p-1,2p+1]} u\sin\left(\frac{\pi u}{2}\right) \geq 1$ and so the change in sign of this term causes a change in sign for $z(u)$ with a corresponding zero

in the interior of the interval. At the boundaries, there are no zeroes, since

$$z(2p \pm 1) = 1 + (-1)^p(1 \pm 2p) \neq 0, \quad p \in \mathbb{N}^+, \tag{E.14}$$

and therefore there is exactly one zero and it is within the interior of each interval $[2p - 1, 2p + 1]$.

For each such interval, there is one $u_{0,p} = 2p$ within that interval. By the results of Theorem E.1 together with the bound from Lemma E.3, we have that the Newton sequence starting with $u_{0,p}$ converges to a zero within

$$\begin{aligned}
\overline{B(u_{p,0}, s_p^*)} &= \left[2p - \frac{1 - \sqrt{1 - 2M_p\beta_p\eta_p}}{M_p\beta_p}, 2p + \frac{1 - \sqrt{1 - 2M_p\beta_p\eta_p}}{M_p\beta_p}\right] \\
&\subseteq \left[2p - \frac{2}{\pi p}, 2p + \frac{2}{\pi p}\right] \\
&\subseteq [2p - 1, 2p + 1], \quad \forall p \in \mathbb{N}^+.
\end{aligned}$$

Therefore, the Newton sequence generated by $u_{p,0}$ converges to the unique zero within $[2p - 1, 2p + 1]$ for every p. □

This theorem ensures that our Newton-Raphson method gives a good approximation of every zero of $z(u)$ and that we can approximate any product or sum over the zeros as a product or sum over the Newton-Raphson approximate zeroes without any skipping or double-counting.

APPENDIX F

WEIERSTRASS FACTORIZATION

In order to construct a factorization of the meromorphic function

$$\alpha(u) \equiv \frac{\beta(u)}{\gamma(u)} \equiv \frac{1 + u \sin\left(\frac{\pi u}{2}\right)}{2\cos\left(\frac{\pi u}{2}\right)}$$

we will apply a strengthening of the factorization theorem of Weierstrass due to Hadamard [70, 71]:

Theorem F.1. *Let $f : \mathbb{C} \to \mathbb{C}$ be an entire function of finite order ω. Let 0 be a zero of f of multiplicity m, and let $(u_n)_{n\in\mathbb{N}}$ be the sequence of other zeroes of f, repeated according to their multiplicities. Further, define*

$$E_n(z) \equiv \begin{cases} 1 - z & : n = 0 \\ (1-z)\exp\left(z + \frac{z^2}{2} + \cdots + \frac{z^n}{n}\right) & : \textit{otherwise} \end{cases}$$

Then, f has finite rank $p \leq \omega$ and there exists a polynomial g of degree at most ω such that

$$f(z) = z^m e^{g(z)} \prod_{n=1}^{\infty} E_p\left(\frac{z}{a_n}\right)$$

Remark. *The order of an entire function is the smallest number ω such that*

$$f(z) = \mathcal{O}(|z|^{\omega})$$

The rank, p, of a function f with the set of non-zero zeroes $\{u_n\}$ is the smallest integer such that

$$\sum_{\{u_n\}} |u_n|^{-p-1} < \infty$$

Because $\gamma(u)$ is proportional to a cosine function, we can utilize the well-know factorization for a cosine,

$$\begin{aligned}\cos\left(\frac{\pi u}{2}\right) &= \prod_{q\in\mathbb{Z}}\left(1+\frac{u}{2q+1}\right)e^{\frac{u}{2q+1}} \\ &= \prod_{q=0}^{\infty}\left(1-\frac{u^2}{(2q+1)^2}\right)\end{aligned} \tag{F.1}$$

For the numerator, $\beta(u)$, the sine here has order 1, which is unchanged by multiplying by u or adding a constant. The order of β, then, $\omega_\beta = 1$. For the rank, β has only two zeroes away from the real axis, and so only the real zeros are relevant. Since β is even we may consider the sum over only the positive zeroes, u_n. As we have shown, $|u_n - 2n \leq \frac{2}{\pi n}|$, and therefore

$$\sum_{n=1}^{\infty}|u_n|^{-p-1} \leq \sum_{n=1}^{\infty}\left|2n-\frac{2}{\pi n}\right|^{-p-1}, \tag{F.2}$$

which converges only when $p > 0$, and therefore β is of rank $p = 1$.

Order the zeroes of β with non-negative real and imaginary parts by increasing absolute value. Because β is an even function and there is no zero at the origin, we may then write

$$\begin{aligned}\beta(u) &= e^{c_0+c_1u}\prod_{n=0}^{\infty}\left(1-\frac{u}{u_n}\right)\left(1+\frac{u}{u_n}\right)e^{\frac{u}{u_n}}e^{-\frac{u}{u_n}} \\ &= e^{c_0+c_1u}\prod_{n=0}^{\infty}\left(1-\frac{u}{u_n}\right)\left(1+\frac{u}{u_n}\right),\end{aligned}$$

where c_0 and c_1 must be determined.

Note that $\beta(0) = 1$ and thereforce $c_0 = 0$. Further, taking the logarithmic derivative of our factorization of β at $u = 0$ and comparing with the direct calculation of the same, we have that

$$\frac{\beta'(0)}{\beta(0)} = c_1 = 0,$$

and therfore

$$\beta(u) = \prod_{n=0}^{\infty}\left(1-\frac{u^2}{u_n^2}\right). \tag{F.3}$$

Combining results, we have that

$$\begin{aligned}\alpha(u) &= \frac{1}{2}\prod_{n=0}^{\infty}\frac{\left(1-\frac{u^2}{u_n^2}\right)}{\left(1-\frac{u^2}{(2n+1)^2}\right)} \\ &= \frac{1}{2}\prod_{n=0}^{\infty}\frac{(2n+1)^2}{u_n^2}\frac{(u_n^2-u^2)}{((2n+1)^2-u^2)} \\ &= -\frac{1}{2}\prod_{n=0}^{\infty}\frac{(2n+1)^2}{|u_n|^2}\frac{(u_n^2-u^2)}{((2n+1)^2-u^2)}\end{aligned} \tag{F.4}$$

APPENDIX G

PROPERTIES OF THE MODIFIED BESSEL FUNCTION OF THE SECOND KIND

The modified Bessel functions of the second kind, sometimes also called the Macdonald functions, appear repeatedly throughout this thesis, and so rather than scatter facts about them throughout, we concisely summarize the important points in this appendix.

Typically denoted $K_\nu(z)$, the modified Bessel function of the second kind of order ν is one of two linearly independent solutions to the differential equation

$$\left(z^2\frac{d^2}{dz^2} + z\frac{d}{dz} - (z^2+\nu^2)\right) K_\nu(z) = 0. \tag{G.1}$$

Such differential equations and the associated solutions arise frequently when studying and solving second order partial differential equations in hyper-spherical coordinates via separation of variables. The same is true in this work; the modified Bessel functions enter our problems as factors in the Green's functions of the Helmholtz equation in even dimensions, which can be seen from the following Fourier transform identity for $k, r \in \mathbb{R}^n$,

$$\int_{\mathbb{R}^n} \frac{1}{k^2+\alpha^2} e^{ik\cdot r}\, d^n k = 2\pi \left(\frac{2\pi\alpha}{|r|}\right)^{n/2-1} K_{\frac{n}{2}-1}\left(\alpha|r|\right). \tag{G.2}$$

(Strictly speaking, this integral converges only when $n < 4$, but for $n \geq 4$ we should understand this identity as the Fourier transform of a tempered distribution). In odd dimensions, this relation involves half-integer order modified Bessel functions, which reduce to more elementary functions: exponentials times algebraic functions. However, in even dimensions we find integer order modified Bessel functions, which cannot be written in closed form using more elementary functions.

The behavior of the modified Bessel functions at large and small positive arguments

also arises and so we show the general expansions for $z \to 0$, where the behavior depends on the order

$$K_\nu(z) \sim \begin{cases} -\log \frac{z}{2} - \gamma & \nu = 0 \\ \frac{1}{2}\left(|\nu| - 1\right)! \left(\frac{z}{2}\right)^{-|\nu|} & |\nu| \in \mathbb{N} \\ \frac{1}{2}\Gamma(\nu)\left(\frac{z}{2}\right)^{-\nu} + \frac{1}{2}\Gamma(-\nu)\left(\frac{z}{2}\right)^{\nu} & \nu \notin \mathbb{Z} \end{cases} \tag{G.3}$$

and also for $z \to \infty$, where the behavior is independent of the order

$$K_\nu(z) \sim \sqrt{\frac{\pi}{2z}} e^{-z} \left(1 + \mathcal{O}\left(\frac{1}{z}\right)\right). \tag{G.4}$$

The behaior for small arguments is particularly notable in two cases in our studies

1. When we have a modified bessel function of purely imaginary order, the function has log-periodic oscillations for small arguments. The value remains between -1 and 1, but it oscillates with ever-increasing frequency.

2. Modified Bessel functions of integer order have poles where the argument is zero. In several cases this means that the kernels of our integral equations are singular, hence the regularized integrals.

Together, these facts about the small argument behavior mean that the modified Bessel functions is never continuously differentiable at zero argument, which sometimes complicates our analysis.

Some relevant additional facts are that $K_\nu(z)$ is an even function of ν

$$K_{-\nu}(z) = K_\nu(z). \tag{G.5}$$

The general characteristics of K on the complex plane are also sometimes useful to know. $K_\nu(z)$ is an entire function of ν for fixed z. For fixed ν, $K_\nu(z)$ is a single-valued function of z, provided that we cut the plane along $z \in (-\infty, 0)$. It is continuous when approaching this branch cut from positive imaginary values.

As we introduce the modified Bessel functions during the body of the thesis, we will sometimes refer the reader to this Appendix.

REFERENCES

[1] L. H. Thomas, "The interaction between a neutron and a proton and the structure ofH3," *Physical Review*, vol. 47, no. 12, pp. 903–909, 1935.

[2] J. J. Sakurai, *Modern quantum mechanics; rev. ed.* Addison-Wesley, 1994.

[3] H. Bethe and R. Peierls, "Quantum theory of the diplon," *Proceedings of the Royal Society A: Mathematical, Physical and Engineering Sciences*, vol. 148, no. 863, pp. 146–156, Jan. 1935.

[4] R. P. H. A. Bethe, "The scattering of neutrons by protons," *Proceedings of the Royal Society of London. Series A, Mathematical and Physical Sciences*, vol. 149, no. 866, pp. 176–183, 1935.

[5] H. A. Bethe, "Theory of the effective range in nuclear scattering," *Phys. Rev.*, vol. 76, pp. 38–50, 1 Jul. 1949.

[6] J. M. Blatt and J. D. Jackson, "On the interpretation of neutron-proton scattering data by the schwinger variational method," *Phys. Rev.*, vol. 76, no. 1, pp. 18–37, Jul. 1949.

[7] S. Albeverio and R. Høegh-Krohn, "Schrödinger operators with point interactions and short range expansions," *Physica A: Statistical Mechanics and its Applications*, vol. 124, no. 1-3, pp. 11–27, Mar. 1984.

[8] P. G. Burke and C. J. Joachain, "Analytic properties of the scattering amplitude," in *Theory of Electron—Atom Collisions*, Springer US, 1995, pp. 103–142.

[9] C. R. de Oliveira, *Intermediate Spectral Theory and Quantum Dynamics*. Springer Basel AG, 2008, ISBN: 3764387947.

[10] E. Braaten and H.-W. Hammer, "Universality in few-body systems with large scattering length," *Physics Reports*, vol. 428, no. 5–6, pp. 259 –390, 2006.

[11] V. Efimov, "Energy levels arising from resonant two-body forces in a three-body system," *Physics Letters B*, vol. 33, no. 8, pp. 563 –564, 1970.

[12] P. Naidon and S. Endo, "Efimov physics: A review," *Reports on Progress in Physics*, vol. 80, no. 5, p. 056 001, 2017.

[13] C. H. Greene, P. Giannakeas, and J. Pérez-Ríos, "Universal few-body physics and cluster formation," *Reviews of Modern Physics*, vol. 89, no. 3, 2017.

[14] B. D. Esry, C. D. Lin, and C. H. Greene, "Adiabatic hyperspherical study of the helium trimer," *Physical Review A*, vol. 54, no. 1, pp. 394–401, 1996.

[15] A. S. Jensen, A. Cobis, D. V. Fedorov, E. Garrido, and E. Nielsen, "Adiabatic hyperspherical expansion and three-body halos," in *Few-Body Problems in Physics '98*, Springer Vienna, 1999, pp. 19–26.

[16] K. M. Case, "Singular potentials," *Physical Review*, vol. 80, no. 5, pp. 797–806, 1950.

[17] K. Meetz, "Singular potentials in nonrelativistic quantum mechanics," *Il Nuovo Cimento*, vol. 34, no. 3, pp. 690–708, 1964.

[18] A. M. Perelomov and V. S. Popov, "?fall to the center? in quantum mechanics," *Theoretical and Mathematical Physics*, vol. 4, no. 1, pp. 664–677, 1970.

[19] P. F. Bedaque, H.-W. Hammer, and U. van Kolck, "Renormalization of the three-body system with short-range interactions," *Physical Review Letters*, vol. 82, no. 3, pp. 463–467, Jan. 1999.

[20] H. E. Camblong, L. N. Epele, H. Fanchiotti, and C. A. G. Canal, "Renormalization of the inverse square potential," *Physical Review Letters*, vol. 85, no. 8, pp. 1590–1593, 2000.

[21] J. Wang, J. P. D'Incao, B. D. Esry, and C. H. Greene, "Origin of the three-body parameter universality in efimov physics," *Physical Review Letters*, vol. 108, no. 26, 2012.

[22] V. Efimov, "Low-energy Properties of Three Resonantly Interacting Particles," *Sov. J. Nucl. Phys.*, vol. 29, p. 546, 1979.

[23] A. O. Gogolin, C. Mora, and R. Egger, "Analytical solution of the bosonic three-body problem," *Phys. Rev. Lett.*, vol. 100, p. 140 404, 14 2008.

[24] S. Tan, "Energetics of a strongly correlated fermi gas," *Annals of Physics*, vol. 323, no. 12, pp. 2952 –2970, 2008.

[25] ——, "Large momentum part of a strongly correlated fermi gas," *Annals of Physics*, vol. 323, no. 12, pp. 2971 –2986, 2008.

[26] ——, "Generalized virial theorem and pressure relation for a strongly correlated fermi gas," *Annals of Physics*, vol. 323, no. 12, pp. 2987–2990, Dec. 2008.

[27] E. Braaten, D. Kang, and L. Platter, "Universal relations for identical bosons from three-body physics," *Physical Review Letters*, vol. 106, no. 15, 2011.

[28] F. Werner and Y. Castin, "General relations for quantum gases in two and three dimensions. ii. bosons and mixtures," *Phys. Rev. A*, vol. 86, p. 053 633, 5 2012.

[29] Y. Nishida and S. Tan, "Liberating efimov physics from three dimensions," *Few-Body Syst*, vol. 51, no. 2-4, pp. 191–206, 2011.

[30] S. Tan, "Universal bound states of two particles in mixed dimensions or near a mirror," *Phys. Rev. Lett.*, vol. 109, p. 020 401, 2 2012.

[31] Y. Nishida, S. Moroz, and D. T. Son, "Super efimov effect of resonantly interacting fermions in two dimensions," *Phys. Rev. Lett.*, vol. 110, p. 235 301, 23 2013.

[32] S. Moroz and Y. Nishida, "Super efimov effect for mass-imbalanced systems," *Phys. Rev. A*, vol. 90, no. 6, 2014.

[33] D. K. Gridnev, "Three resonating fermions in flatland: Proof of the super efimov effect and the exact discrete spectrum asymptotics," *Journal of Physics A: Mathematical and Theoretical*, vol. 47, no. 50, p. 505 204, 2014.

[34] Z. Yu, J. H. Thywissen, and S. Zhang, "Universal relations for a fermi gas close to a p-wave interaction resonance," *Phys. Rev. Lett.*, vol. 115, p. 135 304, 13 2015.

[35] C. Luciuk, S. Trotzky, S. Smale, Z. Yu, S. Zhang, and J. H. Thywissen, "Evidence for universal relations describing a gas with p-wave interactions," *Nat Phys*, vol. 12, no. 6, pp. 599–605, Jun. 2016.

[36] S.-G. Peng, X.-J. Liu, and H. Hu, "Large-momentum distribution of a polarized fermi gas and p -wave contacts," *Physical Review A*, vol. 94, no. 6, 2016.

[37] S. B. Emmons, D. Kang, and L. Platter, "Operator product expansion beyond leading order for two-component fermions," *Physical Review A*, vol. 94, no. 4, 2016.

[38] X. Cui and H. Dong, "High-momentum distribution with a subleading k-3 tail in odd-wave interacting one-dimensional fermi gases," *Physical Review A*, vol. 94, no. 6, 2016.

[39] S.-G. Peng, C.-X. Zhang, S. Tan, and K. Jiang, "Contact theory for spin-orbit-coupled fermi gases," *Physical Review Letters*, vol. 120, no. 6, 2018.

[40] C.-X. Zhang, S.-G. Peng, and K. Jiang, "Universal relations for spin-orbit-coupled fermi gases in two and three dimensions," *Physical Review A*, vol. 101, no. 4, 2020.

[41] O. Hen, L. B. Weinstein, E. Piasetzky, G. A. Miller, M. M. Sargsian, and Y. Sagi, "Correlated fermions in nuclei and ultracold atomic gases," *Physical Review C*, vol. 92, no. 4, 2015.

[42] R. Weiss, B. Bazak, and N. Barnea, "Generalized nuclear contacts and momentum distributions," *Physical Review C*, vol. 92, no. 5, 2015.

[43] M. Alvioli, C. C. degli Atti, and H. Morita, "Universality of nucleon-nucleon short-range correlations: The factorization property of the nuclear wave function, the relative and center-of-mass momentum distributions, and the nuclear contacts," *Physical Review C*, vol. 94, no. 4, 2016.

[44] R. Weiss, R. Cruz-Torres, N. Barnea, E. Piasetzky, and O. Hen, "The nuclear contacts and short range correlations in nuclei," *Physics Letters B*, vol. 780, pp. 211–215, 2018.

[45] R. Weiss, I. Korover, E. Piasetzky, O. Hen, and N. Barnea, "Energy and momentum dependence of nuclear short-range correlations - spectral function, exclusive scattering experiments and the contact formalism," *Physics Letters B*, vol. 791, pp. 242–248, 2019.

[46] J. T. Stewart, J. P. Gaebler, T. E. Drake, and D. S. Jin, "Verification of universal relations in a strongly interacting fermi gas," *Physical Review Letters*, vol. 104, no. 23, 2010.

[47] E. D. Kuhnle, H. Hu, X.-J. Liu, P. Dyke, M. Mark, P. D. Drummond, P. Hannaford, and C. J. Vale, "Universal behavior of pair correlations in a strongly interacting fermi gas," *Physical Review Letters*, vol. 105, no. 7, 2010.

[48] E. Kuhnle, P. Dyke, S. Hoinka, M. Mark, H. Hu, X.-J. Liu, P. Drummond, P. Hannaford, and C. Vale, "Universal structure of a strongly interacting fermi gas," *Journal of Physics: Conference Series*, vol. 264, p. 012 013, 2011.

[49] C. Shkedrov, G. Ness, Y. Florshaim, and Y. Sagi, "In situ momentum-distribution measurement of a quantum degenerate fermi gas using raman spectroscopy," *Physical Review A*, vol. 101, no. 1, 2020.

[50] R. J. Wild, P. Makotyn, J. M. Pino, E. A. Cornell, and D. S. Jin, "Measurements of tan's contact in an atomic bose-einstein condensate," *Physical Review Letters*, vol. 108, no. 14, 2012.

[51] P. Makotyn, C. E. Klauss, D. L. Goldberger, E. A. Cornell, and D. S. Jin, "Universal dynamics of a degenerate unitary bose gas," *Nature Physics*, vol. 10, no. 2, pp. 116–119, 2014.

[52] D. H. Smith, E. Braaten, D. Kang, and L. Platter, "Two-body and three-body contacts for identical bosons near unitarity," *Physical Review Letters*, vol. 112, no. 11, 2014.

[53] R. J. Fletcher, R. Lopes, J. Man, N. Navon, R. P. Smith, M. W. Zwierlein, and Z. Hadzibabic, "Two- and three-body contacts in the unitary bose gas," *Science*, vol. 355, no. 6323, pp. 377–380, 2017.

[54] M. A. Kasevich, D. S. Weiss, and S. Chu, "Normal-incidence reflection of slow atoms from an optical evanescent wave," *Opt. Lett.*, vol. 15, no. 11, pp. 607–609, 1990.

[55] I Manek, R Grimm, and Y. B. Ovchinnikov, "Surface trap for cs atoms based on evanescent-wave cooling," *Physical review letters.*, vol. 79, no. 12, pp. 2225–2228, 1997.

[56] J. D. Jackson, *Classical Electrodynamics*. John Wiley & Sons Inc, Jul. 27, 1998, 832 pp., ISBN: 047130932X.

[57] R. Kress, "On the numerical solution of a hypersingular integral equation in scattering theory," *Journal of Computational and Applied Mathematics*, vol. 61, no. 3, pp. 345–360, 1995.

[58] N. Nishimura, K. ichi Yoshida, and S. Kobayashi, "A fast multipole boundary integral equation method for crack problems in 3d," *Engineering Analysis with Boundary Elements*, vol. 23, no. 1, pp. 97–105, 1999.

[59] G. Krishnasamy, L. W. Schmerr, T. J. Rudolphi, and F. J. Rizzo, "Hypersingular boundary integral equations: Some applications in acoustic and elastic wave scattering," *Journal of Applied Mechanics*, vol. 57, no. 2, pp. 404–414, 1990.

[60] M. S. Tong and W. C. Chew, "A novel approach for evaluating hypersingular and strongly singular surface integrals in electromagnetics," *IEEE Transactions on Antennas and Propagation*, vol. 58, no. 11, pp. 3593–3601, 2010.

[61] M. Bawin and S. A. Coon, "Singular inverse square potential, limit cycles, and self-adjoint extensions," *Physical Review A*, vol. 67, no. 4, 2003.

[62] C. Burgess, P. Hayman, M. Williams, and L. Zalavári, "Point-particle effective field theory i: Classical renormalization and the inverse-square potential," *Journal of High Energy Physics*, vol. 2017, no. 4, 2017.

[63] H.-W. Hammer and T. Mehen, "A renormalized equation for the three-body system with short-range interactions," *Nuclear Physics A*, vol. 690, no. 4, pp. 535–546, 2001.

[64] R. Mohr, R. Furnstahl, H.-W. Hammer, R. Perry, and K. Wilson, "Precise numerical results for limit cycles in the quantum three-body problem," *Annals of Physics*, vol. 321, no. 1, pp. 225–259, 2006.

[65] S. Moroz, S. Floerchinger, R. Schmidt, and C. Wetterich, "Efimov effect from functional renormalization," *Physical Review A*, vol. 79, no. 4, 2009.

[66] E Nielsen, "The three-body problem with short-range interactions," *Physics Reports*, vol. 347, no. 5, pp. 373–459, 2001.

[67] I. S. Gradshteyn, I. M. Ryzhik, D. Zwillinger, and V. Moll, *Table of Integrals, Series, and Products*. Elsevier LTD, Oxford, Nov. 1, 2014, ISBN: 0123849330.

[68] L. Debnath, *Integral transforms and their applications*. Boca Raton: Chapman & Hall/CRC, 2007, ISBN: 9781420010916.

[69] N. Bleistein, *Asymptotic expansions of integrals*. New York: Dover Publications, 1986, ISBN: 0486650820.

[70] J. Hadamard, "Etude sur les propriétés des fonctions entières et en particulier d'une fonction considérée par riemann," *Journal de Mathématiques Pures et Appliquées*, pp. 171–216, 1893.

[71] L. Ahlfors, *Complex analysis : an introduction to the theory of analytic functions of one complex variable*. New York: McGraw-Hill, 1979, ISBN: 0070006571.

[72] M. Kontorovich and N. Lebedev, "About a method of solution of some problems in diffraction theory and related problems," *Journal of Experimental and Theoretical Physics*, pp. 1192–1206, 1938.

[73] N. Lebedev and M. Kontorovich, "On the application of inversion formulae to the solution of some electrodynamics," *Journal of Experimental and Theoretical Physics*, pp. 729–742, 1939.

[74] M. Gattobigio, M. Göbel, H.-W. Hammer, and A. Kievsky, "More on the universal equation for efimov states," *Few-Body Systems*, vol. 60, no. 2, May 2019.

[75] Y. Castin and F. Werner, "Single-particle momentum distribution of an efimov trimer," *Phys. Rev. A*, vol. 83, p. 063 614, 6 2011.

[76] C. Ji, D. R. Phillips, and L. Platter, "The three-boson system at next-to-leading order in an effective field theory for systems with a large scattering length," *Annals of Physics*, vol. 327, no. 7, pp. 1803–1824, Jul. 2012.

[77] C. Ji and D. R. Phillips, "Effective field theory analysis of three-boson systems at next-to-next-to-leading order," *Few-Body Systems*, vol. 54, no. 12, pp. 2317–2355, Apr. 2013.

[78] F. F. Bellotti, T. Frederico, M. T. Yamashita, D. V. Fedorov, A. S. Jensen, and N. T. Zinner, "Dimensional effects on the momentum distribution of bosonic trimer states," *Phys. Rev. A*, vol. 87, p. 013 610, 1 2013.

[79] M. T. Yamashita, F. F. Bellotti, T. Frederico, D. V. Fedorov, A. S. Jensen, and N. T. Zinner, "Single-particle momentum distributions of efimov states in mixed-species systems," *Phys. Rev. A*, vol. 87, p. 062 702, 6 2013.

[80] M. T. Yamashita, "Single-particle momentum distributions for bosonic trimer states in two and three dimensions," *Few-Body Systems*, vol. 55, no. 8-10, pp. 843–846, Feb. 2014.

[81] "8 hilbert transforms on the real line," in, ser. Pure and Applied Mathematics, P. L. Butzer and R. J. Nessel, Eds., vol. 40, Elsevier, 1971, pp. 305 –333.

[82] T. Kraemer, M. Mark, P. Waldburger, J. G. Danzl, C. Chin, B. Engeser, A. D. Lange, K. Pilch, A. Jaakkola, H.-C. Nägerl, and R. Grimm, "Evidence for efimov quantum states in an ultracold gas of caesium atoms," *Nature*, vol. 440, no. 7082, pp. 315–318, Mar. 2006.

[83] M. Zaccanti, B. Deissler, C. D'Errico, M. Fattori, M. Jona-Lasinio, S. Müller, G. Roati, M. Inguscio, and G. Modugno, "Observation of an efimov spectrum in an atomic system," *Nature Physics*, vol. 5, no. 8, pp. 586–591, Jul. 2009.

[84] L. Blanchet and G. Faye, "Hadamard regularization," *J. Math. Phys.*, vol. 41, no. 11, p. 7675, 2000.

[85] G. Fikioris, "Mellin-transform method for integral evaluation: Introduction and applications to electromagnetics," *Synthesis Lectures on Computational Electromagnetics*, vol. 2, no. 1, pp. 1–67, Jan. 2007.

[86] D. J. Walter, "Computer art representing the behavior of the newton-raphson method," *Computers & Graphics*, vol. 17, no. 4, pp. 487–488, 1993.

[87] P Deuflhard, *Newton methods for nonlinear problems : affine invariance and adaptive algorithms*. Berlin New York: Springer, 2004, ISBN: 3540210997.

[88] J. Fernandez, *Newton's method : an updated approach of Kantorovich's theory*. Cham, Switzerland: Birkhauser, 2017, ISBN: 9783319559759.